POLYTECHNIQUE MONTRÉAL

affiliée à l'Université de Montréal

Identifying the severity of adolescent idiopathic scoliosis during gait by using Machine Learning

BAHARE SAMADI

Institut de génie biomédical

Thèse présentée en vue de l'obtention du diplôme de *Philosophiæ Doctor*

Génie biomédical

Décembre 2020

POLYTECHNIQUE MONTRÉAL

affiliée à l'Université de Montréal

Cette thèse intitulée :

Identifying the severity of adolescent idiopathic scoliosis during gait by using Machine Learning

présentée par **Bahare SAMADI**

en vue de l'obtention du diplôme de *Philosophiæ Doctor*

a été dûment acceptée par le jury d'examen constitué de :

Marek BALAZINSKI, président
Maxime RAISON, membre et directeur de recherche
Sofiane ACHICHE, membre et codirecteur de recherche
Carole FORTIN, membre et codirectrice de recherche
Samuel KADOURY, membre
David LABBÉ, membre externe

DEDICATION

To my beloved family

"What is research but a blind date with knowledge?"
Will Harvey

ACKNOWLEDGEMENTS

This adventurous journey would not have been possible without the contribution and valuable assistance of many people, who throughout the past four years, not only influenced my work but also supported me in many ways.

First and foremost, I would like to express my deep and sincere gratitude to my advisors, Professor Sofiane Achiche and Professor Maxime Raison, who mentored me during my Ph.D. Their endless patience and invaluable guidance in all aspects of being a good research scientist are greatly appreciated and will not be forgotten. I sincerely thank them for their support and confidence in me, which allowed me to follow my dreams. I am thankful to Maxime for his dedicated advice and overall insights throughout this research, which made this an inspiring experience for me. I greatly appreciate Sofiane for his sincerity, empathy, great sense of humor and brilliant ideas. I would also like to thank Professor Carole Fortin, my research co-director for her precious guidance and assistance.

I am also grateful to *Fondation Arbour*, *Biomedical Science and Technologies Research Centre* (GRSTB) and *Fond de recherche du Québec-Nature et technologies* (FRQNT) for their financial support during my Ph.D.

A sincere thank you to the participants in the gait analysis evaluation as part of my research project and to the researchers, physiotherapists, students and trainees of the Technopole of Marie Enfant Rehabilitation Center for making this research experience both friendly and fulfilling. My appreciation to my colleagues in the COSIM Lab at Polytechnique for the great times and conversations, especially to Olivier Barron who was always there listening to me. I am indebted to my lovely family and friends all over the world for their friendship and motivation, especially to Katayoon Safaei, Lili Azari and Elahe Serri.

And finally I would like to say a heartfelt thank you to my parents, Forough and Reza, who guided me in the right direction all through my life with their infinite love, support and encouragement; to my brother Payman for his unconditional love and ability to make me smile and remain inspired on difficult days, who never stopped pushing me towards success.

RÉSUMÉ

La scoliose idiopathique de l'adolescent (SIA) est une déformation de la colonne vertébrale dans les trois plans de l'espace objectivée par un angle de Cobb ≥ 10°. Celle-ci affecte les adolescents âgés entre 10 et 16 ans. L'étiologie de la scoliose demeure à ce jour inconnue malgré des recherches approfondies. Différentes hypothèses telles que l'implication de facteurs génétiques, hormonaux, biomécaniques, neuromusculaires ou encore des anomalies de croissance ont été avancées. Chez ces adolescents, l'ampleur de la déformation de la colonne vertébrale est objectivée par mesure manuelle de l'angle de Cobb sur radiographies antéropostérieures. Cependant, l'imprécision inter / intra observateur de cette mesure, ainsi que de l'exposition fréquente (biannuelle) aux rayons X que celle-ci nécessite pour un suivi adéquat, sont un domaine qui préoccupe la communauté scientifique et clinique. Les solutions proposées à cet effet concernent pour beaucoup l'utilisation de méthodes assistées par ordinateur, telles que des méthodes d'apprentissage machine utilisant des images radiographiques ou des images du dos du corps humain. Ces images sont utilisées pour classer la sévérité de la déformation vertébrale ou pour identifier l'angle de Cobb. Cependant, aucune de ces méthodes ne s'est avérée suffisamment précise pour se substituer l'utilisation des radiographies.

Parallèlement, les recherches ont démontré que la scoliose modifie le schéma de marche des personnes qui en souffrent et par conséquent également les efforts intervertébraux. C'est pourquoi, l'objectif de cette thèse est de développer un modèle non invasif d'identification de la sévérité de la scoliose grâce aux mesures des efforts intervertébraux mesurés durant la marche. Pour atteindre cet objectif, nous avons d'abord comparé les efforts intervertébraux calculés par un modèle dynamique multicorps, en utilisant la dynamique inverse, chez 15 adolescents atteints de SIA avec différents types de courbes et de sévérités et chez 12 adolescents asymptomatiques (à titre comparatif). Par cette comparaison, nous avons pu objectiver que les efforts intervertébraux les plus discriminants pour prédire la déformation vertébrale étaient la force et le couple antéro-postérieur et la force médio-latérale. Par la suite, nous nous sommes concentrés sur la classification de la sévérité de la déformation vertébrale de 30 AIS ayant une courbure thoraco-lombaire / lombaire. Pour ce faire, nous avons testé différents modèles de classification. L'angle de Cobb a été identifié en exécutant différents modèles de régression. Les caractéristiques (*features*) servant à alimenter les algorithmes d'entraînement ont été choisies en fonction des

efforts intervertébraux les plus pertinents à la déformation vertébrale au niveau de la charnière lombo-sacrée (vertèbres allantes de L5-S1). Les précisions les plus élevées pour la classification exécutant différents algorithmes ont été obtenues par un algorithme de classification d'ensemble comprenant les “K-nearest neighbors”, “Support vector machine”, “Random forest”, “multilayer perceptron”, et un modèle de “neural networks” avec une précision de 91.4% et 93.6%, respectivement. De même, le modèle de régression par “Decision tree” parmi les autres modèles a obtenu le meilleur résultat avec une erreur absolue moyenne égale à 4.6° de moyenne de validation croisée de 10 fois.

En conclusion, nous pouvons dire que cette étude démontre une relation entre la déformation de la colonne vertébrale et les efforts intervertébraux mesurés lors de la marche. L'angle de Cobb a été identifié à l'aide d'une méthode sans rayonnement avec une précision prometteuse égale à 4.6°. Il s’agit d’une amélioration majeure par rapport aux méthodes précédemment proposées ainsi que par rapport à la mesure classique réalisée par des spécialistes présentant une erreur entre 5° et 10° (ceci en raison de la variation intra/inter observateur). L’algorithme que nous vous présentons peut être utilisé comme un outil d'évaluation pour suivre la progression de la scoliose. Il peut être considéré comme une alternative à la radiographie. Des travaux futurs devraient tester l'algorithme et l’adapter pour d’autres formes de SIA, telles que les scolioses lombaire ou thoracolombaire.

ABSTRACT

Adolescent idiopathic scoliosis (AIS) is a 3D deformation of the spine and rib cage greater than 10° that affects adolescents between the ages of 10 and 16 years old. The true etiology is unknown despite extensive research and investigation. However, different theories such as genetic and hormonal factors, growth abnormalities or biomechanical and neuromuscular reasons have been proposed as possible causes. The magnitude of spinal deformity in AIS is measured by the Cobb angle in degrees as the gold standard through the X-rays by specialists. The inter/intra observer error and the cumulative exposure to radiation, however, are sources of increasing concern among researchers with regards to the accuracy of manual measurement. Proposed solutions have therefore, focused on using computer-assisted methods such as Machine Learning using X-ray images, and/or trunk images to classify the severity of spinal deformity or to identify the Cobb angle. However, none of the proposed methods have shown the level of accuracy required for use as an alternative to X-rays. Meanwhile, scoliosis has been recognized as a pathology that modifies the gait pattern, subsequently impinging upon intervertebral efforts. The present thesis aims to develop a radiation-free model to identify the severity of idiopathic scoliosis in adolescents based on the intervertebral efforts during gait.

To accomplish this objective, we compared the intervertebral efforts computed using a multibody dynamics model, by way of inverse dynamics, among 15 adolescents with AIS having different curve types and severities, as well as 12 typically developed adolescents. This resulted in the identification of the most relevant intervertebral efforts influenced by spinal deformity: mediolateral (ML) force; anteroposterior (AP) force; and torque. Additionally, we focused on the classification of the severity of spinal deformity among 30 AIS with thoracolumbar/lumbar curvature, testing different classification models. Lastly, the Cobb angle was identified running regression models. The features to feed training algorithms were chosen based on the most relevant intervertebral efforts to the spinal deformity on the lumbosacral (L5-S1) joint. The highest accuracies for the classification were obtained by the ensemble classifier algorithm, including “K-nearest neighbors”, “support vector machine”, “random forest”, and “multilayer perceptron”, as well as a neural network model with an accuracy of 91.4% and 93.6%, respectively. Likewise, the “decision tree regression” model achieved the best result with a mean absolute error equal to 4.6 degrees of an averaged 10-fold cross-validation.

This study shows a relation between spinal deformity and the produced intervertebral efforts during gait. The Cobb angle was identified using a radiation-free method with a promising accuracy, providing a mean absolute error of 4.6°. Compared to measurement variations, ranging between 5° and 10° in the manual Cobb angle measurements by specialists, the proposed model provided reliable accuracy. This algorithm can be used as an assessment tool, alternative to the X-ray radiography, to follow up the progression of scoliosis. As future work, the algorithm should be tested and modified on AIS with other types of spine curvature than lumbar/thoracolumbar.

TABLE OF CONTENTS

LIST OF TABLES

LIST OF FIGURES

LIST OF SYMBOLS AND ABBREVIATIONS

This list presents the symbols and abbreviations used in the thesis or dissertation in alphabetical order, along with their meanings.

AIS Adolescents with idiopathic scoliosis

AP Anteroposterior

ATR Angle of Trunk Rotation

ANN Artificial Neural Network

CNN Convolutional Neural Network

EMG Electromyography

MAE Mean Absolute Error

MBD Multibody dynamics

ML Mediolateral

TDA Typically developed adolescents

CoP Center of Pressure

CNS Central Nervous System

4D Four-dimensional

3D Three-dimensional

V Vertical

CHAPTER 1 INTRODUCTION

1.1 Background information and problem definition

Adolescent idiopathic scoliosis (AIS) is an abnormal curvature of the spine higher than 10° in the sagittal plane in "S" or "C" shape, as well as rotation and twist of the spine bones. These abnormalities are classified based on the location of the curvature on the spine as thoracic, thoracolumbar/lumbar, and double [1] (Figure 1.1). The AIS is the most common form of scoliosis in children and adolescents (80% of the scoliosis cases) which affects girls 7 times more than boys [2]. The true aetiopathogenesis of this disorder remains unknown with different hypotheses such as genetics, growth hormone secretion, connective tissue structure, muscle and fibrous tissue, vestibular dysfunction, melatonin secretion, and platelet microstructure [3]. However, physiotherapy treatments are aimed at controlling progression of the spinal deformity in adolescents with AIS [4].

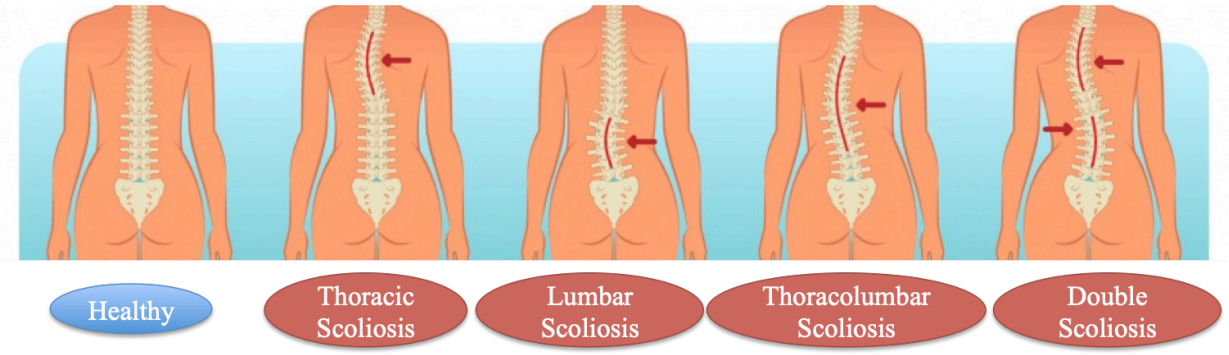

Figure 1.1 Scoliosis types, adapted from [5]

To assess the progression of spine curvature, the magnitude of the spinal deformity is measured by the Cobb angle [6] as the gold standard, in degrees, using X-ray images as shown in Figure 1.2. However, the accuracy of the Cobb angle measurement and repetitive exposure to X-ray radiations presents a big challenge.

1.2 Research scope and objectives

This study aims to develop a radiation-free model to identify the severity of idiopathic scoliosis in adolescents based on the intervertebral efforts during gait. To achieve this objective, it is required to identify the intervertebral efforts associated with the spinal deformity, by comparing the intervertebral efforts among the adolescents with AIS and typically developed adolescents (TDA).

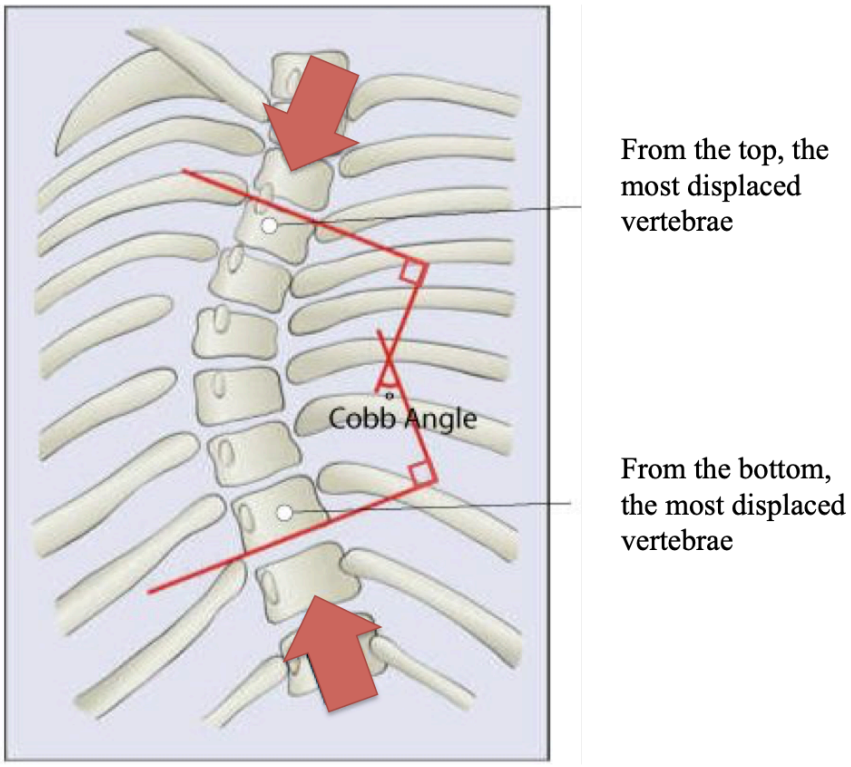

Figure 1.2 Cobb angle measurement, adapted from [7]

1.3 Thesis outline

This thesis is comprised of nine chapters. Chapter 1 is the introduction of the research project. A literature review on AIS gait patterns, effects of physiotherapy treatments on AIS, scoliosis evaluation methods and related challenges are presented in Chapter 2. In Chapter 3, the problematic, general objective and sub-objectives of the study are summarized. Chapter 4 briefly

presents the methodology. Chapter 5 identifies the intervertebral efforts most influenced by spinal deformity during gait in AIS (Article 1). Chapter 6 discusses the use of Machine Learning algorithms (Article 2) to classify the severity of spinal deformity among AIS based on the relevant intervertebral efforts during gait. Chapter 7 uses Machine Learning models to present a radiation-free model that identifies the Cobb angles based on the intervertebral efforts in the lumbosacral joint (Article 3). Chapter 8 is a general discussion of achievements, limitations, and outputs. The final chapter (Chapter 9), consists of the conclusion, suggestions for future studies, and recommendations.

CHAPTER 2 LITERATURE REVIEW

2.1 Impact of the severity of spinal deformity on gait pattern

2.1.1 Pre-surgery

Gait analysis has been known as a non-invasive method used to diagnose different musculoskeletal diseases. Studies on the scoliosis gait patterns have confirmed that there are some differences between the gait pattern of AIS and typically developed adolescents (TDA). AIS experience balance abnormality during the stance phase and asymmetry in the frequency characteristics [8]. These differences also depend on the type and severity of scoliosis. For instance, the AIS with S (double) curves have demonstrated poorer balance compared to those with the C (single) curve type. This, despite a more symmetrical trunk posture [9] among AIS with S (double) curves.

As per Mahaudens et al. [10] findings, a restriction occurs in the frontal pelvis, hip, shoulder and transversal hip motion in thoracolumbar and lumbar AIS during gait, even in scoliosis with mild severity. It can be explained by the stiffness of the spinal deformity or by the bilateral extended activation timing of the pelvic and lumbar muscles. Scoliosis also leads to asymmetry in gait patterns in the frontal and transverse planes, resulting in asymmetrical ground reaction forces in the mediolateral (ML) direction [11]. The changes in global postural control strategies during gait may be the reason for asymmetrical gait. Studies have shown that there is a relationship between this asymmetry, neurological dysfunction and spinal deformity. That is, the left side of the spinal curve has greater symmetry indices for a left side impulse and vice versa [12]–[14].

It has also been found that the severity of the spinal deformity has an influence on the gait pattern. Sycxewska et al. demonstrated a direct relationship between the obliquity and Cobb angle, and an inverse relationship between the length of the step and the Cobb angle [15]. Additionally, they confirmed that the severity of the spinal deformity and the type of pelvic misalignment have a correlation with the gait pathology in adolescents with the thoracolumbar curve type [16].

In terms of investigating kinetic parameters of scoliosis gait patterns, Yazji et al. [17] showed that ML forces at the right hip were significantly lower for the AIS with moderate left lumbar and

thoracolumbar, compared to TDA. Moreover, the abduction and adduction angles of the hip joint in the single support phase are reported to be significantly different than TDA[18].

Schizas et al. [19] compared the rate of application, contact time and magnitude of the two peaks of the vertical ground reaction forces during gait between right thoracic AIS, left thoracolumbar AIS and TDA. Subsequently, they reported no relation between gait asymmetry and curve magnitude, aside from the asymmetry of at least one kinetic parameter. In another study, Kramers-de Quervain et al. found an asymmetry in hip, knee and ankle motion in the sagittal plane, trunk rotational motion in the transverse plane, as well as a ground-reaction-force asymmetry of the free rotational movement [20]. As well, the right thoracic spinal curvature leads to slower dynamic patterns compared to a straight spine [21]. Scoliosis severity also influences the distribution of the center of pressure (CoP) during gait [22]. For instance, it has been reported that individuals with moderate scoliosis walk with more foot inversion motion than others [22]. The position of the major curve causes asymmetrical trunk kinematics during gait. Trunk motions with a single lumbar curve and thoracic curve cause asymmetry in the coronal plane and transverse plane, respectively [23].

In summary, based on previous studies, we conclude that spinal deformity and its severity modify the gait pathology characteristics, influencing overall function among those with AIS. Therefore, the evaluation of the gait pattern is essential to assess the progression of scoliosis and its treatments.

2.1.2 Post-surgery

Surgical treatment is recommended for patients with a spine curvature greater than 45° or 50° after skeletal maturity or for patients with progressive spinal deformity [24]. Spinal surgery has shown improvement in the sagittal plane posture, C7-Pelvic offsets, axial plane motion, center of mass displacement and gait phases as compared with TDA [14], [25], [26]. However, no post-surgery individual has demonstrated a gait pattern exactly similar to that of individuals with a healthy spine. Indeed, surgery does not cause any interference in daily functions such as walking. According to Mahaudens et al. [27]**,** one year after the reduction of spinal curvature by surgery, AIS patients demonstrated kinematics similar to mild AIS and abnormal EMG, and excessive energy expenditure compared to TDA. The same research group performed an evaluation 10 years after spinal surgery to draw comparisons with results one year after the surgery [28]. This

showed the Cobb angle reduced by 55% one year post-surgery to have reduced to 37% when measured 10 years post-surgery. The Frontal plumb line C7-S1 and lower limb kinematics remained stable over 10 years. However, Schimmel et al. [9] did not report any improvement in postural balance one year after the surgery in spite of better spinal alignment.

2.2 The biomechanical effects of physiotherapy and bracing treatments on AIS

Small lateral curvature and misalignment of the spine cause the weight of the body segment superior to the curve to generate a lateral bending moment as shown in Figure 2.1. This moment exacerbates the spinal deformity during the growth ages [29]–[32]. Furthermore, asymmetry in muscle activation leads to greater asymmetries in the biomechanical force patterns of body postures and body motions than the etiology factor of spinal curvature [33], [34].Therefore, the goal of scoliosis treatment strategies is to eliminate or reduce the lateral bending moment by the spine alignment [35].

To treat scoliosis through physiotherapy treatments, the biomechanical principles of axial and transverse forces are taken into account. The axial forces are the main factors in correcting the bending moment, while transverse loads are responsible for correcting function. The combination of these two loads presents the most effective way for postural correction for all severity types of scoliosis [36].

Physical exercise has been demonstrated as an effective method to treat AIS in terms of reducing the progression of the spine curvature, neuromotor control, respiratory function, biomechanical reduction of postural collapse, mobility, and balance [37]–[43]. Physiotherapy treatment also enables patients to correct their posture using their trunk muscles. Manual help by the therapists in the form of dynamic passive forces and static forces is also required [44]. Postural correction in AIS should account for the interactions between the central nervous system (CNS) and body biomechanics from a globally functional and systematic perspective [45]. The type of scoliosis should also be considered in global postural correction - a single thoracic curve causes asymmetrical trunk movement in the transverse plane while a single lumbar curve causes asymmetrical trunk movement in the coronal plane [23].

Bracing is recommended for AIS with the Cobb angle between 25° and 45° and the skeletal maturity index smaller or equal to 2, or for those with the Cobb angle less than 25° showing 5° progression at the 4 to 6 months follow-up stage [46]. The mechanical compression on the spine in AIS reduces the number of new cells in the proliferative zone of the growth plate. Meanwhile, bracing treatment aims to unload the growth plate by applying the corrective forces on the spine, releasing the load on the concave (inner) part of the spine curvature, and increasing the load on the convex (outer) part of the spine curvature [47], [48].

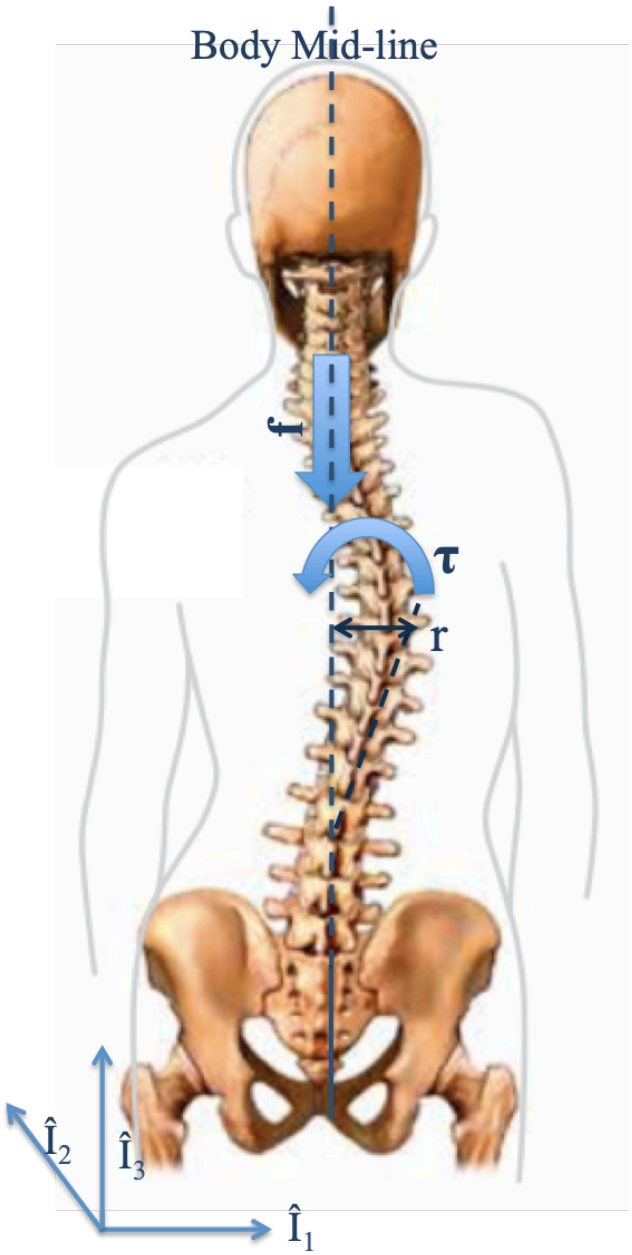

Figure 2.1 Schematic diagram of the produced moment on the scoliosis spine due to spine curvature.

τ: Moment of the force at the apex level due to the lateral offset (**τ = f** × r**), f**: Body weight of the segments above the apex level, r: Lateral translation of the apical vertebrae from the body midline

2.3 Scoliosis assessment

The initial evaluation for scoliosis is based on screening programs that are performed by physical examination with Adam's forward bending test (Figure 2.2) [49] and a scoliometer measurement (Figure 2.2) [50]. In Adam's forward bending test the patient is asked to bend forward as far as possible. In this position, should one side of the rib cage be higher than the other, the protruding side of the spine is convex. The scoliometer is a tool used to measure the angle of trunk rotation (ATR). A patient with an ATR greater than 10° is referred for an immediate orthopedic evaluation. An ATR of less than 5° is dismissed, while patients with an ATR between 5° and 9° are referred for two subsequent screenings conducted within 6 months of each other, during the year following the first screening [51]. Upon screening, to diagnose scoliosis, the Cobb angle should be measured using spinal X-rays in the standing postero-anterior position. The Cobb angle, i.e. the magnitude of the spinal curvature, is considered the gold standard measurement to determine and track the progression of scoliosis [6]. This is measured by considering a line parallel to the upper end of the upper vertebra and the lower end of the lowest vertebra of the curve and the angle between two perpendicular lines to these two lines (Figure 2.3). As proposed by Cobb, the measurement is carried out in degrees [6]. The severity of scoliosis is categorized based on the value of the Cobb angle. A Cobb angle between 10° and 25° is categorized as mild scoliosis, one between 25° and 45° as moderate scoliosis, and one greater than 45° as severe scoliosis [52]. However, there are challenges in measuring the Cobb angle in terms of accuracy and exposure to X-rays. It has been reported that there is a 5-10° measurement error due to the intra-observer, which may be further increased due to inter-observer measurement variations [53]–[55]. Radiography acquisition and measurement methods may also cause measurement variation of up to 7° [56]. This underscores the importance of replacing manual measurement methods with automated methods to measure the Cobb angle. These methods necessitate repeated exposure of the entire spine to X-ray radiations so as to monitor the progression of the spine curvature. The frequency of such exposure in adolescents presents growth challenges and increases health risks such as cancer [57]. The accuracy of the evaluation is important for determining the appropriate treatments. Initial treatments are physiotherapy exercises and bracing, whereas the most invasive form of treatment used to correct curvature in severe and progressive cases of scoliosis is spine surgery.

To minimize radiation exposure, several studies have been performed to propose radiation-free methods to evaluate scoliosis. Sections 2.3.1 and 2.3.2 review and draw comparisons between the accuracy levels of proposed automated methods using X-ray images and radiation-free methods to identify the Cobb angle.

Figure 2.2 Scoliosis screening using Adam's forward bending test and scoliometer, adapted from [58], [59]

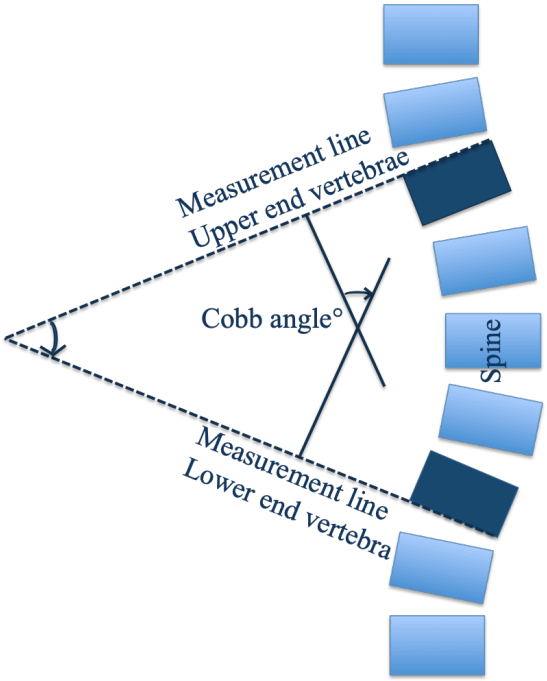

Figure 2.3 Cobb angle measurement on the X-ray image (frontal plane of the spine)

2.3.1 Computer assisted methods to measure the Cobb angle using radiography images

The manual measurement of the Cobb angle requires considerable time and effort by physicians. Even so, as mentioned in 2.3, this may lead to variations in measurements. Meanwhile, the accuracy of this measurement is crucial to avoiding misdiagnosis and failure in determining the appropriate treatment method. To overcome this problem, automated and computer-assisted methods have been proposed to measure the Cobb angle on radiography images. For instance, Sardjono et al. [60], proposed a curve fitting algorithm to fit the spine curvature and tested three curve fitting methods (piece-wise linear, splines, and polynomials) for the best fit. Among these, the most accurate result was obtained using the polynomial method (6^{th} degree), with a mean absolute error (MAE) equal to 3.91°. Samuvel et al. [61] presented a mask-based segmentation method applied on X-ray images to measure the Cobb angle. Samuvel et al. developed an algorithm that divides the X-ray image into segments, and proceeds to measure the angle between the lower and upper end vertebras, i.e. the Cobb angle. In this method, the Cobb angle measured provided a tolerance of 3-4° as compared with the manual measurement by an expert physician. Other studies have focused on automated detection of the upper-end and lower-end vertebrae to

decrease the variation in measurements carried out by clinicians. Results show that computer-assisted methods are clinically advantageous and more reliable than manual measurement, with average error values ranging from 1.7° to 6.5°. The proposed computer-assisted methods, therefore, showed the potential to obviate the measurement variation problems, with an average error of 4°. However, such methods continued to expose patients to X-ray radiations.

2.3.2 Computer-assisted methods to measure the Cobb angle using 3D reconstruction of the trunk or from topography as less invasive methods

To minimize the frequency of radiation exposure, which lead to increased health risks, researchers have tried to replace radiography images with radiation-free methods to assess scoliosis. In doing so, they report that these measurement techniques cannot be used in clinical recordings. Pearsal et al. [62] compared the performance of three different methods: scoliometer; back counter device; and topographic images to measure the Cobb angle. Patias et al. [63], used a multi-camera system setup to view the trunk from different views and then computed the 3D coordinates of a large number of surface points using automatic image matching. As a result, they proposed a number of indices linked to the spine shape to assess scoliosis. Findings from this study [64] and another by Goldberg et al. [65] showed that, although the back surface image data cannot substitute for radiographs in the diagnosis of scoliosis, it can be used as additional quantitative data to complement the radiologic study. Frerich et al. [66] used a Formetric 4D surface topography system to project stripes of white light on the back of a person in the standing position, whereby the system captures a digital photo to evaluate surface asymmetry and to identify bony landmarks. The value of the Cobb angle, however, cannot be measured using this device.

Although several studies have been conducted to develop radiation-free Cobb angle measurement by using back images and topography, still more improvement is required in this field. The existing solutions have been recognized as complementary to X-ray images. That is, the value of the Cobb angle cannot be measured with the accuracy required to be proposed as a radiation-free solution for treatment purposes. Therefore, the need for radiation-free solutions with promising accuracy that could be used as a reliable measurement method for treatment strategies is still valid.

2.4 Use of Machine Learning algorithms to assess the severity of scoliosis

In addition to the mentioned computer-assisted methods to measure the Cobb angle and severity of scoliosis, researchers have found that Machine Learning and Deep Learning algorithms are reliable and interesting methods to assess scoliosis. Zhang et al., developed a fuzzy Hough transform technique to detect the vertebral endplates and measure the Cobb angle automatically to decrease the variability in measurement [67]. They used a deep neural network (DNN) to determine the slopes of vertebrae and reported a mean absolute difference of up to 5° for intra-observer measurement variations. In [68]–[70], different models were developed using the convolutional Neural Network (CNN) algorithm to segment the X-ray images. The results obtained were subsequently used to calculate the Cobb angle. In one instance, Wu et al., [77] segmented the spine on the X-ray images and removed the outlier features to minimize the intraclass variance of the feature space and reported a mean squared error of 0.0046 on 50 test images. They also proposed [78] a multi-view Correlation Network architecture that provided an MAE of 4° in Cobb angle estimation. Horng et al. [79] segmented the vertebrae by using a CNN, which was then reconstructed into a complete segment to determine the Cobb angle with an MAE of 2°. They believed that their model was a robust automated tool to assess scoliosis for clinical purposes. Vergari et al. used a CNN with discriminant analysis to classify the treatment of scoliosis. In this study, [71], brace use, spinal implant, or neither together with radiography images as the dataset with an accuracy score of 98.3% . Tu et al. [72] segmented the radiography images by removing unrelated regions by way of programming the DU-Net network to segment the spine in contours. Therefore, the spine curve could be fitted by the spine contour and the Cobb angle could be automatically measured by the tangent line of the spine curve, with an average error of 2.9°, compared to the manual measurement by a specialist. Zhang et al. used a Deep Neural Network with vertebral patches extracted from spinal radiography images to identify the Cobb angle based on the vertebral slopes which resulted in an MAE of less than 3° [73]. Wu et al. reported Artificial Neural Network (ANN) as a promising technique to define the scoliosis progression. They used four values of the Cobb angle and lateral deviations at the apex level of the patients for six and twelve month intervals (coronal plane) as features to train their algorithm. In doing this, [74] used the scan of the entire torso surface of each patient by an optical imaging system and X-ray images of the whole spine for the mathematical 3D reconstruction of the spine and rib cage. They reported 0.99 and 0.97 for R-values of the linear

regression. Although the aforementioned methods eliminated the inconvenience of manual measurements, they cannot be considered as radiation-free methods.

Ramirez et al. [75] classified the severity of scoliosis (Cobb angle inferior to 30° or superior to 30°) based on the surface topographic images of patients with idiopathic scoliosis and their clinical data, using a support vector machine (SVM) classifier with an accuracy between 69-85% in the testing dataset. In fact, the treatment strategies are not the same for all individuals with the Cobb angle inferior to 30°, and for all of the individuals with the Cobb angle superior to 30°. The treatments strategies are based on the severity of scoliosis that is divided into three categories, as explained in section 2.3. Therefore, the proposed classifier cannot be used as a scoliosis evaluation tool even if the accuracy was promising. Ajemba et al. [76] proposed an SVM classifier algorithm on the basis of preoperative standing Lenke indicators measured from AP and ML radiographs, to predict the risk of progression in moderate AIS. They reported 100% accuracy in training and 65-80% accuracy in testing.

Seo et al. [77] trained multiple regression analysis by feeding standing posture parameters correlated with spine deformity as features and tested the proposed method on five patients. The reported errors were approximately 5°. Recently, Cho et al. [18] (2018), developed a gait recognition method based on the kinematic parameters (72 gait features) during gait to recognize scoliosis and non-scoliosis gait patterns and severity of scoliosis using an SVM classifier with accuracy scores of 95.2% and 85.7%, respectively.

The complexity of AIS geometry and progression calls for accurate assessment of treatment and evaluation. However, radiation exposure is also an important factor, which should be seriously considered. The mentioned methods in sections 2.3 and 2.4 show that there is interest and potential in utilizing automatic radiation-free methods based on Machine Learning algorithms as a follow-up tool in AIS. However, to our knowledge, there is no model with acceptable accuracy, which could be used for clinical purposes.

The majority of proposed Machine Learning methods reviewed in this section, have used the X-ray images to train their learning algorithms. Those, which have used other types of data, have not provided reliable or promising results for clinical assessments. Therefore, the challenge of developing a radiation-free method to identify the severity of idiopathic scoliosis as an alternative to X-rays remains an active field of research.

2.5 Multibody dynamics applied to AIS

Scoliosis has been recognized as a parameter that modifies the gait pattern and therefore leads to the modification of the intervertebral efforts during gait i.e. three-dimensional (3D) forces and torques during gait resulting from the mechanical modulations, according to the Hueter-Volkmann Law [47]. Furthermore, an increase of 30% of the energy consumption was detected during gait in AIS. This is explained due to the excessive postural muscle contractions to control the posture and maintain the spine [10]. Therefore, the understanding and quantification of the intervertebral efforts are crucial for posture correction and scoliosis evaluation[78]. To obtain the intervertebral forces and torques, a multibody dynamics model (MBD) is required. An MBD system is a mechanical system, consisting of solid or flexible bodies, linked to each other by joints, which restrict their relative motions (Figure 2.4). The MBD model calculates the required forces to make the system move with the inverse dynamics [79].

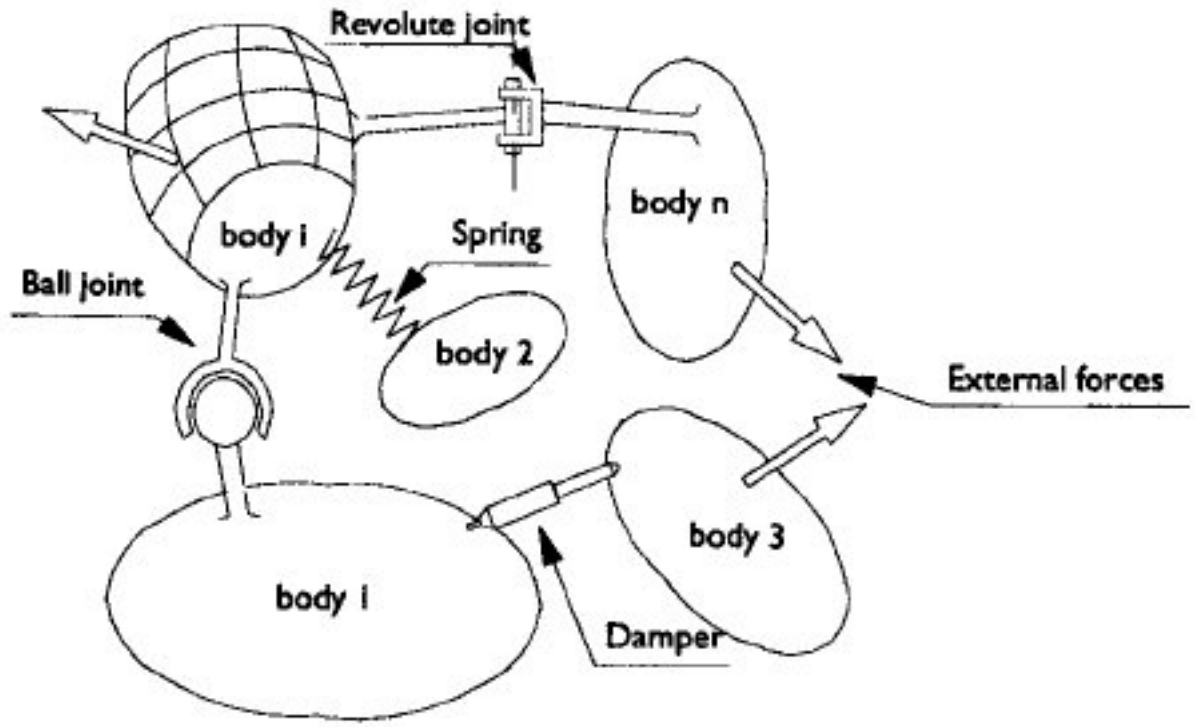

Figure 2.4 Schematic representation of a multibody system [80]

The quantification of joint efforts has been known as an essential tool to develop rehabilitation techniques for patients with musculoskeletal pathologies such as scoliosis [81]. An MBD model

of the human body can quantify the efforts of all human body articulations including the intervertebral efforts along the spine [17], [82]. In this study, we used two previous studies, which developed an MBD model to calculate the intervertebral joint efforts. The principle of inverse dynamics to calculate the joint efforts has been shown in Figure 2.5.

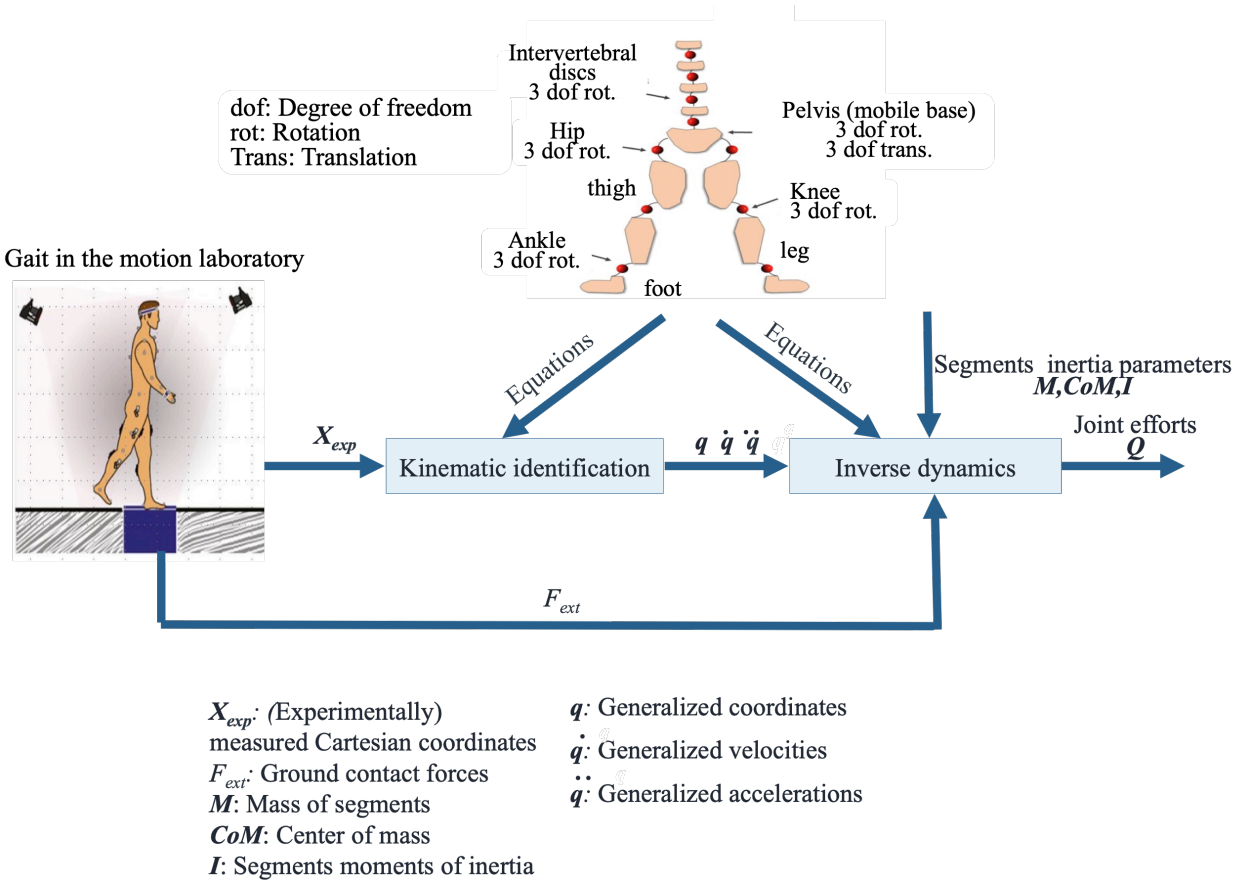

Figure 2.5 Procedure of joint efforts quantification using inverse dynamics in the multibody model [17]

To obtain the joint efforts by using an MBD model, a motion capture system, including cameras and force platforms/treadmill are required. The force platforms/treadmill are equipped with strain gauges to measure the 3D ground contact forces and the motion capture system records the 3D joint coordinates by placing markers on the specific anatomical joints of the human body. The

model is customized to each individual with measurements taken on them i.e. the mass, height, width of the knees and ankles, as well as the feet length. Then, the Cartesian coordinates i.e. the center of each joint is calculated as proposed by Davis et al. [83]. The segments inertia parameters, i.e. the mass of the segments (M), segments moments of inertia (I) and center of mass (CoM) for each body segment, are computed from the inertia tables from de Leva [84] by using the total mass, height, and gender. The inertial parameters of the vertebrae are computed following Kiefer et al. [85].

Then the joints' coordinates q are numerically defined by a global optimization method [86] that estimates the joint coordinates of the MBD model that best fit the position of the experimental joint centers [17]. For each data frame, the optimal position of the MBD model is computed based on globally minimizing the least square distance between the marker coordinates of the experimental and the model-defined. Finally, with applying a numerical derivative the corresponding velocities $\dot{q}$ and accelerations $\ddot{q}$ are computed from q using cubic splines. To obtain the dynamical equations, the Newton-Euler formalism is used [87]. As shown in *Equation 2-1*, this algorithm provides the vector Q of the internal interaction forces and torques at the joints for any configuration of the multibody system, in the form of an inverse dynamical model, generated with Robotran software [88] as shown in Figure 2.5.

$$Q = f(q, \dot{q}, \ddot{q}, F_{ext}, g) \qquad \textit{Equation 2-1}$$

Where Q is the vector of forces and torques between each vertebra, q is the vector of joint relative coordinates, $\dot{q}$ are the corresponding joint velocities, $\ddot{q}$ the corresponding joint accelerations, F_{ext} is the vector of the external forces and g is the gravity field.

CHAPTER 3 RATIONALE

3.1 Problematic

To assess the spinal deformity in adolescents with idiopathic scoliosis, it is generally required to measure the Cobb angle through radiography images. To perform that, on the one hand, the patients are exposed to radiation at least every six months, during the growth ages. On the other hand, the variations in measurement due to the measurement errors reduce the accuracy of identification of the Cobb angle. The cumulative exposure to radiation increases the risk of certain types of cancer and organ tissue damage and the variability in the Cobb angle measurement decreases the accuracy of treatments and the reliability of surgical decisions. Consequently, a radiation-free computer-assisted method with reliable and promising accuracy would mitigate these deficiencies.

3.2 Objectives

3.2.1 General objectives

The general objective of this research project is to develop a radiation-free model to identify the severity of idiopathic scoliosis in adolescents based on the intervertebral efforts during gait. To achieve the general objective, the following sub-objectives are required to be accomplished.

3.2.2 Sub-objectives

SO1: Define the intervertebral efforts among the six intervertebral forces and torques i.e. anteroposterior (AP), mediolateral (ML) and vertical (V) forces and torques during gait, which are relevant to the spinal deformity.

SO2: Define the relevant features from the intervertebral efforts during gait cycles to feed the training algorithms.

SO3: Classify the severity of scoliosis and identify the Cobb angle in AIS with lumbar/thoracolumbar scoliosis based on the lumbosacral joint efforts during gait using Machine Learning algorithms.

CHAPTER 4 GENERAL METHODOLOGY

This chapter briefly explains the methodology since the details are presented in chapters 5 to 7.

Spinal deformity modifies the kinematics parameters during gait, causes postural asymmetry, asymmetrical loading on the spine and progression of the spine curvature. To quantify the intervertebral efforts, kinematics identification is required. Additionally, different muscle function patterns due to the spinal deformity compared to a healthy spine may result in different behaviour in intervertebral efforts. Studies have been shown that an increase in the Cobb angle impacts on apical vertebral rotation, apical vertebral wedging and intervertebral discs wedging. It has also been reported that the deformation of the apical intervertebral disc is an important parameter in the progression of spinal deformity. Concluding mentioned observations and studies on intervertebral efforts in AIS during gait[89], confirm that intervertebral efforts during gait can be used as a parameter to be affected by the spinal deformity and therefore the Cobb angle. To identify the Cobb angle based on the intervertebral efforts during gait, first we defined the intervertebral efforts that are being influenced by scoliosis. The intervertebral efforts during gait along the spine were computed using an MBD model [82] for 15 adolescents with AIS with different types of scoliosis and severity and 12 TDA. The intervertebral efforts of the adolescents with AIS in the level of the apex (the vertebra with the greatest rotation or farthest deviation from the center of the spine) were compared to the average of intervertebral efforts of TDA at the same level to define the intervertebral efforts sensitive to the spinal deformity. The details are presented in chapter 5 (Article 1). The specifications of the participants are presented in Table 4.1.

Table 4.1 Specification of the participants in SO1 (article 1)

	Age (y) mean (SD)	**Weight (kg) mean (SD)**	**Height (m) mean (SD)**	**Cobb angle (°) mean (SD)**	**Scoliosis type**
Adolescents with AIS (5 males)	14.1 (1.3)	48.9 (9.4)	1.6 (0.1)	26 (7) Range (12-37)	Thoracic (6) Lumbar/ thoracolumbar (6) Double (3)
TDA (5 males)	13.4 (1.8)	44.4 (13)	1.55 (0.1)	NA	NA

To proceed with the training of the classification algorithm, we focused on the AIS with lumbar/thoracolumbar scoliosis, choosing a longitudinal database, including 30 adolescents, that was collected in [10], [17], presented in Table 4.2. Based on the results obtained from the first part of the present study (SO1), [17], [82], we defined the features using the lumbosacral (L5-S1) joint efforts during gait, associated the most with the spinal deformity i.e. ML force and torque and AP torque to feed the classification training algorithm.

Different supervised Machine Learning classification algorithms were run to achieve the model that provides the most accurate result to classify the severity of scoliosis, as explained in detail in chapter 6 (Article 2). The features used to feed the classification algorithms are presented in Table 4.3.

Table 4.2 Specification of the participants in SO2 and SO3 (Article 2 and Article 3)

	No.	**Age (y) mean (SD)**	**Weight (kg) mean (SD)**	**Height (m) mean (SD)**	**Cobb angle (°) (lumbar region) mean (SD)**
Mild scoliosis 10° < Cobb angle < 25°	9	14 (2)	45 (9)	1.58 (0.1)	20 (3)
Moderate scoliosis 25° < Cobb angle < 45	14	15 (2)	52 (8)	1.63 (0.08)	36 (4)
Severe scoliosis Cobb angle > 45°	7	16 (1)	53 (8)	1.67 (0.09)	52 (7)

Table 4.3 Features used to train the classification algorithms (SO2 and SO3 (Article 2))

NO.	**Features fed to classification algorithms**		
	Mediolateral force	**Anteroposterior torque**	**Mediolateral torque**
1	Maximum (|Maximum-mean|,|Minimum-mean|)		

2	Maximum (|Variance-mean|,|Variance+mean|)
3	Maximum (|Max|,|Min|)
4	|mean|
5	Standard deviation

To identify the value of the Cobb angle, the same database, presented in Table 4.2 was used, as explained in detail in chapter 7 (Article 3). The features fed to train the regression algorithms are presented in Table 4.4.

Table 4.4 Features to train the regression algorithms (SO3 (Article 3))

No.	**Features**		
	Mediolateral force	**Anteroposterior torque**	**Mediolateral torque**
1	Maximum (|Maximum-mean|, |Minimum-mean|)		
2	Maximum (|Variance-mean|, |Variance+mean|)		
3	Maximum (|Max|, |Min|)		
4	|mean|		
5	Standard deviation		
6	|Max-Min|		

To estimate the performance of algorithms on unseen data and in general due to the limited number of data, k-fold cross-validation was applied. The value of k refers to the number of groups that a dataset is to be split into. The value of k for both classification and regression was chosen based on the size of the dataset to give each test sample the opportunity of being used in the hold out dataset. Generally, a larger value of k leads to a decrease in the bias, since the difference in size between the training set and the resampling subsets gets smaller [90].

CHAPTER 5 ARTICLE 1: IDENTIFICATION OF THE MOST RELEVANT INTERVERTEBRAL EFFORT INDICATORS DURING GAIT OF ADOLESCENTS WITH IDIOPATHIC SCOLIOSIS

Samadi B [a, b], Raison M [a, b], Achiche S [a], Fortin C [c, d]

[a]*Department of Mechanical Engineering École Polytechnique de Montréal, Canada;* [b]*Technopole in Pediatric Rehabilitation Engineering, Sainte-Justine UHC, Montréal, Canada;* [c]*Research center CHU Sainte-Justine, Montréal, Canada,* [d]*School of Rehabilitation, Faculty of Medicine, Université de Montréal, Canada*

Journal of Computer Methods in Biomechanics and Biomedical Engineering. Submitted 05 November 2019; Accepted 16 April 2020, Published online 13 May 2020; doi: 10.1080/10255842.2020.1758075

5.1 Abstract

Introduction: The intervertebral efforts, i.e. forces and torques, during gait have been recognized as influencing the progression of scoliosis, due to the mechanical modulations according to the Hueter-Volkmann Law. Therefore, these efforts are key variables for posture correction and to control the progression of scoliosis. Using the intervertebral efforts during gait for the clinical follow-ups has never been performed. For this, it would be necessary to identify amongst all these efforts the most relevant ones, which is the objective of this study. **Methods:** A previously developed dynamical model of the human body was used to compute the 3D intervertebral efforts during the gait of 15 participants with adolescent idiopathic scoliosis (AIS) and 12 typically developed adolescents (TDA). Kolmogorov-Smirnov and Two-sample t-test were applied on the calculated intervertebral efforts and the graphs of intervertebral efforts were studied. **Results:** Anteroposterior (AP) forces and torques and mediolateral (ML) forces are the most relevant intervertebral efforts amongst the other efforts in adolescents with AIS during gait. **Discussion:** Gait analysis in adolescents with AIS based on the relevant intervertebral efforts could be an effective means to follow-up and evaluate the progression of scoliosis during their treatment period. **Conclusion:** This study highlights the most relevant intervertebral efforts of individuals with AIS during gait. As future work, the identified intervertebral efforts could be implemented

in a quantified and visual feedback tool for therapeutic and performance evaluation or interactive sessions in physiotherapy, e.g. via video games for dynamic posture self-correction.

Keywords: musculoskeletal model, Idiopathic Scoliosis, intervertebral efforts, visual feedback, gait pattern, inverse dynamics

5.2 Introduction

Adolescent idiopathic scoliosis (AIS) is a pathology characterized by a complex three-dimensional (3D) deformation of the spine and rib cage of 10 degrees or more, which is prevalent in 1-3% of the adolescents aged between 10 and 16 years [91]–[93]. The Trunk 3D deformities of the spine are referred to as any abnormality in the alignment or shape of the spine, which lead to posture asymmetries, asymmetric loading on the spine and disharmony during gait [94]. The repetitive asymmetric movements during gait may increase the deformity of the spine and affect the whole body structure, change the position and the performance of other organs in the body such as lungs and heart in more severe cases [95], [96]. Gait studies on AIS have shown the presence of asymmetry in kinematics and kinetics parameters such as reduced shoulder, hip and pelvis motion in frontal plane, hip motion in transversal plane and knee motion in the sagittal plane in adolescents with AIS compared to healthy controls [93], [97], [98]. Additionally, adolescents with AIS displayed reduced step length, stance phase, increased energy expenditure and changes in load distribution during gait [93], [97]–[99].

The true etiology and aggravation of the AIS mechanism remain unclear and are categorized widely as abnormalities at the genetic level, hormonal and central nervous system during growth [91].Thus, controlling the progression of scoliosis is the main challenge. It is well accepted that early clinical interventions help to control the progression of scoliosis and improve the functional performance of the AIS population in their daily motions [100]. Therefore, re-education of gait pattern is one of the therapeutic challenges in rehabilitation, as this movement is involved in the main daily activities.

Several studies [17], [81], [82], [101], [102] are consistent with the fact that intervertebral efforts i.e. the three components of forces and torques (Figure 5.1) are crucial variables for AIS gait analysis since they have a significant impact on the progression of the Cobb angle and spine deformity. According to the “Hueter-Volkmann Law” vertebral growth is slowed by mechanical

compression [103]. Additionally, the intervertebral efforts quantification is based on the kinematics, geometric and inertial parameters of the individuals with AIS, which are very sensitive to these parameters. Consequently, the quantification of the intervertebral efforts of the spine would provide an effective means for rehabilitation and instrumentation purposes in AIS.

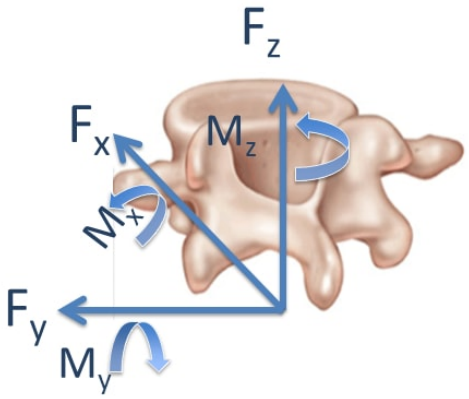

Figure 5.1 Directions of 3D efforts components on the vertebrae, F_x: Anteroposterior force, F_y: Mediolateral force, F_z: Vertical force, M_x: Anteroposterior torque, M_y: Mediolateral torque, M_z: Vertical torque.

Raison et al. (2008, 2012) developed a method to quantify the intervertebral efforts, enabling the reporting of different intervertebral efforts between a healthy adolescent and one with AIS, and that adolescent with AIS after arthrodesis [104], [105]. Furthermore, Yazji et al. (2015) demonstrated that there are differences in calculated intervertebral efforts between healthy and pre-operative individuals with AIS. However, following spinal surgery, these efforts were more similar between healthy and postoperative individuals with AIS [17]. In their model, Yazji et al., assumed that the spine 3D reconstruction is fixed during gait [17], however; spinal gait kinematics is a critical factor for adolescents with AIS [106]. Abedrabbo et al. (2012) quantified the efforts of L5-S1 of one adolescent with AIS by proposing a multibody biomechanical model based on kinematics and kinetics parameters and muscle activities [107]. Recently, Guilbert et al. (2019) developed a multibody model paired with the kinematics model of the spine to identify the intervertebral efforts in real-time of one healthy adolescent, and one with AIS [82]. They reported a higher amount of mediolateral force and torque in the adolescent with AIS compared

to the healthy one. They revealed that the pathological efforts are distributed along the spine and are not only concentrated around critical points [82].

These findings may help determine the effect of conservative treatment in AIS. Self-correction exercises used in specific physiotherapy approaches for scoliosis treatments showed promising results to momentarily correct or prevent scoliosis progression [108], [109]. Therefore, providing a therapeutic tool based on the intervertebral effort indicators would allow a better understanding of the effect of these exercises on the spine deformity and would have a strong potential of interest in the follow-up and control of the scoliosis progression.

To achieve this goal, one of the main problems is to identify the most relevant efforts, among the 90 possible indicators; i.e. 6 force and torque components in 15 levels of vertebrae (L3-L2 to T1-C7), a task that has never been carried out. These components are along the anteroposterior, mediolateral and vertical directions, which are referred to the walking direction (X-axis), the perpendicular direction to the walking direction (Y-axis) and the direction along the spine (Z-axis), respectively (Figure 5.1).

These efforts can show how they are distributed along the spine during gait when comparing adolescents with AIS and different curve types to typically developed adolescents (TDA). This could help to discern and evaluate the progression of scoliosis during their treatment periods.

Therefore, the objective of this study is to identify the most relevant indicators among the 3D intervertebral efforts along the spine (L3-L2 to T1-C7) between different curve types of AIS and TDA to be used as a follow-up for the scoliosis progression. The motivation is to enable the possibility of implementing these indicators in therapeutic and feedback tools for rehabilitation, such as virtual reality and visual feedback for posture self-correction, clinician guide and therapeutic follow-up in AIS.

5.3 Methods

5.3.1 Multibody model

This section briefly presents the multibody model used in this paper, called model hereafter, developed by Guilbert et al. (2019)[82]. This model quantifies the intervertebral efforts in real-time using the kinematics of the spine. It does not assume that the spine is fixed during gait,

enabling one to study the impact of spinal deformity on the produced efforts along the spine.

The model is composed of 25 rigid bodies (the lower limbs (6), pelvis (1) and spine (18)), as shown in Figure 5.2a. The Cartesian coordinates of the anatomical landmarks, and the ground reaction forces during gait were obtained in a motion laboratory equipped with a motion-capture system and force platforms, respectively. However, to compute the intervertebral efforts, the force platforms are not required, but they remain essential to obtain the lower limb efforts. To obtain the joint kinematics from recorded Cartesian coordinates, an inverse kinematics process using the Levenberg-Marquardt (LM) optimization algorithm developed by ALGLIB®[110] with a global optimization [111] was applied. The LM algorithm developed in the early 1960's to solve non-linear least square problems which combines the gradient descent and Gaussian-Newton minimization methods. This algorithm is an iterative procedure, acts more like a gradient-descent method when the parameters are far from their optimal value, and acts more like the Gauss-Newton method when the parameters are close to their optimal value (*Equation 5-2*) [112]. In the inverse kinematics, the error-damped factor of the LM method prevents the algorithm from escaping a local minimum [113]. It improves the convergence performance and the numerical accuracy and robustness of the optimization algorithm [114].

$$[J^T W J + \lambda I] h_{lm=} J^T W (y - \hat{y}) \qquad \textit{Equation 5-2}$$

Where J is the m×n Jacobian matrix, W is the weighting matrix, λ, is the damping parameter, I is the identity matrix, $h_{lm}$is the parameter update of Levenberg-Marquardt optimization algorithm, y is the measured data, $\hat{y}$ is the predicted value for y.

The efforts, i.e. forces and torques between each vertebra based on a dynamical equation system (inverse dynamics) were then computed from a Newton-Euler equation (*Equation 5-3*). To generate the symbolic equations, Robotran software was used [115] (Figure 5.2.a.).

$$Q = f(q, \dot{q}, \ddot{q}, F_{ext}, g) \qquad \textit{Equation 5-3}$$

Where Q is the forces and torques between each vertebra, q is the joint angles, $\dot{q}$ is the joint speeds, $\ddot{q}$ is the joint accelerations, F_{ext} is the external forces and g is the gravity. Six components of efforts, i.e. three forces (N/kg) and three torques (Nm/kg), are computed in the anteroposterior (AP), mediolateral (ML) and vertical (V) directions (Figure 5.1 and Figure 5.2.b).

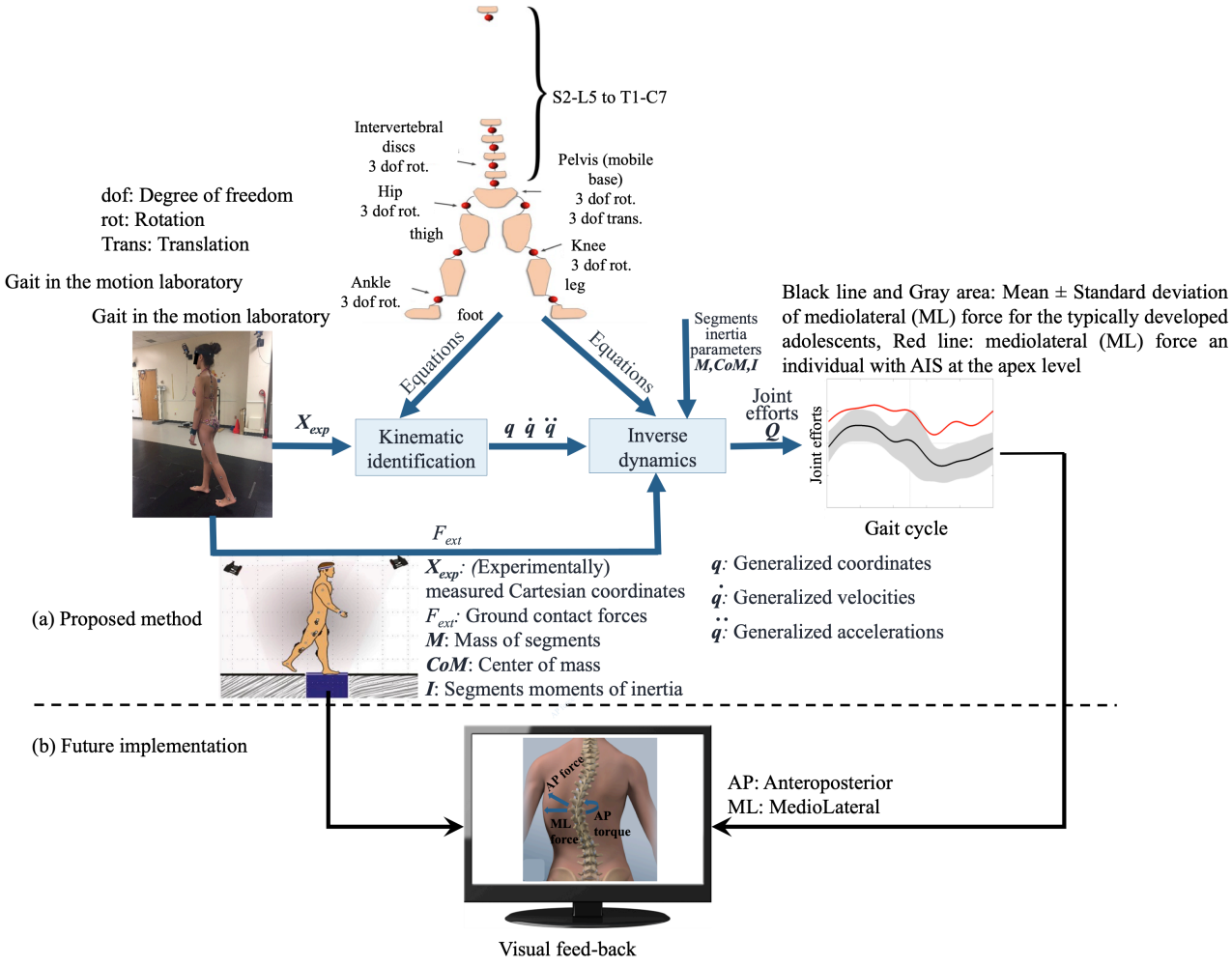

Figure 5.2 (a) The proposed method and the fundamental of inverse dynamics to quantify the efforts in the multibody model of the human body [116], [117] (b) The future motivation of the proposed method.

5.3.1.1 Equipment and measurements

The participants were asked to walk with their own preferred pace without targeting their steps in a motion lab. The motion lab was equipped with 12 cameras (Vicon, UK) to capture the movements and three separate force platforms (AMTI, USA) embedded in the floor in the middle of the walkway in the lab to measure the applied ground reaction forces to each foot. Data from one complete cycle was retained for this study. The cycle started when the first foot hit the first platform and ended at the last frame before the same foot hit the floor for the second time.

5.3.1.2 Data collection procedure

To perform the data collection procedure, 15 adolescents with AIS (5 males, mean (SD)- age: 14.1 y (±1.3) (range: 12-16 years), weight: 48.9 kg (±9.4), height: 1.60 m (±0.1) and 12 TDA as the control group (5 males, mean (SD) age: 13.4 y (±1.8) (range: 11-16 years), weight: 44.4 kg (±13), height: 1.55m (±0.10) were recruited in this study. The AIS group included six thoracic, six lumbar/thoracolumbar and three double curve types, with a Cobb angle between 12 to 37 degrees (mean(±SD): 26 (±7)). Inclusion criteria: the participants with AIS with a Cobb angle of more than 10 degrees and fewer than 50 degrees were recruited. The healthy participants with less than 5 degrees of trunk asymmetry measured by the scoliometer [118] and without any neuro-musculoskeletal conditions were included. All of the participants/parents signed the written consent approved by the research ethics committee of Sainte-Justine University Hospital Centre (UHC) prior to the test.

5.3.1.3 Data analysis

For each participant, the model is customized with the measurements taken by a physiotherapist prior to the data collection. These measurements include mass, height, foot length, knee and ankle width. The centre of rotation of each articulation is then calculated on the basis of Davis III's model [119]. The body and vertebrae inertia parameters were obtained from de Leva's table [120] and Kiefer et al. [121], respectively.

All data were synchronized at 100 Hz and were fed to a C++ real-time routine [116] to calculate the intervertebral forces and torques along the spine. The duration of the gait cycle was normalized between 0 and 100 and the efforts were normalized to the body weight to have the

same scale for all of the participants. To verify the normality of the distribution of 3D intervertebral efforts, i.e. to compare the curve pattern of each intervertebral effort during a complete gait cycle, a Kolmogorov-Smirnov (K-S) test [122] was performed. The K-S is sensitive to differences in both location and shape of the empirical cumulative distribution functions of the two samples. We compared the components of efforts of each adolescent with AIS at the apex level (the vertebra with the greatest rotation or farthest deviation from the center of the spine, shown in Figure 5.3) to the average efforts of TDA. After testing the equality of the variances on the intervertebral efforts at the apex level, to compare the means during a gait cycle, a t-test [123] was applied. For each participant with AIS, we obtained the mean during one gait cycle, which is continuous data. For the TDA group, first we obtained the mean of each gait cycle for each participant and then we calculated the mean of the group. Finally, we performed a t-test comparing the mean of one gait cycle (continues data) for each participant with AIS and the mean of the TDA. The reason behind applying both K-S and t-test is that the position of the major curve on the spine influences the trunk kinematics parameters leading to asymmetrical trunk movements [124], [125], which affects their gait pattern. Therefore, considering only the means during the gait cannot be representative of the whole duration of a cycle and all types of scoliosis.

Visual analysis plays an important role in exploring, analyzing and presenting data, detecting the expected and discovering the unexpected results [126]. Therefore, to visually analyze the curve pattern of the intervertebral efforts, we compared the graphs of the intervertebral efforts for each individual with AIS i.e. forces and torques along the three axes, with the graphs of average ±standard deviation of the same efforts of TDA during one gait cycle. To enhance the understanding of the impact of spinal deformity on the pattern of the intervertebral efforts curves, the radiography of the spine of each participant with AIS is provided.

5.4 Results

The obtained *p*-values applying t-test and Kolmogorov-Smirnov to compare the differences between each participant with AIS and average of TDA are presented in Table 5.1. The parameters with the *p*-value less than 0.05 are considered as the ones with the significant differences between the adolescents with AIS and TDA.

Table 5.5 *P*-value for t-test and Kolmogorov-Smirnov (K-S) test of the 3D forces and torques of AIS at the apex level and mean of TDA

	P-value					
	Anteroposterior Force (line 1) Torque (line 2)		**Mediolateral Force (line 1) Torque (line 2)**		**Vertical Force (line 1) Torque (line 2)**	
Participants (P) with AIS (type)	t-test	K-S test	t-test	K-S test	t-test	K-S test
P1	0.000	0.000	0.000	0.000	0.241	0.000
(Thoracic)	0.066	0.069	0.481	0.005	0.000	0.000
P2	0.000	0.000	0.000	0.000	0.536	0.344
(Thoracic)	0.020	0.000	0.000	0.000	0.448	0.005
P3	0.004	0.008	0.000	0.000	0.014	0.013
(Thoracic)	0.000	0.000	0.000	0.000	0.000	0.000
P4	0.000	0.000	0.000	0.000	0.872	0.794
(Thoracic)	0.001	0.000	0.000	0.000	0.905	0.193
P5	0.000	0.000	0.000	0.000	0.600	0.314
(Thoracic)	0.000	0.000	0.004	0.005	0.982	0.000
P6	0.000	0.000	0.000	0.000	0.034	0.000
(Lumbar)	0.000	0.000	0.472	0.005	0.139	0.099
P7	0.000	0.000	0.000	0.000	0.000	0.000
(Lumbar)	0.000	0.000	0.935	0.001	0.717	0.021
P8	0.000	0.000	0.650	0.047	0.202	0.000
(Thoracolumbar)	0.000	0.000	0.169	0.193	0.000	0.000
P 9	0.000	0.000	0.036	0.003	0.066	0.069
(Thoracolumbar)	0.000	0.000	0.415	0.008	0.000	0.000

P10	0.001	0.003	0.000	0.000	0.000	0.000
(Thoracolumbar)	0.000	0.000	0.000	0.000	0.000	0.0000
P11	0.000	0.031	0.000	0.000	0.000	0.000
(Thoracolumbar)	0.000	0.000	0.001	0.001	0.018	0.000
P12	0.000	0.000	0.000	0.000	0.000	0.000
(Thoracolumbar)	0.424	0.099	0.448	0.069	0.147	0.000
P13	0.000	0.000	0.000	0.000	0.294	0.013
(Double)	0.000	0.000	0.039	0.047	0.029	0.047
P14	0.000	0.000	0.000	0.000	0.028	0.000
(Double)	0.000	0.000	0.094	0,001	0.000	0.000
P15	0.000	0.000	0.002	0.000	0.531	0.140
(Double)	0.000	0.000	0.000	0.000	0.461	0.008

Table 5.6 is the summary of Table 5.5 showing the intervertebral efforts with significant differences in distribution and average comparing the entire two groups included in this study. As seen, all of the intervertebral efforts show significant differences in terms of distribution and significant differences of AP forces and torques and ML forces in terms of means comparing the efforts during one complete gait cycle.

Table 5.6 Kolmogorov-Smirnov (K-S) test and t-test results of intervertebral efforts of all participants with AIS

Test **Efforts (Apex)**	**Kolmogorov-Smirnov**	**Two sample t-test**
Anteroposterior force	Significant difference in distribution	Significant difference between the means
Mediolateral force	Significant difference in distribution	Significant difference between the means
Vertical force	Significant difference in distribution (< 68%)	No significant difference between the means (< 68%)
Anteroposterior torque	Significant difference in distribution	Significant difference between the means
Mediolateral torque	Significant difference in distribution	No significant difference between the means (< 68%)

Vertical torque	Significant difference in distribution	No significant difference between the means (< 68%)

Figure 5.3. a to f show the intervertebral efforts i.e. ML, AP and V forces and ML, AP and V torques respectively, of one individual with thoracic scoliosis chosen as a sample, along the spine and the mean ± SD of TDA. As demonstrated, black curves and gray areas indicate the mean ± standard deviation related to intervertebral forces/torques of TDA, blue curves are related to the intervertebral forces/torques of AIS along the spine and red curves show the forces/torques of the AIS at the apex level. These figures present the impact of spinal deformity and spine right or left curve on the intervertebral efforts curve pattern of the adolescents with AIS. Figure 5.4 is the enlargement of Figure 5.3 at the apex level and one level higher and lower than it the apex level.

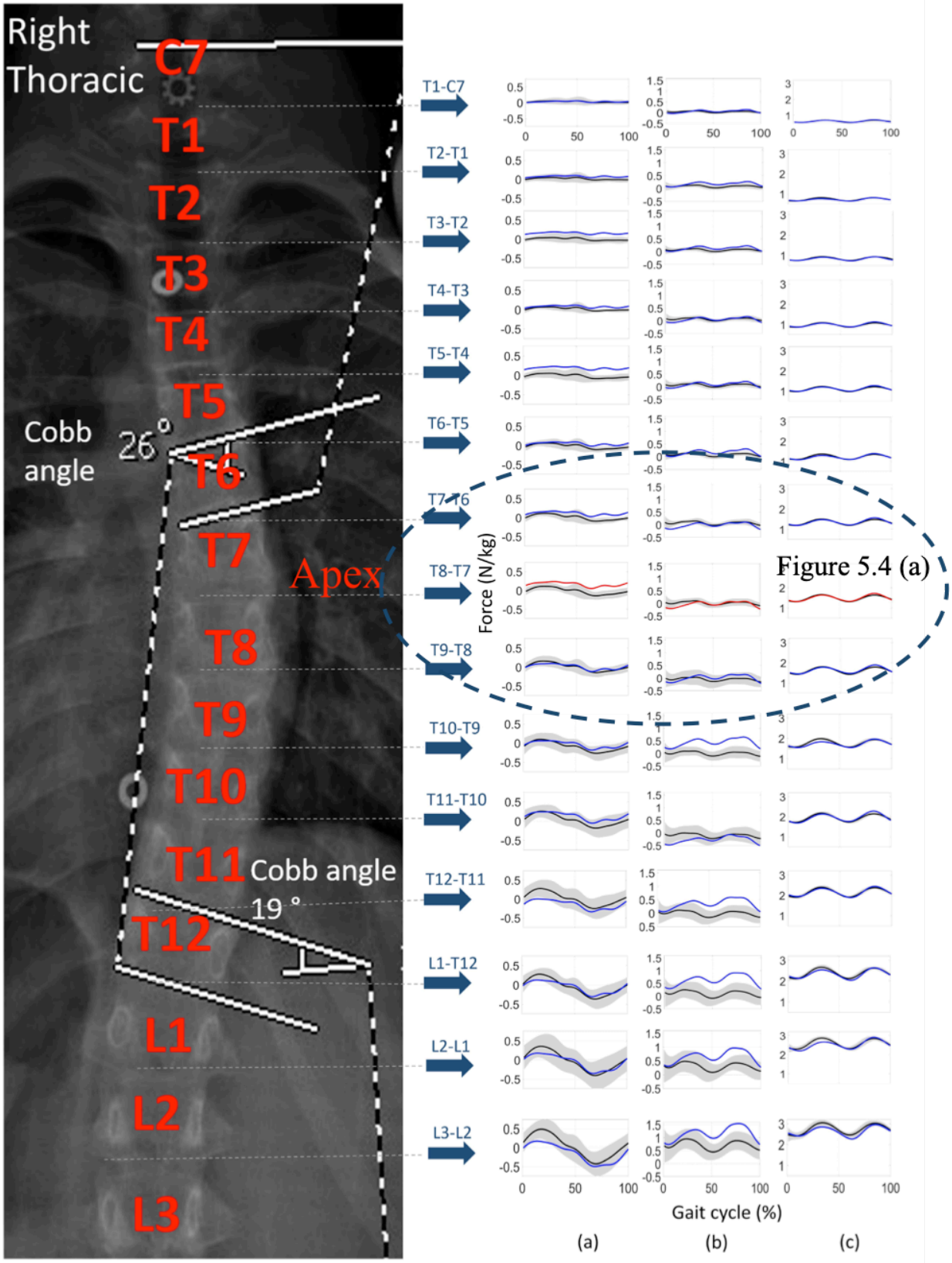
Right
Thoracic
C7
T1
T2
T3
T4
T5
Cobb
angle
26°
T6
T7
Apex
T8
T9
T10
T11
Cobb angle
19°
T12
L1
L2
L3
T1-C7
T2-T1
T3-T2
T4-T3
T5-T4
T6-T5
T7-T6
T8-T7
T9-T8
T10-T9
T11-T10
T12-T11
L1-T12
L2-L1
L3-L2
Force (N/kg)
Gait cycle (%)
(a)
(b)
(c)

Figure 5.4 (a)

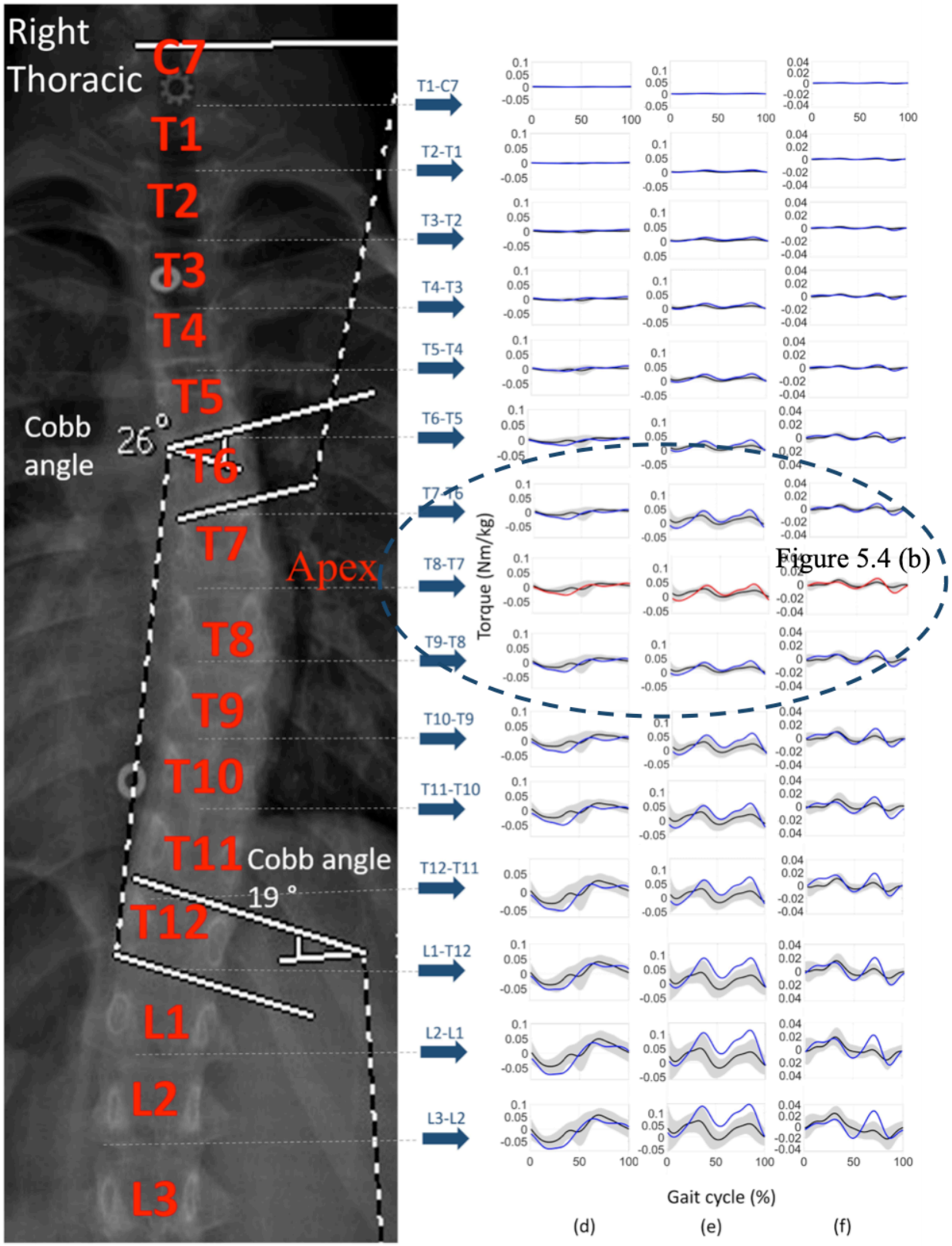
Right
Thoracic
C7
T1
T2
T3
T4
T5
Cobb
angle
26°
T6
T7
Apex
T8
T9
T10
T11
Cobb angle
19°
T12
L1
L2
L3
T1-C7
T2-T1
T3-T2
T4-T3
T5-T4
T6-T5
T7-T6
T8-T7
T9-T8
T10-T9
T11-T10
T12-T11
L1-T12
L2-L1
L3-L2
Torque (Nm/kg)
Gait cycle (%)
(d)
(e)
(f)

Figure 5.4 (b)

Figure 5.3 Above, left to right: a. mediolateral (ML), b. anteroposterior (AP) and c. vertical (V) force along the spine (N/kg). Below, left to right: d. anteroposterior, e. mediolateral and f. vertical torque along the spine (Nm/kg). Black line and Gray area: Mean ± Standard deviation for the typically developed adolescents, Blue line: An individual with thoracic idiopathic scoliosis, Red line: An individual with thoracic idiopathic scoliosis at the apex level.

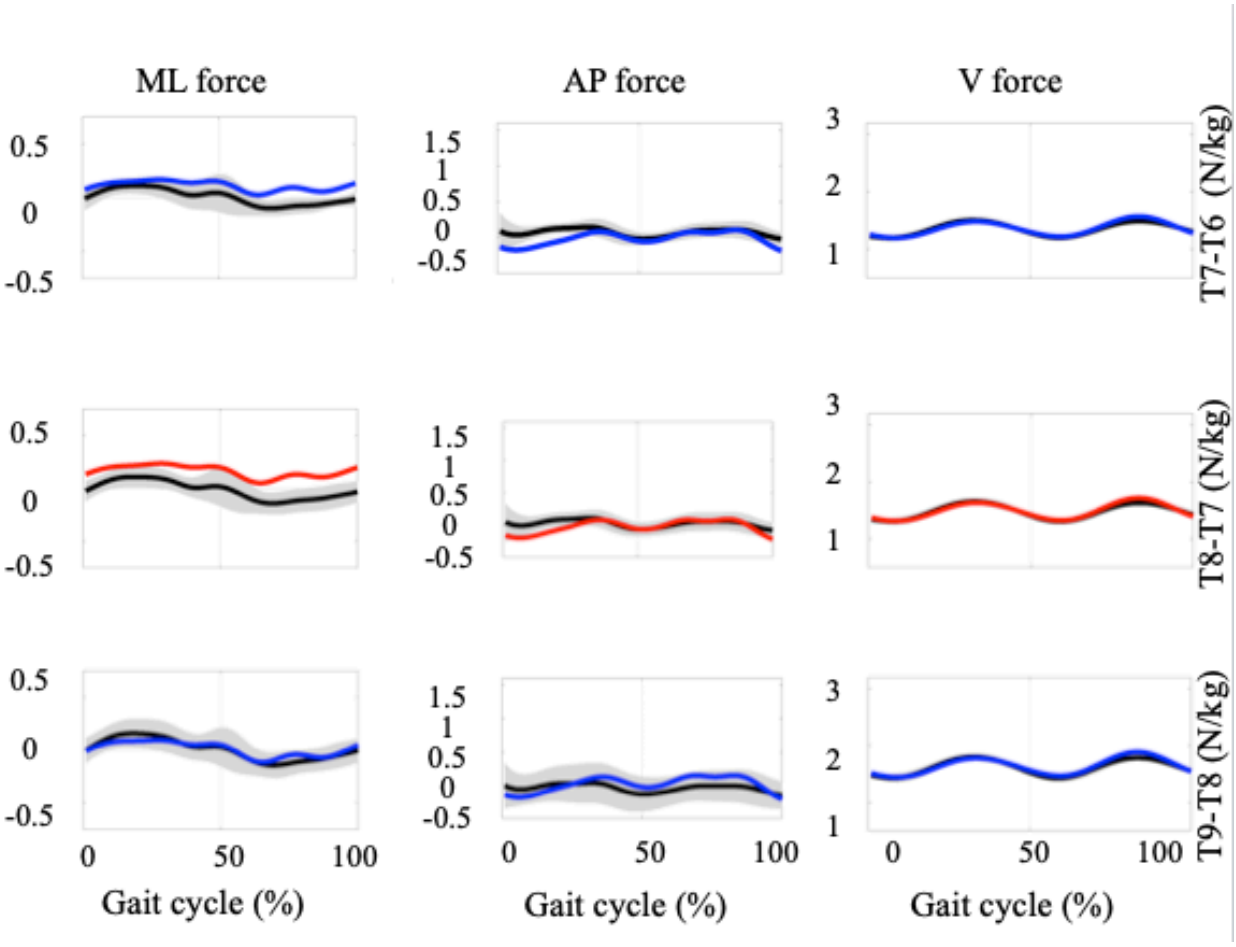

a. b. c.

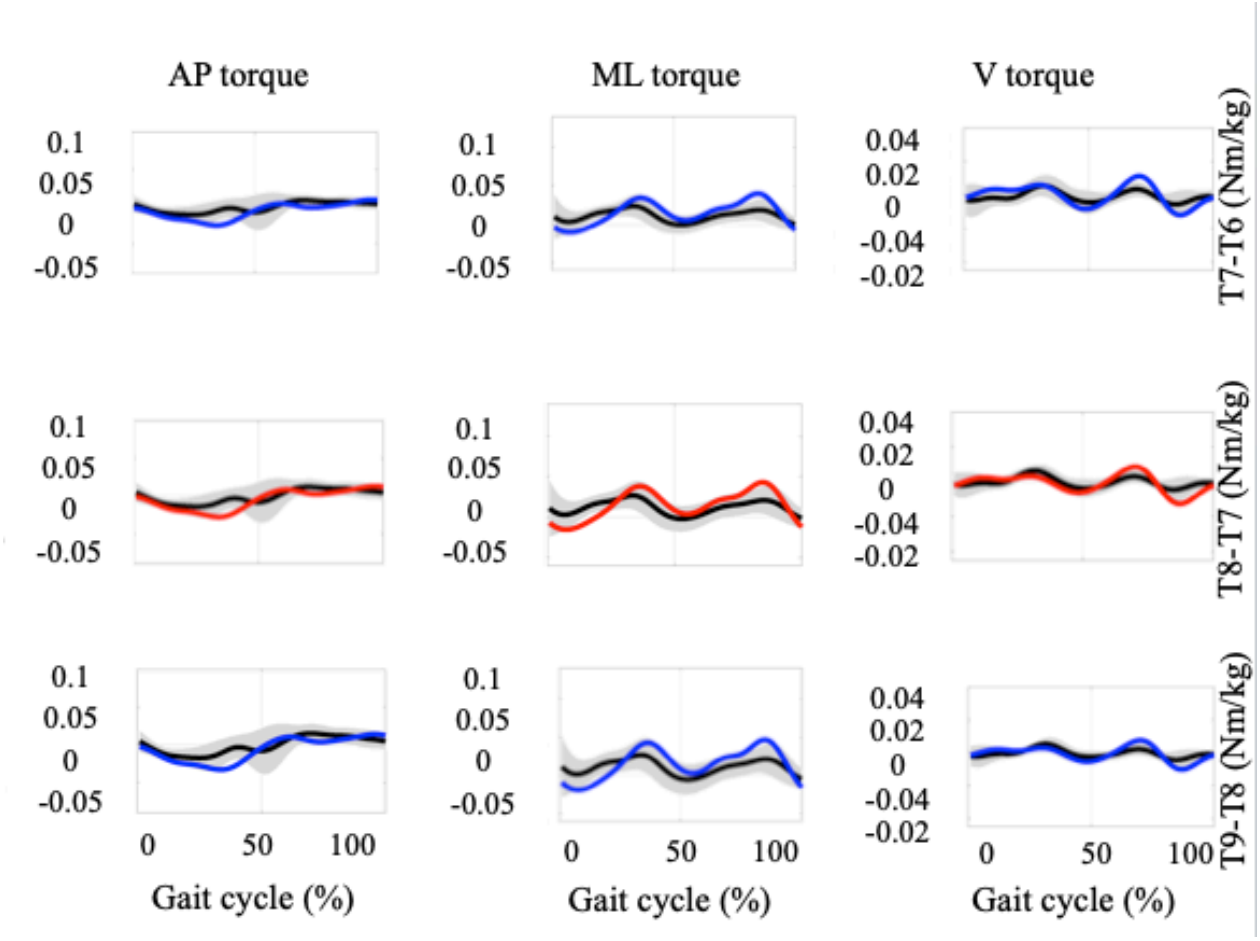

Figure 5.4 Enlargement of Figure 5.3 in the level of apex (above) Above left to right: a. ML, b. AP and c. V force along the spine (N/kg). Below, left to right: d. AP, e. ML and f. V torque along the spine (Nm/kg). Black line and Gray area: Mean ± Standard deviation for the typically developed adolescents, Blue line: An individual with thoracic idiopathic scoliosis, Red line: An individual with thoracic idiopathic scoliosis at the apex level.

To compare the differences and similarities in participants with different types of AIS to the mean of TDA, Figure 5.5a to f present the graphs of ML force and AP torque of one thoracic, one lumbar and one double scoliosis, respectively. The curves of the intervertebral efforts show different patterns compared to the TDA during walking.

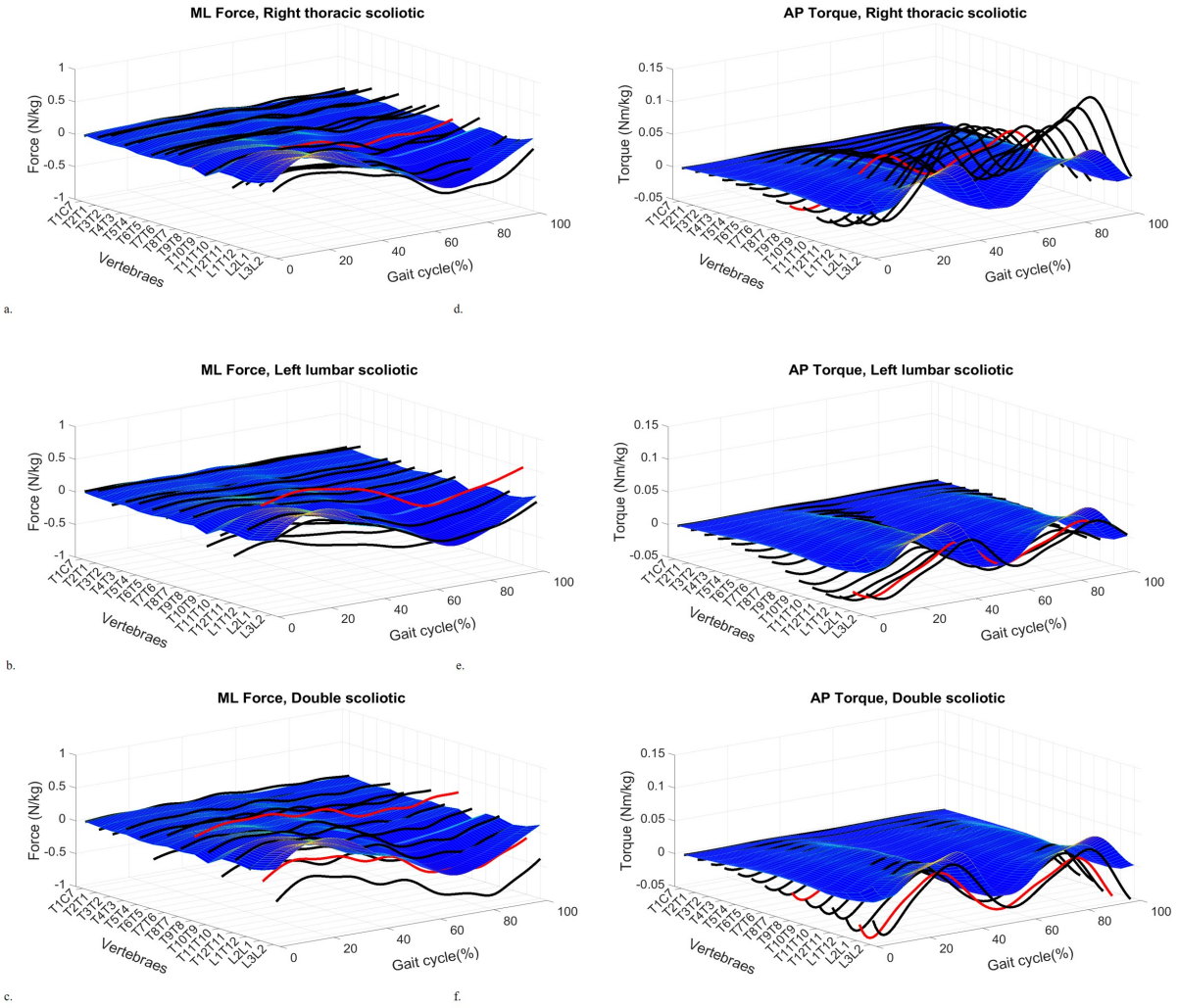

Figure 5.5 Mediolateral force of a. thoracic scoliosis, b. lumbar scoliosis, c. double scoliosis, and anteroposterior torque of d. thoracic scoliosis, e. lumbar scoliosis f. double scoliosis. Black/ Red line: The intervertebral efforts of an adolescent with AIS: along the spine / at the apex level, Blue area: The mean of intervertebral efforts of TDA group

5.5 Discussion

The objective of this study was to identify the most relevant intervertebral efforts as indicators during gait of adolescents with idiopathic scoliosis. The participants recruited in this study were chosen from all types of AIS (i.e. thoracic, lumbar/thoracolumbar and double scoliosis) and a

wide range of severity, since to our knowledge there is no study that compared the intervertebral efforts along the spine for all types of AIS. In the literature there are comprehensive studies on lumbosacral joint efforts during gait in lumbar/thoracolumbar AIS as presented in [17], [81], [127] but not other types. Comparing one gait cycle of the adolescents with AIS and mean of TDA demonstrates that the distribution of all efforts except the vertical force and the mean of AP and ML force and AP torque respectively, differ significantly between these two groups (Table 5.1 and 5.2).

Figure 5.3a. illustrates the ML force along the spine during one gait cycle of an adolescent with AIS. This could be observed that the ML force curve of the individual with AIS is out of the ±SD area of the mean of TDA when there is a curvature between the two adjacent vertebrae. For instance, at the apex level, it is fully out of the ±SD area of the mean of TDA. However, the curvature side of the spine, i.e. right or left curvature seems to make the AIS ML force curve shift to the top or below the mean TDA of ML force curve, respectively. The ML force is the lateral force on the spine, which is perpendicular to the walking direction. It could be explained by the greater muscle activity found on the convex side of the spine compared to the concave side [33][32] and it confirms the necessity of 3D correction of the spine to decrease the asymmetry as proposed in physiotherapeutic scoliosis-specific exercises approaches [100], [108], [109] .

The graph of AP force (Figure 5.3b) shows that the differences are eventually more in the lower part (L2 to T9) of the spine than the upper part. It could be due to the multifidus muscle function that stabilizes the lumbar spine [129]. This may also explain the higher amount of energy use found during gait in adolescents with thoracolumbar or lumbar curves compared to controls [130].

Figure 5.3c exhibits that the spinal deformity does not influence the vertical force during gait. It could be explained by the correlation between the vertical force to the mass of the participants [131], [132]. The average weight among the two groups has similar values (mean weight (SD): adolescents with AIS: 48.9 kg (±9.4), TDA: 44.4 kg (±13)), therefore it could explain the similarity of the curve pattern of vertical force between adolescents with AIS and TDA. The same results could be noticed in Figures 5.3d and 5.3f, i.e. the graphs of ML torque and V torque. They look similar when comparing the scoliosis and the healthy spine. However, they differ at the lower part of the spine. In terms of AP torque curves (Fig. 5.3e), the scoliosis spine has an

impact on the curve pattern and the AP torque curve of the participants with AIS is mostly out of the ±SD area of the mean of TDA. It seems that by studying the graphs of intervertebral efforts, similar results to the statistical tests could be obtained, i.e. the ML and AP forces and AP torque are the most relevant ones, compared to the rest to be used as indicators for treatment purposes.

These findings are similar to the results reported by Guilbert et al. (2019)[82] and Raison et al. (2008) tested on only two individuals [105], whereas the current study includes a larger population to validate the previous studies.

There are also differences in curve patterns observed in the graphs among the individuals with different scoliosis types due to the dissimilarity of spinal deformity as shown in Figure 5.5a-f. For instance, in thoracic scoliosis, the curve of ML force at the apex (Figure 5.5a) is partly below and partly above the mean TDA curve. In lumbar scoliosis, the curve of ML force (Figure 5.5b) is above the curve of mean TDA. In the double scoliosis (Figure 5.5c) at the apex level of the lumbar part of the spine, the ML force curve is below the curve of the mean TDA and at the thoracic part of the spine, the curve of ML force is above of the mean TDA curve. In terms of AP torque, for thoracic scoliosis (Figure 5.5d), all curves are above the mean TDA curve. However, in lumbar (Figure 5.5e) and double scoliosis (Figure 5.5f), the curves are mostly under the mean TDA curves. Fuji et al. (2007) also reported that, the thoracic scoliosis produces more movement in rotation than the lumbar scoliosis [133].

Studies also show that adolescents with AIS have different gait patterns compared to the TDA [97], [134], [135]. This may be due to the type and severity of the scoliosis creating different impacts on trunk kinematics parameters during gait [136], [137]. This difference is also due to the sensitivity of the intervertebral efforts to the kinematics parameters [104], [134], [138]. Syczewska et al. (2006) showed that scoliosis changes body orientation and mechanics of the pelvis at least in one plane [98]. These indicators can be implemented in a biofeedback tool. Therefore, it may help clinicians to optimize their treatments by providing feedback while undertaking the manual posture correction, i.e. they would be able to visualize the impact of their treatment on the intervertebral efforts and consider different strategies for adolescents with AIS according to their type or severity of the scoliosis [100].

5.6 Conclusion

The objective of this study was to identify the most relevant intervertebral effort indicators during the gait of adolescents with AIS. The main results showed ML forces and AP forces and torques (Figure 5.3b) are the most relevant indicators to be used as a therapeutic tool due to their significant differences when compared to the typically developed adolescents. It is worth noting that, due to the differences between the intervertebral efforts among different scoliosis types (Figure 5.5 a-f); the strategies for their treatment should be personalized based on the scoliosis classification. Therefore, these efforts are essential variables for posture correction and may be useful to monitor scoliosis progression when comparing to typically developed adolescents as the reference. In fact, the proposed method could be used as an evaluation tool to assess the efficiency of the treatments during the specific time interval while the patients follow the treatment process.

As future work, the identified intervertebral efforts could be implemented in a quantified and visual feedback tool in a virtual reality environment such as GRAIL[139] for clinical evaluation or interactive sessions in physiotherapy, e.g. via video games for posture self-correction. For example, this could be carried out, during gait, presenting the graphs of intervertebral efforts indicators in real-time, considering the mean ± SD of efforts of the healthy individuals as the reference for the clinicians. The patients would adapt their posture during gait with visual feedback and aid of the physiotherapist, as shown schematically in figure 52.b. This should make the treatment sessions more interactive and interesting to follow for the individuals and for avoiding repetitive and incorrect exercises.

Acknowledgements

Funding: This work has been supported by the Interactive Technologies of Engineering in Rehabilitation (INTER) program of the Fonds de Recherche du Québec – Nature et Technologies (FRQNT). B. Samadi is supported by a scholarship of the Fonds de Recherche du Québec – Nature et Technologies (FRQNT). C. Fortin is currently supported by a Fonds de Recherche du Québec – Santé (FRQS) Junior 1 salary award. The authors would like to thank Jean-François

Aubin-Fournier, Samuel Clark and Karl Chemali for their assistance in data collection as well as Soraya Barchi for recruiting participants and the participants.

CHAPTER 6 ARTICLE 2: CLASSIFICATION OF THE SEVERITY OF SPINE DEFORMATION IN ADOLESCENTS WITH IDIOPATHIC SCOLIOSIS USING MACHINE LEARNING ALGORITHMS BASED ON LUMBOSACRAL JOINT EFFORTS DURING GAIT

Bahare Samadi [a, b], Maxime Raison [a, b], Philippe Mahaudens [c,d], Christine Detrembleur [d], Sofiane Achiche [a]

[a]Department of Mechanical Engineering Polytechnique Montréal, Canada; [b] Technopole in Pediatric Rehabilitation Engineering, Sainte-Justine UHC, Montreal, Canada; [c] Cliniques Universitaires Saint-Luc, Service d'Orthopédie et de Traumatologie de l'Appareil Locomoteur, Brussels, Belgium ; [d] Université catholique de Louvain, Secteur des Sciences de la Santé, Institut de Recherche Expérimentale et Clinique, *Neuro Musculo Skeletal Lab (NMSK),* Brussels, Belgium

European Spine Journal. Submitted on 16 January 2021

6.1 Abstract

Introduction: To assess the severity and progression of adolescents with idiopathic scoliosis (AIS), radiography with X-rays is usually used. The methods based on statistical observations have been developed from 3D reconstruction of the trunk or from topography. Machine Learning has shown great potential to classify the severity of scoliosis on imaging data, generally X-ray measurements. However, it is also known that AIS leads to the development of gait disorder. To our knowledge, Machine Learning has never been tested on spine intervertebral efforts during gait as a radiation-free method to classify the severity of spinal deformity in this clinical population. **Purpose:** Develop automated Machine Learning algorithms to classify the severity of spinal deformity on AIS based on the lumbosacral joint (L5-S1) efforts during gait. **Methods:** The lumbosacral joint efforts of 30 individuals with AIS were used as distinctive features fed to the Machine Learning algorithms. Several tests were run using various classification algorithms. The labeling consisted of three classes reflecting the severity of scoliosis using the Cobb angle (10° to 25° Cobb angle, 25° to 45° Cobb angle and more than 45° Cobb angle) performing six

walking cycles. **Results:** The ensemble classifier algorithm including K-nearest neighbours, support vector machine, random forest and multilayer perceptron, and a Neural Networks model achieved the most promising results, with accuracy scores of 91.4% and 93.6%, respectively. **Conclusion:** This study shows lumbosacral joint efforts can be used to classify the severity of spinal deformation in AIS. This algorithm can be used as an assessment tool to follow-up the progression of AIS as a radiation-free method, alternative to the X-ray radiography.

Key Words: Idiopathic scoliosis, Cobb angle, Radiation-free scoliosis assessment, Machine Learning classification algorithms, Gait analysis, Lumbosacral joint efforts.

6.2 Introduction

Adolescent idiopathic scoliosis (AIS) is a progressive spinal growth disease resulting in the occurrence of one or more coronal curvatures of the spine exhibiting a Cobb angle equal to or greater than 10° with spinal rotation [141], [142]. It affects up to 4% of schoolchildren worldwide [142] without any known etiology. The Lenke classification has been created to group similar curves into clusters enabling appropriate treatment recommendations and allowing comparison of different treatment strategies [1]. These curves are classified by their location along the spine and the magnitude of the coronal deviation of the curve which is expressed by the Cobb angle as the gold standard to evaluate AIS [6].

To support physicians and surgeons to follow-up and evaluate the progression of spinal deformation more accurately and efficiently, patients are monitored with large a series of radiographs i.e. at least every six months, during their growth years [143]. However, these cumulative roentgenograms represent a real risk of increase in organ carcinogenic due to x-ray radiation as reported in [144], [145]. For this reason, and due to the three-dimensional (3D) deformation of the spine in AIS, many researchers have tried to develop alternative methods to evaluate the severity of the deformation in a radiation-free manner as a robust follow-up tool. Up until now, mainly optical surface measurement systems have been developed based on static 3D models of the spine. Adankon *et al.* [146] showed that it was possible to perform follow-ups on AIS patients using 3-D trunk image analysis combined with a genetic algorithm. Tabard-Fougère

et al. [147] introduced rasterstereography as an automatic, fast, and system capable of monitoring the progression of AIS with an acceptable validity compared to X-Rays. Liu *et al.* [148] used the Quantec spinal image system to quantify and classify the spinal deformity. Weisz *et al.* [149] used the integrated shape imaging system (ISIS), a surface shaped method capable of identifying the curve growth of the spine. However, the results obtained from these mentioned research works reported prediction accuracy levels ranging from 63.5% to 87.5%.

In [75], a support vector machine (SVM) classifier assessed the severity of idiopathic scoliosis (AIS) based on surface topographic images of human backs with the accuracy of between 69% to 85%. Seoud *et al.* [150] proposed a semi-supervised classifier algorithm with an accuracy of 87% to predict the scoliosis curve types. More recently (2019), Roy et al. [151] presented an ionizing radiation- free method to estimate the trajectory of the spine with good results in the estimations of the lateral deviation of the spine for mild and moderate scoliosis. However, their proposed method was not intended to replace the X-ray radiography, but as complimentary to X-ray images.

Most measurement techniques are only applied for a static posture of the patient and based on the trunk surface images. However, it is known that AIS also affects spino-pelvic mobility and can consequently modify human locomotion [10]. Therefore, it seems promising to investigate the impact of scoliosis severity on gait patterns. To our knowledge, very few studies have investigated the effect of scoliosis on walking ability, which is a prior effect of AIS. Two studies [127], [152] evaluated the impact of brace wearing on gait in AIS, respectively on the very short term and on the long term. In both cases, the quality of frontal pelvis and hip motion were affected. Another study [10] analyzed the effect of scoliosis and scoliosis severity on kinematic and electromyographic (EMG) gait variables, compared to an able-bodied population. Scoliosis patients showed significant but slight modifications in gait, the pelvic frontal motion being reduced, as was the motion in the hips and shoulder. Similarly, a comparison of lumbosacral joints efforts during gait was made between healthy and individuals with scoliosis [81]. Participants with severe idiopathic scoliosis presented higher mobility resulting in higher joint efforts at the lumbosacral level than healthy adolescents, i.e. the lumbosacral joint is the most mobile part of the spine during gait [10], [81]. Two recent studies (2019 and 2020) [78], [82] by Guilbert *et al.* and Samadi *et al.*, respectively, presented the differences of intervertebral efforts along the spine by comparing adolescents with AIS and typically developed ones. All these

studies attest to the major impact of AIS on mobility; therefore, dynamical intervertebral efforts acting between vertebrae are affected by the spinal deformity.

Therefore, in this paper, we propose a radiation-free method, based on the lumbosacral joint efforts during gait, which uses Machine Learning algorithms to classify the individuals with AIS with different curve severity without the need for image or topography of patients' bodies.

6.3 Materials and methods

6.3.1 Patient samples and data acquisition

The gold standard mean to define the severity and progression of scoliosis is measuring the Cobb angle. Therefore, we considered it as the parameter to identify the severity of scoliosis. The data set used in this paper as longitudinal data was obtained from a previous study conducted in [10] which has been collected and tracked since 2009. A total of 30 individuals with similar location of spine curvature (Lenke 5-6 [1]: main thoracolumbar/lumbar curves) with no spine surgery were included in this study. Thirty individuals in three different classes in terms of severity of the spinal deformity i.e. mild scoliosis (10° < Cobb angle < 25°), moderate scoliosis (25° < Cobb angle < 45°) and severe scoliosis (Cobb angle > 45°) as shown in Table 6-1 participated in this study. The dataset includes six successive gait cycles on a treadmill for each participant.

Table 6.1 Specification of participants

	Mild scoliosis	**Moderate scoliosis**	**Severe scoliosis**
Number	9	14	7
Age, years mean(SD)	14(2)	15(2)	16 (1)
Weight, kg mean(SD)	45(9)	52 (8)	53 (8)
Height, cm mean(SD)	158(10)	163 (8)	167 (9)

This study takes ground on a precedent study [17] that evaluated intervertebral joints efforts by inverse dynamics. These efforts were determined as features for the learning algorithm. The participants were asked to walk at 4 km/h on an instrumented treadmill in a motion lab with reflective markers attached to their skin on different anatomical joints of their body during gait. A motion capture system composed of optokinetic sensors measured the kinematics of 26 anatomical landmarks, and a treadmill equipped with force sensors measured the ground reaction forces (GRF) applied to each foot. The intervertebral forces and torques in the lumbosacral joint were calculated using a dedicated three-dimensional or inverse dynamics model of the human body, through ROBOTRAN software [17], [88] as shown in Figure 6.1.

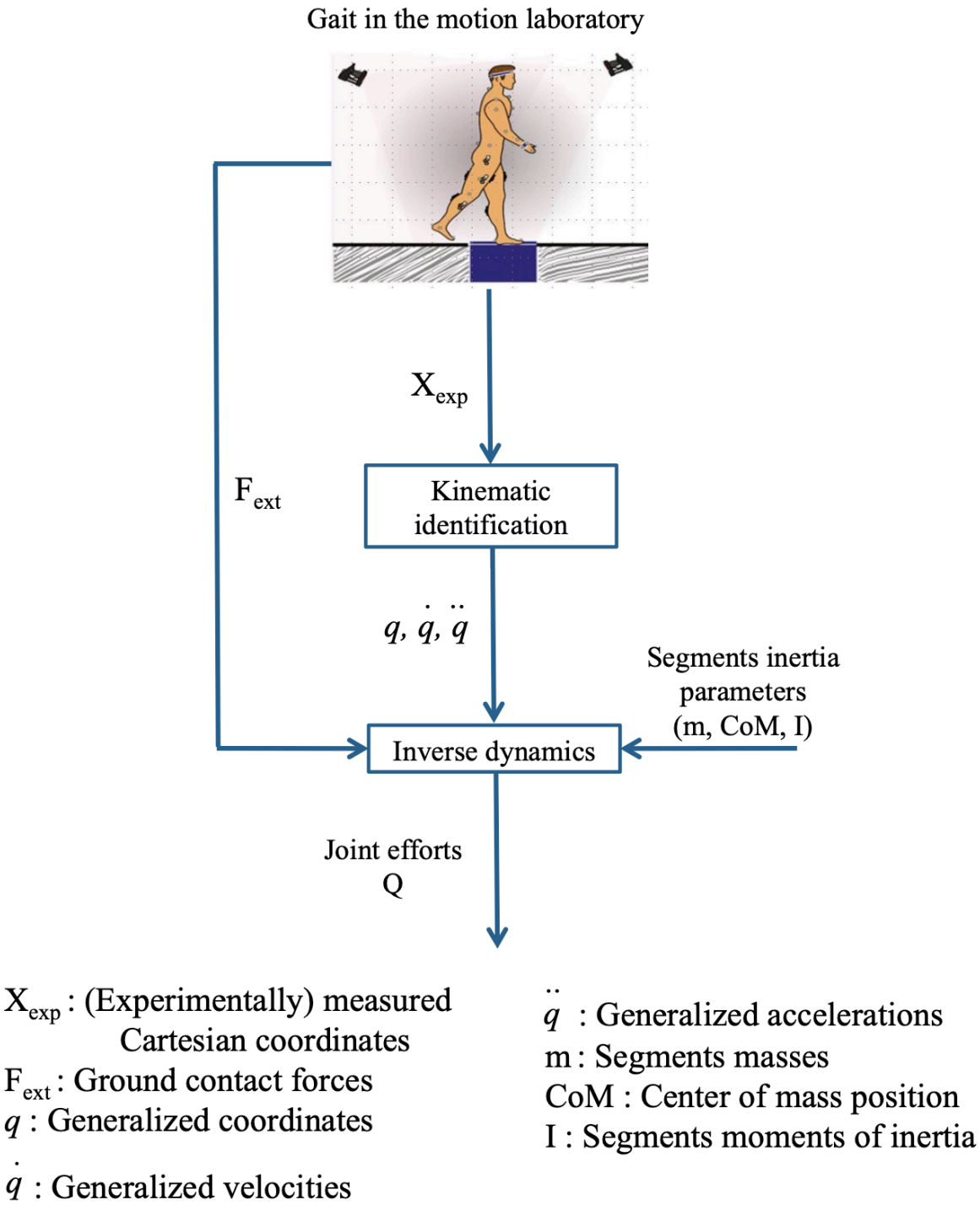

Figure 6.1 Process of quantifying the intervertebral joint efforts by inverse dynamics

6.3.2 Feature selection

As presented by Mahaudens et al.[10] and Raison et al. [81], adolescents with severe idiopathic scoliosis showed higher mobility resulting in higher joint efforts in the lumbosacral joint (L5-S1) than healthy adolescents. Therefore, the efforts at the lumbosacral joint that are produced while walking could be relevant indicators for classification of the severity of spinal deformity.

Based on previous studies [78], [81], [101] as well as observation of the data as shown in Figure 6.2 and 6.3 , mediolateral (ML) forces and torques and anteroposterior (AP) torques at the lumbosacral joint were chosen as features due to the greater influence of the spinal deformity on these mentioned efforts . AP is the axis along with the walking direction and ML is the axis perpendicular to the walking direction, when participants are walking during the data collection sessions. The impact of the spinal deformity on the mentioned efforts could be explained due to the asymmetry between the left and right side of the body in AIS and the impact of the lumbar curve on asymmetrical trunk movement in the coronal plane. In fact, the adaptive dynamic strategies in AIS have been distinguished by an asymmetry between right and left limbs for lateral and forward initiation due to the impact of spinal deformity on dynamic motions [153].

These mentioned efforts of one adolescent with AIS and one healthy adolescent chosen from the database collected in [10] (Height: 164 cm, weight: 65kg, age: 17 years) during a complete gait cycle are presented in Figure 6.2, as an example.

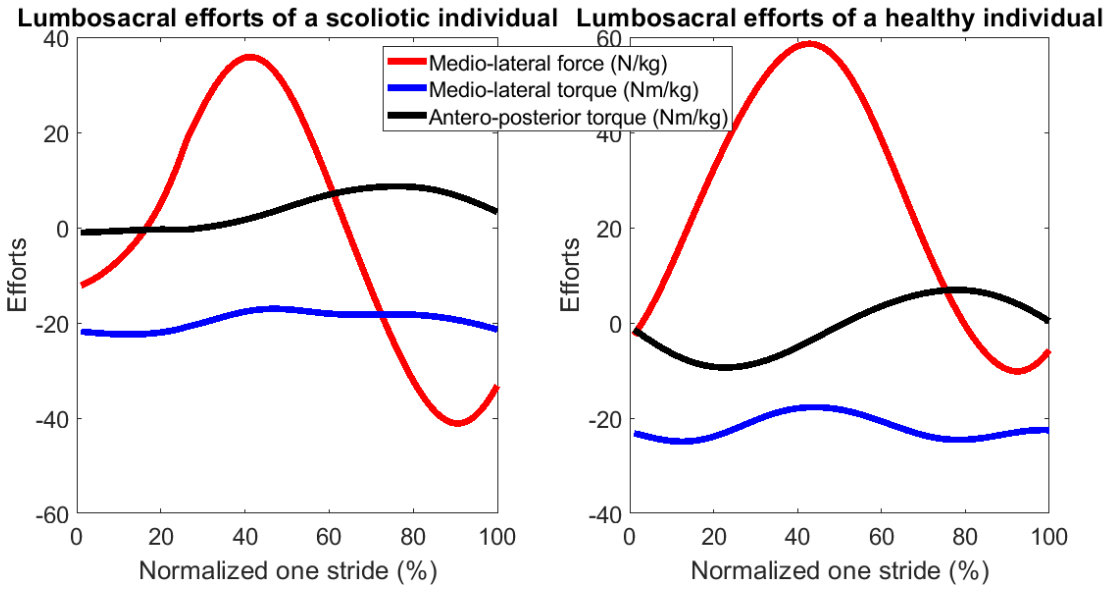

Figure 6.2 *left*: Lumbosacral joint effort of an adolescent with AIS during one complete gait cycle, *right*: Lumbosacral joint effort of a healthy individual during one complete gait cycle

The 15 parameters from six gait cycles shown in Table 6.2 were considered as features for the learning algorithms. We considered the fact reported in [81] that magnitude, maxima and minima of ML force and torque and AP torque efforts are being influenced by the severity of spinal deformity and defined the features. To have a better understanding of the chosen features, Figure 6.3 was prepared. As demonstrated in Figure 6.3, the chosen parameters as features show significant differences between healthy individuals and those with scoliosis.

Table 6.2 Features to feed classification algorithms

NO.	**Features**		
	Mediolateral force	**Anteroposterior torque**	**Mediolateral torque**
1	Maximum (|Maximum-mean|,|Minimum-mean|)		
2	Maximum (|Variance-mean|,|Variance+mean|)		
3	Maximum (|Max|,|Min|)		
4	|mean|		
5	Standard deviation		

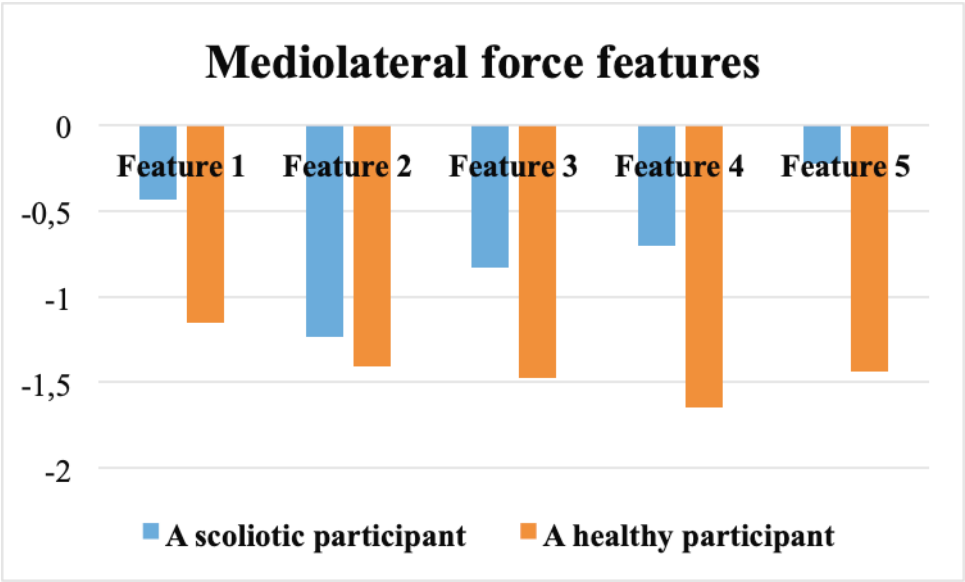
Mediolateral force features
0
-0,5
-1
-1,5
-2
Feature 1
Feature 2
Feature 3
Feature 4
Feature 5
A scoliotic participant
A healthy participant

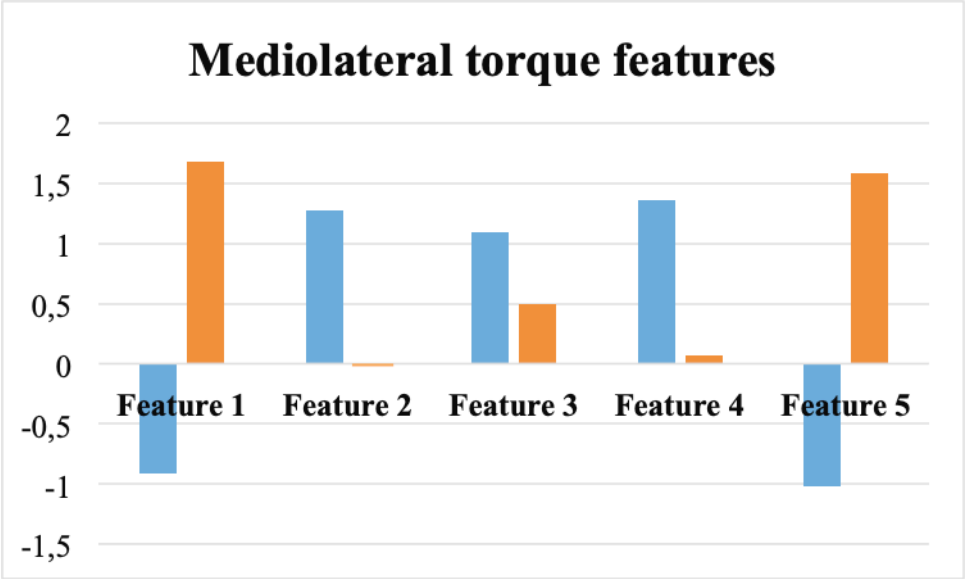
Mediolateral torque features
2
1,5
1
0,5
0
-0,5
-1
-1,5
Feature 1
Feature 2
Feature 3
Feature 4
Feature 5

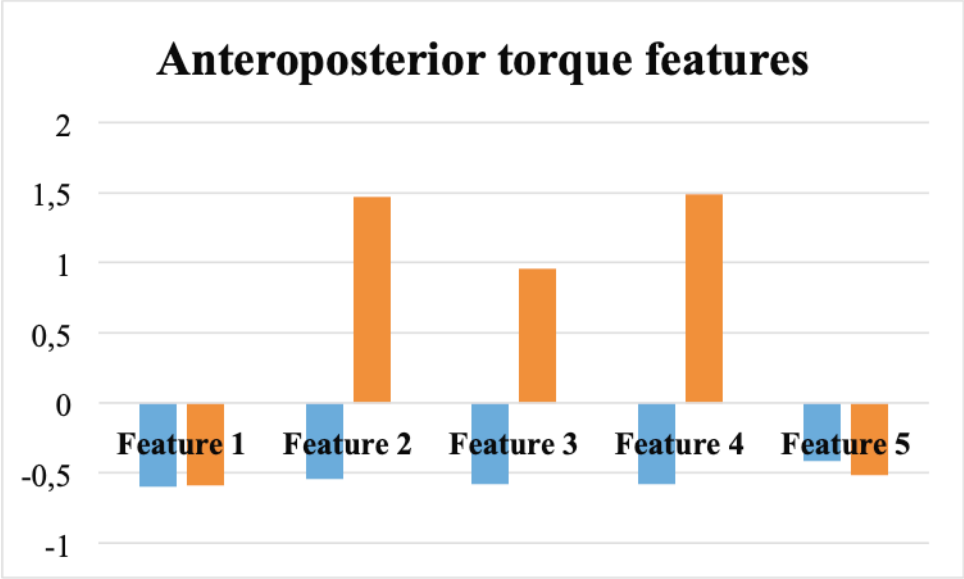

Figure 6.3 top: Mediolateral force, middle: Mediolateral torque, bottom: Anteroposterior torque features, comparison between an adolescent with AIS and a typically developed adolescent

6.3.3 Sampling process

Following the feature selection step, to maintain the compatibility between the features, StandardScaler [154] was applied to arrange the data in a standard normal distribution as a pre-processed step. The features were calculated over the 6 complete gait cycles i.e. 12 steps for each individual.

6.3.4 Model selection

Several supervised classifier methods, as listed in Table 6.3, were implemented, since our training dataset is labeled. Gridsearch was used to automatically tune the hyperparameters for each learning algorithm. Grid search methodically builds and evaluates the model for each combination of algorithm parameters specified in a grid, by performing a cross validation process through a given list of parameters and the range of values for each parameter. It finds the optimal hyperparameters that provide the best accuracy for each model.

Three different classes based on the surgeons measurement of the Cobb angle on radiography images were considered as the labels [155]: Individuals with the Cobb angle between 10° and 25°

(class 1), 25° and 45° (class 2) and superior to 45° (class 3), respectively. To select the learning model, a comparative study was carried out in terms of the accuracy score of different learning algorithms on a cross-validation set. To evaluate the performance of each model on unseen data we performed the k-fold cross validation process. K-fold cross validation separates the data to k folds and each time it holds one fold for a test and training the model on the rest of the folds. It means that every data point has the chance to be in a test dataset once and to be in the training dataset k-1 times. The overall performance of the model then calculates based on the average of all folds over each time training process.

To improve the accuracy score, we implemented an ensemble of learning methods using the voting classifier algorithm adding several models. The developed models with their hyperparameters are summarized in Table 6.3.

Table 6.3 Parameters used in each algorithm

No.	**Classifier Algorithm**	**Parameters**
1	K-nearest neighbours [156]	Number neighbours=3 (Number of the nearest neighbours in the dataset to include in the voting process)
2	Radius neighbours [157]	metric=chebyshev (The distance metric to use for the tree, Chebyshev distance: The maximum distance between two vectors) radius=3.0 (The given radius of a point or points to find neighbours within it) weights=distance (Weight function used in prediction, when distance is chosen, closer neighbours of a query point have a greater influence than

		neighbours which are further away)
3	SVM with Polynomial (degree 3) Kernel [158]	C = 0.9 (Regularization parameter, to avoid overfitting)
4	SVM with Gaussian Kernel [158]	C = 100 (Regularization parameter, to avoid overfitting)
5	Random forests [159]	criterion=entropy (The function to measure the quality of a split, "entropy" criteria calculates the information gain by making a split) max_depth=20 (The maximum depth of the tree) max_features=auto (The number of features to consider when looking for the best split. If "auto" is chosen, it means that it is equal to square root of number of features)
6	Logistic regression [160]	penalty=L2 (Regularization parameter, to avoid overfitting, L2 (Ridge regression), adds "squared magnitude" of coefficient as a penalty term to the loss function) solver = lbfgs (Chosen algorithm for the optimization, "lbfgs" for multiclass problems) C = 0.09 Inverse of regularization strength
7	Gaussian process [161]	kernel = 10.0 * RBF(1) (To specify the covariance function. RBF: squared exponential kernel)

8	Multilayer perceptron [162]	activation= ReLU (The function to activate the hidden layer, ReLU *f(x) = max(0, x))*, rectified linear unit function) hidden_layer_sizes=(60) (Number of hidden neurons) learning_rate=constant (updates the weight) learning_rate_init=0.003 (It controls the step-size in updating the weights) max_iter=500 (Number of epochs when the solver is "adam") n_iter_no_change=10 (Number of iterations with no improvement to wait before termination training procedure) solver=adam (Optimizes the weight, "adam": stochastic gradient-based optimizer)
9	AdaBoost [163]	n_estimators=500 (The maximum number of estimators at which boosting is terminated) learning_rate=0.01 (Shrinks the contribution of each classifier)

		algorithm=SAMME.R (SAMME.R for fast convergence)
10	Gaussian naïve Bayes [164]	var_smoothing=3 (Portion of the largest variance of all features that is added to variances for calculation stability)
11	Linear discriminant analysis [165]	solver = lsqr (Least squares solution)
12	Bootstrap aggregating (Bagging) [166]	KneighboursClassifier (The used algorithm)
13	Extra trees [167]	criterion=gini (It measures the quality of a split, Gini Impurity is a measurement of the likelihood of an incorrect classification of a new instance of a random variable, if that new instance were randomly classified according to the distribution of class labels from the dataset) max_depth=None (The maximum depth of the tree, "None": nodes are expanded until all leaves are pure or all leaves contain less than min_samples_split samples) max_features=auto (max_features=square root of (n_features))
14	Ensemble methods [168]	K nearest neighbours SVM Random forest multilayer perceptron
15	Neural Network model [169]	6 hidden layer Activation function of input and hidden

		layers: tanh(x) = $(\frac{e^x - e^{-x}}{e^x + e^{-x}})$ Activation function of output layer: Softmax = $\frac{exp(x_i)}{\sum_j exp(x_j)}$) (Exponential and enlarges differences - push one result closer to 1 while another closer to 0) Dropout [170] = 0.2 (It is used to avoid overfitting by randomly dropping out nodes during training) Optimizer: Stochastic gradient descent (SGD) (Computation is performed on a small subset or random selection of data example instead of whole dataset) Learning rate=0.001 Momentum=0.4 (Regularization parameter when optimizer is SGD)

6.3.5 Classifier algorithms

Ensemble method and Neural Networks models showed the best results; therefore we explain these mentioned algorithms in the following section and the related parameters in Table 6.3:

- **Ensemble voting classifier** [168] is a combination of a set of classifiers which uses a majority vote to predict the class labels :
  - K nearest neighbours (KNN): it stores all of the available possibilities and classifies new data based on a similarity to the stored data [171]. The label is predicted as the class with the highest frequency from the most similar samples.

Each sample in the training dataset votes for the class of the sample in the test and the class with the most votes is the final prediction [172].

- SVM (Gaussian kernel) [173], [174]: finds the hyper plane in an N-dimensional space which N is the number of features that classifies the data points. Its classification algorithm is based on finding an optimal boundary between the possible outputs.

- Random forest: consists of many decision trees. The parameters are the variables and thresholds, which are used to split each node that is learned during training. It consists of several decision tree models that split on a subset of features on each split.

- Multilayer perceptron (MLP) [170], [175]: is a feed forward artificial Neural Network that generates a set of outputs from a set of inputs. It uses the backpropagation technique for training, which is based on the calculation of loss. The loss between the model predicted and the real label is calculated and then the value of all the weights is calculated from the last layer to the first layer aiming to decrease the loss over the network.

- **Neural Networks model** [176]: is a series of algorithms to recognize underlying relationships in a set of data through a process that mimics the way the human brain operates. We implemented a sequential Neural Network densely connected with six hidden layers, i.e. each neuron in a layer receives an input from all neurons of the previous layer and all the neurons in a layer are connected to the neurons in the next layers.

We developed different classification algorithms to have a comprehensive observation on performance of different methods as shown in Table 6.3. To account for the randomness of the splitting of the dataset, we launched seven simulations based on the size of the database and then averaged the results to obtain the final result.

6.4 Results

6.4.1 Performance of the classifiers

The performance of each model has been shown by presenting the accuracy score, precision, recall (sensitivity) and F1-score in Table 6.4. The equation for each of the evaluation methods is shown in equations 6-1 to 6-4.

$$Accuracyscore: \frac{Numberofcorrectpredictions}{Totalnumberofpredictions} \quad \textit{Equation 6-1}$$

$$Precision: \frac{Numberoftruepositives}{Numberoftruepositives+Numberoffalsepositives} \quad \textit{Equation 6-2}$$

$$Recall(sensitivity): \frac{Numberoftruepositives}{Numberoftruepositives+Numberoffalsenegatives} \quad \textit{Equation 6-3}$$

$$F1Score: \frac{2*Precision.Recall}{Precision+Recall} \quad \textit{Equation 6-4}$$

Table 6.4 Performance of each classification algorithm for AIS severity classification (cross-validation)

No.	Classifier Algorithm	Accuracy (%)	Precision (%)	Recall (%)	F1 Score (%)
1	K-nearest neighbours	77.9	67.9	77.9	71.7
2	Radius neighbours	60	40.1	60.7	47.3
3	SVM with Polynomial (degree 3) Kernel	57.1	36.6	57.1	43.7
4	SVM with Gaussian Kernel	84.3	78.2	84.3	79.6
5	Random forests	83.6	80.1	83.6	80.2
6	Logistic regression	77.9	70.2	77.9	73.1
7	Gaussian process	77.1	65.7	77.1	69.3

8	Multilayer tron	87.9	83.6	87.9	84.3
9	AdaBoost	85.7	85.1	85.7	83.1
10	Gaussian naïve Bayes	67.9	52.0	67.9	57.8
11	Linear discriminant analysis	77.9	72.6	77.9	74.5
12	Bootstrap aggregating (Bagging)	57.1	78.2	71.4	65.0
13	Extra trees	80.7	75.8	80.7	75.8
14	Ensemble methods (K nearest neighbours, SVM, Random forest, Multilayer perceptron)	91.4	89.5	91.4	89.3

The accuracy score obtained by the sequential Neural Networks model was 93.6%. Figure 6.4 shows the accuracy score (left) and categorical cross entropy (right) as the loss function (see equation 6-5) of one of the folds of the cross-validation for the training and test as an example.

$$Loss: -\sum_{i=1}^{output\ size} y_i \ .\log \widehat{y_i} \qquad \textit{Equation 6-5}$$

where,

$\widehat{y_i}$ is the ith scalar value in the model output, y_i is the target value, and *n* is the number of scalar values in the output of the model.

Loss function is the measurement of distinguishability of two discrete probability distributions from each other. The categorical cross entropy defines the probability of each data point belonging to a specific category (class) in classification tasks, which the model must decide.

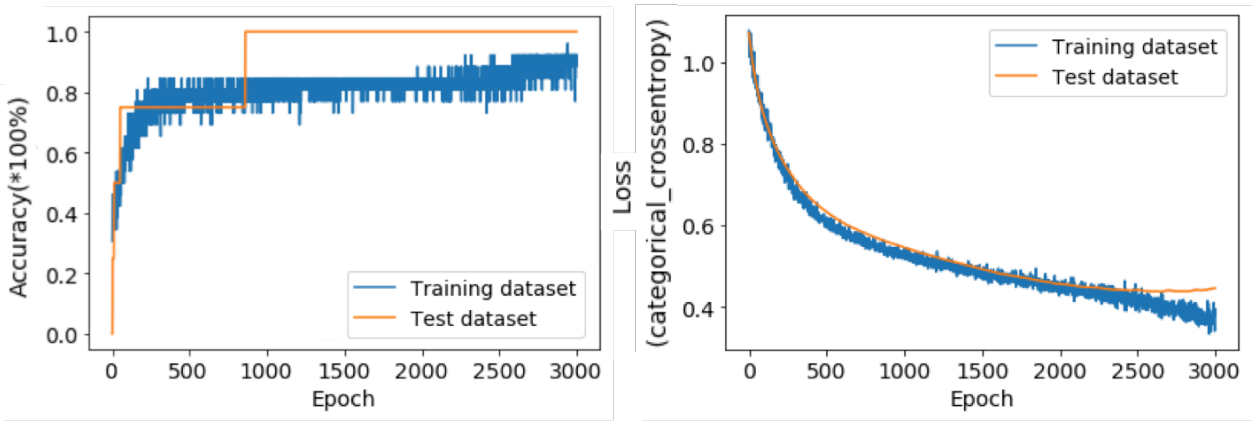

Figure 6.4 *left*: Accuracy score, *right*: Loss function of one fold of Neural Network model for training and test dataset

6.5 Discussion

Gait pattern provides useful information to assess and follow-up musculoskeletal diseases. AIS as a disease that affects trunk symmetry and anatomy of spine can modify human locomotion. Significant differences have been reported in kinematics [177]and ground reaction forces during gait in AIS with different levels of severity[178] . Therefore, the intervertebral efforts as variables, which are computed by using kinematics and ground reaction forces, can provide valuable information to assess and follow-up scoliosis. Raison et al. reported that the magnitude, maxima and minima of intervertebral efforts normalized to the body mass are being influenced by the severity of spinal deformity and we considered that as a feature of the engineering process to train the classification algorithms[81]. Consequently, in the current study, we developed a Machine Learning algorithm based on the lumbosacral (L5-S1) joint efforts during gait as an aid for clinicians to follow-up and assess the progression of scoliosis. The proposed method classified the severity of scoliosis (Cobb angle) in 30 patients without any spinal fusion surgery within the Lenke 5-6 (left lumbar and thoracolumbar scoliosis). Three different classes based on the treatments strategies were considered: AIS individuals with a Cobb angle between 10° and 25° (mild scoliosis), between 25° and 45° (moderate scoliosis) and superior to 45° (severe scoliosis). It is worth noting that the lumbosacral joint is the most mobile part of the spine in lumbar and thoracolumbar scoliosis. Additionally, mediolateral force and torque as well as

anteroposterior torque, in this part of the spine, have shown differences between healthy individuals and the individuals with different severity as shown in Figures 6.2 and 6.3 and studies presented in [10], [78], [81], [82]. Therefore, these mentioned efforts in the lumbosacral joint are promising parameters to be chosen as features for the classifier algorithm. It can be explained by the fact that spinal deformity causes the AIS to compensate on the opposite limb to that of the curve. Furthermore, it has been reported that lumbar curve causes asymmetrical trunk movement in the coronal plane [23] .Therefore the efforts related to the lateral direction, i.e. ML force and torque and AP torque are influenced the most by the spinal deformity during gait, compared to the other components of the intervertebral efforts [178].

To account for the randomness of splitting the data, a k-fold cross-validation was chosen to evaluate the algorithm. To perform a comprehensive observation, we first applied several supervised classification algorithms and then implemented the Ensemble algorithm combined with the ones with higher accuracy scores amongst the others, i.e. KNN (accuracy score: 77.9%), SVM with Gaussian kernel (accuracy score: 84.3%), random forest (accuracy score: 83.6%) and multilayer perceptron (accuracy score: 87.9%). The accuracy score equal to 91.4% was obtained by implementing the Ensemble methods. A Neural Networks (NN) model was also designed to classify the dataset with an accuracy score equal to 93.6%, the highest accuracy score, compared to others as shown in Table 6.4.

KNN is used when the data points are separated into several classes to predict the class of a new data point. It is usually one of the first chosen classification algorithms when there is a lack of knowledge about the distribution of the dataset [172]. It works better than SVM when the number of features is greatly higher than the number of samples. Therefore, the accuracy score of KNN was relatively high. The obtained accuracy score of SVM is higher than KNN since SVM performance in handling the outliers is better than KNN and in this study, the number of features is not higher than the number of samples. Random forest is known as a fast, simple and flexible model. Its good performance among the others can be explained by its ability to search for the best feature among a random subset of features. It is also capable to handle an unbalanced dataset, i.e. a larger class will get a low error rate while a smaller class will have a larger error rate and can provide high accuracy through cross-validation [179]. The higher performance of the NN model compared to the others can be justified by the ability of NN models to solve non-linear and complex problems. Furthermore, NN models are capable of generalizing the model and

predict unseen data once they learn from the initial inputs and their relationships. They can learn hidden relationships in the data without imposing any fixed relationship in the data. The designed NN model in this study includes sequential dense layers. A densely connected layer provides learning features from all the combinations of the features of the previous layer to provide an accurate prediction.

Observing the performance of other models, shows that the performance of linear models were not as good as others. It confirms that the dataset does not have completely linear relationships. The performance of the models such as AdaBoost (adaptive boosting) and extra trees, which are based on the combination of multiple models, i.e. multiple weak classifiers and many decision trees respectively, are better than the others in terms of the accuracy score.

The value of calculated precision, recall and F1-score are high and close to the accuracy score. It means that the proposed ensemble model has provided a low number of false positives due to the high precision (exactness), few false negatives, due to the high recall (completeness) and also there is a balance between the precision and recall as the F1-score shows.

In previous studies, [75], [146]–[150] the focus was on the static posture parameters to assess the severity of AIS. However this survey developed a classification model by using Machine Learning algorithms based on a simple activity like walking. It is worth mentioning that Cho et al. [18] used 72 gait features based on kinematic gait parameters (the Euler angles and 3D acceleration components) to train an SVM model to classify the severity of scoliosis in two classes, i.e. the Cobb angle less and more than 25°. The accuracy score of the classifier was 85.7%, however, considering the 25° as a threshold to classify the severity of AIS, cannot provide required information to make appropriate decisions for treatment strategies. The ones with a Cobb angle more than 45° are subjected to the spinal surgery and the ones with a Cobb angle between 25° and 45° are prescribed to wear bracing. Therefore, the need for radiography images remained valid. Consequently, for the first time we proposed a radiation-free method that classified the severity of AIS, in three classes, i.e. mild, moderate and severe scoliosis with an accuracy score of 93.6%. By using the proposed classifier, the radiation exposure for the follow-up of the progression of the spinal curvature can be limited.

The adolescents with AIS included in this research had similar spinal deformities: Lenke 5-6 corresponding to thoracolumbar and lumbar curves, impacting the pelvis motion. It would be

required to validate the model on AIS with thoracic curves (Lenke 1-2), since the location of the spine curvature is in the middle or thoracic part of the spine.

6.6 Conclusion

For the first time, we developed an efficient radiation-free Machine Learning method to assess the severity of spinal deformity into mild, moderate and severe classes, which corresponds to the related treatments, i.e. physiotherapy exercises, bracing and surgery, respectively. The proposed classifier showed an accuracy score equal to 93.6% for thoracolumbar/lumbar AIS with 7.4% increase in performance compared to the highest reported accuracy score (85.7%) in the state of the art.

The solution presented in this paper is a promising alternative to current follow-up methods i.e. using X-ray images, which only requires performing a gait evaluation session and implementing Machine Learning algorithms.

As future work, the proposed classifier should be tested and modified on other types of spinal curvature located on the middle and/or top of the spine. Furthermore, an algorithm should be developed to identify the value of the Cobb angle to improve the purpose of replacement of this radiation-free method to the radiography images.

CHAPTER 7 ARTICLE 3: DEVELOPMENT OF MACHINE LEARNING ALGORITHMS TO IDENTIFY THE COBB ANGLE IN ADOLESCENTS WITH IDIOPATHIC SCOLIOSIS BASED ON LUMBOSACRAL JOINT EFFORTS DURING GAIT

Bahare Samadi [a, b], Maxime Raison [a, b], Philippe Mahaudens [c,d], Christine Detrembleur [d], Sofiane Achiche [a]

[a]Department of Mechanical Engineering Polytechnique Montréal, Canada; [b] Technopole in Pediatric Rehabilitation Engineering, Sainte-Justine UHC, Montreal, Canada; [c] Cliniques universitaires Saint-Luc, Service d'Orthopédie et de Traumatologie de l'Appareil Locomoteur, Brussels, Belgium ; [d] Université catholique de Louvain, Secteur des Sciences de la Santé, Institut de Recherche Expérimentale et Clinique, *Neuro Musculo Skeletal Lab (NMSK),* Brussels, Belgium

The Spine Journal. Submitted on 16 January 2021.

7.1 Abstract

Background Context: Adolescent idiopathic scoliosis (AIS) is an abnormal curvature of the spine, which affects up to 4% of children between the ages of 10 and 16 years old. To quantify the magnitude of spinal deformities, the Cobb angle in degrees as the gold standard is used based on the radiography with an X-ray of the spine. The amount of continuous exposure to X-ray radiation to follow-up the progression of scoliosis may lead to negative side effects on patients. Furthermore, manual measurement of the Cobb angle needs time and effort and could lead to up to 10° or more of a difference due to intra/inter observer variation. Therefore, recent studies have focused on using computer-assisted, Machine Learning methods, and statistical observations to assess the evolution of scoliosis. However, identification of the Cobb angle by automated radiation-free methods with the accuracy compatible with radiological data is still a challenge in scoliosis treatment and follow-up. **Purpose:** To develop an automated algorithm based on Machine Learning methods to identify the Cobb angle of the spine based on the intervertebral efforts on the lumbosacral (L5-S1) joint during gait. **Study Design:** The participants included in this study are 30 AIS in the lumbar/thoracolumbar category with the Cobb angle between 15° and

66° who performed 6 complete gait cycles. **Methods:** The lumbosacral joint efforts during six walking cycles of participants were used as features to feed training algorithms. Several tests were run using various regression algorithms. **Results:** The decision tree regression algorithm among 15 different regression models achieved the best result with the mean absolute error (MAE) equal to 4.6° of averaged 10-fold cross-validation. Discussion and **conclusion:** This study shows that the lumbosacral joint efforts during gait as radiation-free data are capable of identifying the Cobb angle by implementing Machine Learning algorithms. The proposed model can be used as an alternative, radiation-free method to X-ray radiography to assist the clinicians in Cobb angle identification and treatment strategies.

Key Words: Spinal deformity, Idiopathic scoliosis, Cobb angle, Radiation-free scoliosis assessment, Prediction, Machine Learning regression algorithms, Gait analysis, Lumbosacral joint efforts.

7.2 Introduction

Adolescent idiopathic scoliosis (AIS), which is the most common form of scoliosis, affects up to 4% of adolescents between ages 10 to 16 years old. It is defined by a deformation of the spine and trunk greater than 10 degrees [144], [180], [181]. The etiology is not clear; but various theories such as biomechanical, neuromuscular, genetic, and environmental origins exist [57], [182] . The preliminary diagnosis is performed by screening with Adam's forward bend test and a scoliometer [183]. Although an ultimate diagnosis and assessment cannot be made without measuring the Cobb angle [184] as a gold standard. Cobb angle is the degree of spine curvature on the coronal plane, measured by using spinal radiography in a standing position. The accuracy of the measurement of the Cobb angle is an important basis for selecting therapeutic methods and following the progression of scoliosis. However, it requires submitting the patients to sequential radiographic images i.e. at least every 6 months during their growth stage to measure it.

To define the Cobb angle, two main challenges exist; on the one hand, accurate Cobb angle measurement, utilizing the information of X-rays, requires considerable time and effort, along with associated problems such as inter/intra observer variations [70]. On the other hand,

convolutional exposure to X-ray radiations in growing ages represents a real risk of an increase in organ carcinogenic and can cause tissue damage [57], [144], [180]–[182].

The problem in the accuracy of the measurement is due to the difficulty in visualizing the vertebrae or to poor selection of terminal vertebrae or variations in goniometers [62], [185]. These problems increased the interest of using automated measurements methods such as Machine Learning and radiation-free data such as kinematics parameters instead of manual measurement and using radiographic data.

Jaremko *et al.* [186] used an Artificial Neural Network (ANN) to analyze the asymmetry of 360° torso surface cross-sections to estimate the Cobb angle without the use of X-rays but using torso surface topographic coordinates. They reported a mean absolute error (MAE) equal to 1.9° (SD=5°). Choi *et al.* [187] estimated the Cobb angle by applying a convolutional Neural Network (CNN) on the merged images of moiré and spine radiography with an MAE of 3.42° (SD=2.64°).

Wu *et al.* showed that the SurgimapSpine measurement, a surgical planning software platform [188], is an equivalent measuring tool to the traditional manual measurement in the coronal Cobb angle [64]. Wang *et al.* used Deep Learning to measure the Cobb angle on X-ray images with an MAE of 7.81°[189] in comparison with the manual measurement. Tu *et al.* [72] developed a Deep Learning algorithm that estimated the Cobb angle with an average error of 2.9° compared to the reference Cobb angle which was measured manually by a specialized orthopaedist.

Watanabe *et al.* [185] compared the back morphometric data of moiré images, with radiologic data, using a CNN and achieved an MAE of 3.42°(SD=2.64°) for the Cobb angle. Pearsall *et al.* [62] compared three noninvasive methods including scoliometer, back counter device and moiré topographic imaging to assess scoliosis and the obtained results suggested that these measurement techniques cannot be used in clinical recordings. Pino-Almero *et al.* believed that, even with back surface images, data cannot substitute for radiography images in the diagnosis of scoliosis, they can however offer additional quantitative data that may complement radiologic study[64]. According to the state of the art methods, identifying the Cobb angle on X-ray images using computer-assisted methods and Machine Learning algorithms have been shown more accurate results compared to the manual measurement by specialized clinicians. However, using

the topographic images of the back of the body has been proposed as a complementary method to the radiography images or to evaluate surface asymmetry.

Consequently, it would be more interesting to develop an accurate radiation-free method without the need for topography and X-ray images, which could be an alternative to radiography. Seo *et al.* [77] predicted the Cobb angle with an MAE of 5° by applying multiple regression analysis on posture parameters in the standing position. They trained their model over 85% of the dataset (27 individuals) and tested it on 15% (5 individuals).

Gait analysis studies show that spinal deformity affects spino-pelvic mobility and can accordingly modify human locomotion and walking patterns [17]. Therefore, it is interesting to study the relationship between spinal deformity and gait pattern to identify the Cobb angle. According to Mahaudens et al. research, [10] scoliosis modifies the gait pattern and reduces the pelvic frontal motion. Similarly, Raison et al. [81] showed that severe spinal deformity in AIS presented higher mobility resulting in higher joint efforts in the lumbosacral (L5-S1) joint than of healthy adolescents, i.e. the lumbosacral joint is the most mobile part of the spine during gait. Two recent studies (2019 and 2020) by Guilbert *et al.* and Samadi *et al.*, [78], [82] respectively, presented the differences of gait patterns among adolescents with AIS and TDA by comparing the intervertebral efforts along the spine. All these studies attest to the major impact of scoliosis on mobility.

Accordingly, the aim of this study is to propose a radiation-free method, to identify the Cobb angle in AIS based on the lumbosacral joint efforts during gait, by using Machine Learning algorithms.

7.3 Data acquisition and patient samples

7.3.1 Dataset

Thirty AIS with main thoracolumbar/lumbar spine curvature (Lenke 5-6 [1]) with a Cobb angle between 15 and 66 degrees, without any history of spine surgery, participated in a previous study [10] and were included in this study, as shown in Table 7.1.

Table 7.1 Specification of the participants

Cobb angle, degree (mean ± SD)	Age, years (mean ± SD)	Weight, kg (mean ± SD)	Height, cm (mean ± SD)
35° ± 13° (Range: 15-66°)	15 ± 2	50 ±9	163 ±9

This study takes ground on a previous study [10], which calculated lumbosacral joint efforts utilizing inverse dynamics. This longitudinal dataset is a collection that was started in 2009. The features to train the Machine Learning models have been selected based on the lumbosacral joint efforts, using reflective markers attached to specific anatomical joints on the skin of the participants performing gait cycles. A motion capture system composed of optokinetic sensors measured the kinematics of 26 anatomical landmarks, and ground reaction forces applied to each foot measured with an equipped treadmill with force sensors. The intervertebral forces and torques in the lumbosacral joint were calculated using a precise 3D inverse dynamic model of the human body, through ROBOTRAN software [17], [88] as shown in Figure 6.1.

7.3.2 Feature selection

According to the studies of the impact of the spinal deformity on gait patterns and intervertebral efforts, presented in previous studies. [10], [17], [81] severe lumbar/thoracolumbar scoliosis presents higher mobility on the lumbosacral joint and therefore led to different joint efforts in the lumbosacral joint, compared to the non-scoliosis spine. Furthermore, a single lumbar curve causes asymmetry in trunk motion in the coronal plane. As a result, the produced efforts during gait at the lumbosacral joint could be considered as significant parameters to define the scoliosis severity and to identify the Cobb angle.

As shown in Figure 7.1 and 7.2 and presented in [10], [78], [81], among the 3D intervertebral efforts, mediolateral (ML) forces and torques and anteroposterior (AP) torques are the ones which are affected the most by spinal deformity, therefore the features have been chosen based on these efforts. To have a better understanding and comparison, Figure 7.1 presents these efforts in the lumbosacral joint during gait for two AIS with different severity.

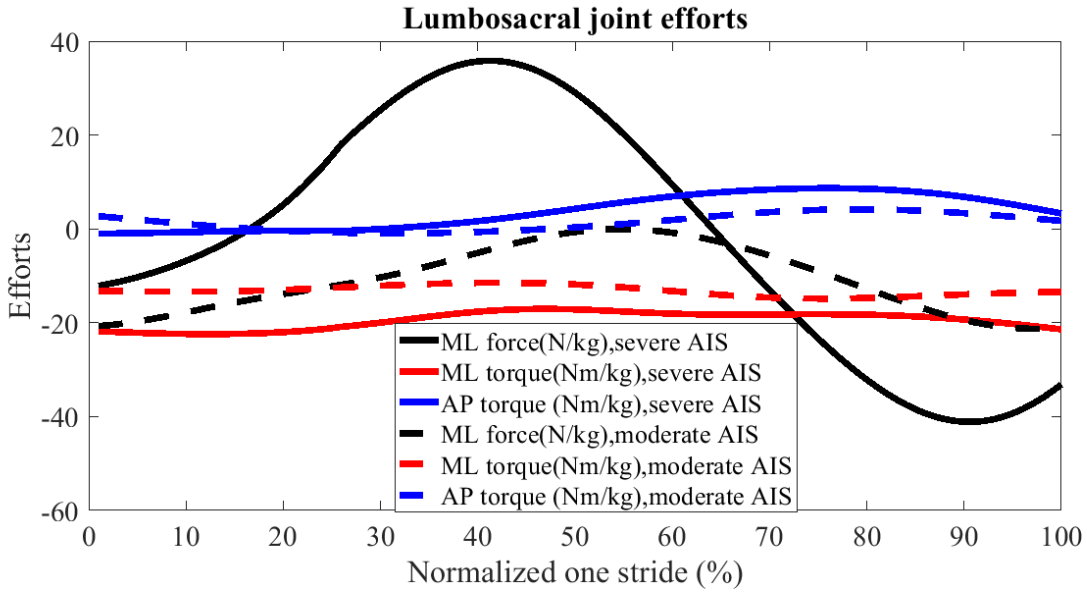

Figure 7.1 Lumbosacral joint effort of one AIS with severe scoliosis (filled line) and one AIS with moderate scoliosis (dashed line)

The 18 parameters from six gait cycles shown in Table 7.2 were considered as features to train the model. As presented in Figure 7.2, these parameters show different behaviors based on the severity of spinal deformity.

Table 7.2 Features to feed regression algorithms

No.	**Features**		
	Mediolateral force	**Anteroposterior torque**	**Mediolateral torque**
1	Maximum (|Maximum-mean|, |Minimum-mean|)		
2	Maximum (|Variance-mean|, |Variance+mean|)		
3	Maximum (|Max|, |Min|)		
4	|mean|		
5	Standard deviation		
6	|Max-Min|		

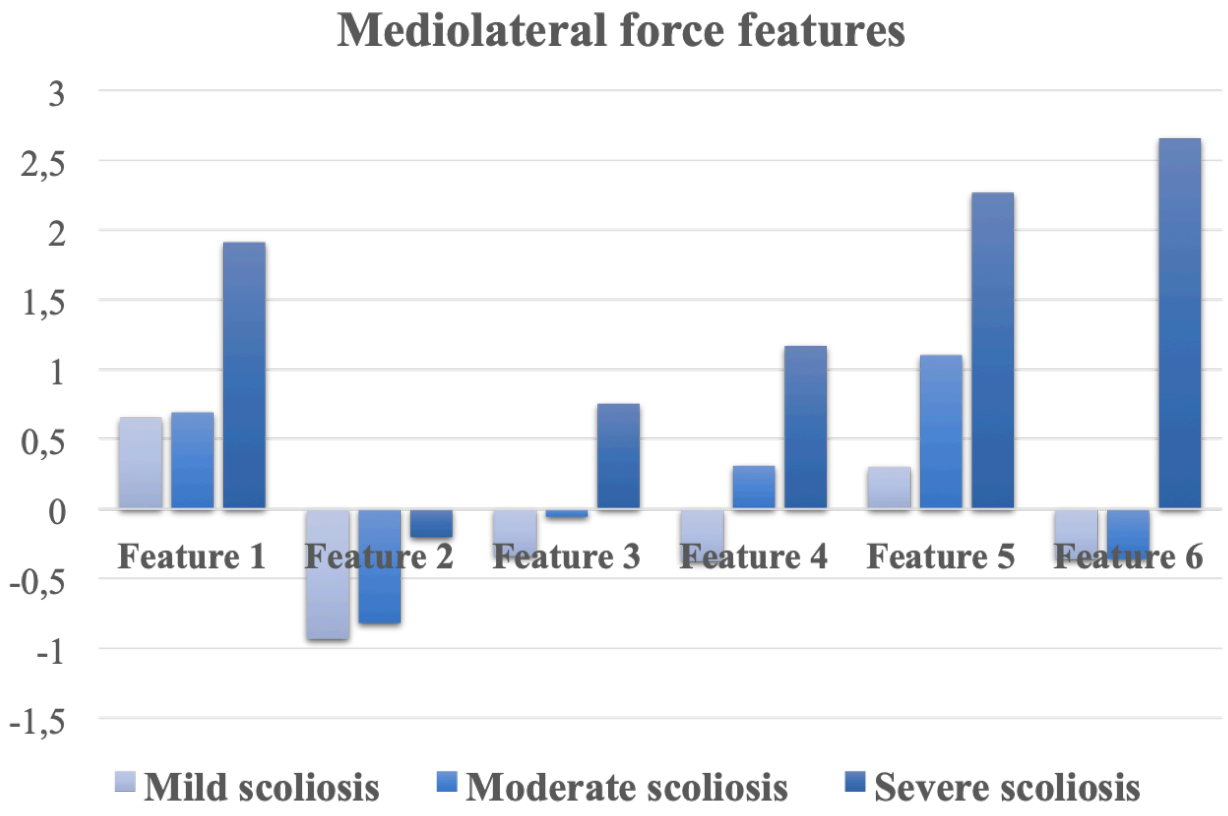
Mediolateral force features
3
2,5
2
1,5
1
0,5
0
-0,5
-1
-1,5
Feature 1
Feature 2
Feature 3
Feature 4
Feature 5
Feature 6
Mild scoliosis
Moderate scoliosis
Severe scoliosis

a.

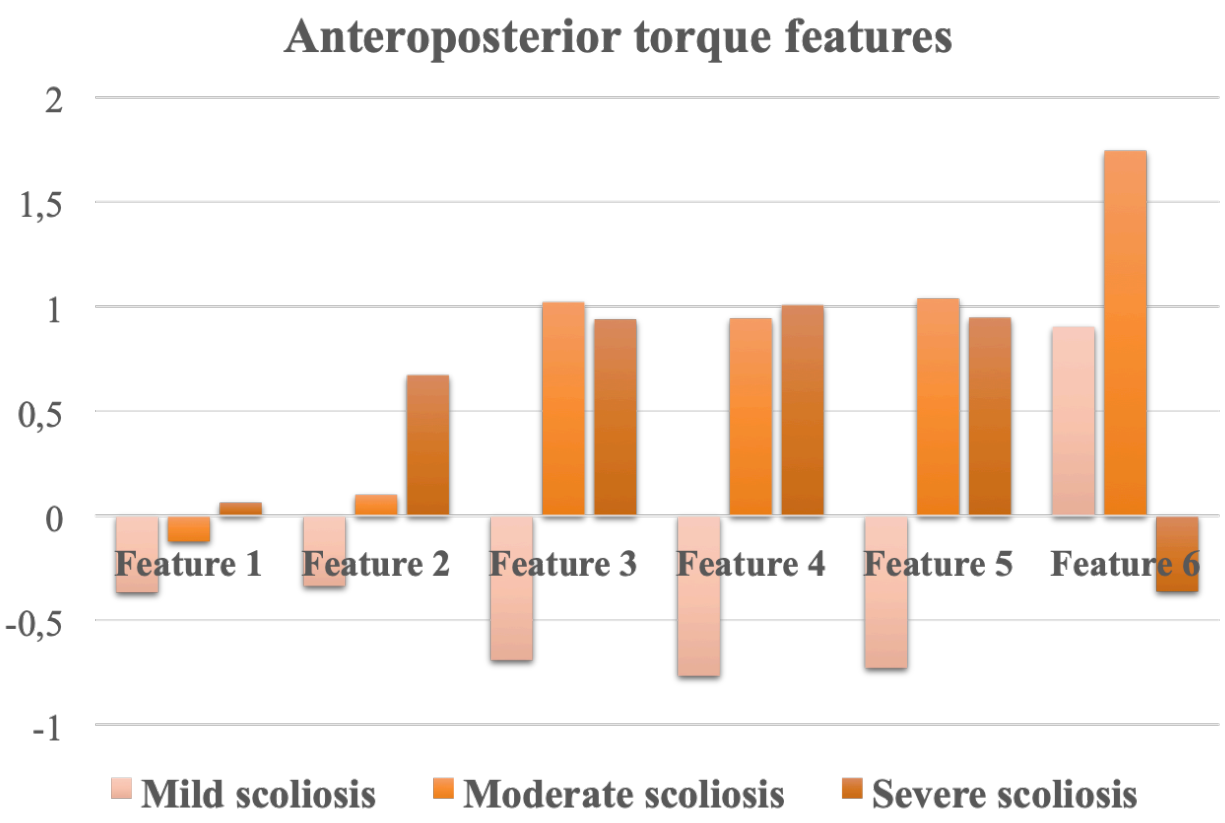
Anteroposterior torque features
2
1,5
1
0,5
0
-0,5
-1
Feature 1
Feature 2
Feature 3
Feature 4
Feature 5
Feature 6
Mild scoliosis
Moderate scoliosis
Severe scoliosis

b.

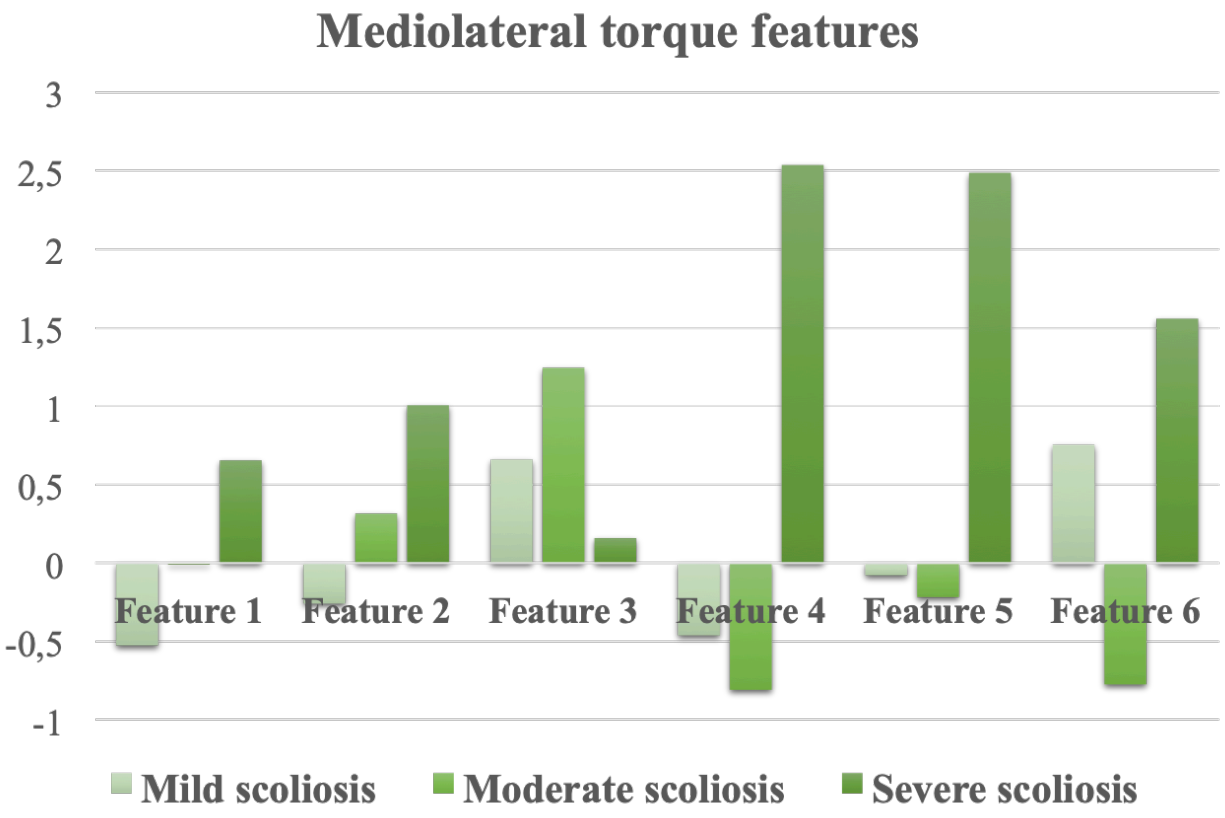

c.

Figure 7.2 a: Mediolateral force, b: Anteroposterior torque, c: Mediolateral torque features, comparison between three AIS with different severities

7.3.3 Sampling process

To avoid any of the features dominating the model and learning algorithm as well as enabling the learning process to learn equally from all features, StandardScaler [190] was applied to the features. StandardScaler aligns the features in the same range of variance. The features were calculated over 360 steps i.e. 12 steps (6 complete successive gait cycles) for each participant. To account for the randomness of the splitting of the data and to evaluate the performance of each model on unseen data, k-fold cross-validation with 10 folds was applied on the algorithm [191]. K-fold cross validation splits the data to k groups and each time it holds one group for the test and it trains the model on the rest of the groups. It means that every data point once is located in a test dataset and k-1 times are located in a training dataset. The overall performance of the model is calculated on the basis of the average of all groups over each time of the training process. The

value of k is chosen based on the size of the dataset. Generally, the larger value of k, decreases the bias, due to the decrease of the difference between the training set and the resampling [90].

7.3.4 Model selection

Several regression models, listed in Table 7.3, were developed to identify the Cobb angle by feeding 18 features to the learning algorithms. To improve the accuracy of each model, Grid-search hyperparameter tuning was used. Hyperparameters are specified parameters to control the behaviour of Machine Learning algorithms by tuning and Grid Search chooses the hyperparameters by going through all possible combinations of hyperparameters to obtain better prediction [192]. Table 7.3 presents the developed models with related parameters. The undefined parameters are the default parameters by scikit-learn software, which is a free Machine Learning library in Python [193]. The model with the smallest MAE, which is the average MAE over the 10 folds, is the selected model to identify the Cobb angle.

Table 7.3 Parameters used in each algorithm

No.	**Regression Algorithm**	**Parameters**
1	K-nearest neighbours [194]	Number neighbours=3 (Number of the nearest neighbours in the dataset)
2	Radius neighbours [195]	metric= minkowski (The distance metric to use for the tree, Minkowski distance: $D(X,Y) = \left(\sum_{i=1}^{n} \lvert x_i - y_i \rvert^p\right)^{\frac{1}{p}}$ $X = (x_1, x_2, \dots, x_n) Y = (y_1, y_2, \dots, y_n) \in R^n$

		$p = 2$ radius=6.0 (The given radius of a point or points to find neighbours within it) weights=distance (Weight function used in prediction, when distance is chosen, closer neighbours of a query point have a greater influence than neighbours which are further away)
3	SVM with linear Kernel [196]	C = 100 (Regularization parameter, to avoid overfitting)
4	Random forests [197]	criterion=mae (The function to measure the quality of a split. mae : mean absolute error) max_depth=15 (The maximum depth of the tree) max_features=log2 (The number of features to consider when looking for the best split. If "log2" is chosen, it means that it is equal to log2 of number of features)
5	Linear regression [198]	
6	Linear ridge regression [199]	alpha=0.1 (To define the regularization strength)

7	Lasso regression [200]	alpha=0.1 max_iter=10000 (The maximum number of iteration) selection=random (It accelerates the convergence) tol=0.0001 The tolerance for the optimization
8	Gaussian process [201]	kernel = DotProduct() + WhiteKernel() (To specify the covariance function)
9	Multilayer Perceptron [37]	activation= logistic (The function to activate the hidden layer, The logistic sigmoid function: $f(x) = \frac{1}{1 + exp\ (-x)}$ hidden_layer_sizes=(60) (Number of hidden neurons) learning_rate=constant (updates the weight) learning_rate_init=0.003 (controls the step-size in updating the weights) max_iter=1000

		(number of epochs when the solver is “adam”) n_iter_no_change=10 (number of iterations with no improvement to wait before termination training procedure) solver=adam (Optimizes the weight, “adam”: stochastic gradient-based optimizer)
10	AdaBoost [202]	n_estimators=250 (The maximum number of estimators at which boosting is terminated) learning_rate=1.1 (Shrinks the contribution of each regressor) loss=linear (To update the weights after each boosting iteration)
11	Decision Tree [203]	max_depth = 4 The maximum depth of the tree Criterion = “mse” (The function to measure the quality of a split. “mse” for the mean squared error, which is equal to variance reduction as feature selection criterion and minimizes the L2 loss using the mean of each terminal node)

12	Bayesian Ridge [204]	Fit a Bayesian ridge model
13	Bootstrap aggregating (Bagging) [205]	base_estimator=Decision Tree (The base estimator to fit on random subsets of the dataset) n_estimators=20 (The number of base estimators in the ensemble)
14	Extra trees [206]	criterion=mae (The function to measure the quality of a split) n_estimators=200 (The number of trees in the forest) max_depth=None (The maximum depth of the tree, “None”: nodes are expanded until all leaves are pure or all leaves contain less than min_samples_split samples) max_features=None (max_features=n_features)
15	Gradient Boosting [207]	alpha=0.85 criterion=mae learning_rate=1 learning rate shrinks the contribution of each

		loss=huber (Huber loss is a combination of both Mean Square Error and Mean Absolute Error) max_depth=3 (maximum depth of the individual regression estimators that limits the number of nodes in the tree)

7.3.5 Decision Tree regression algorithm

As presented in Table 7.4, the decision tree model, presented the best result, therefore in this section, we go through the details of this model.

The decision tree regression model has an empirical tree structure that breaks down the dataset into smaller subsets by applying a series of simple rules learned from features, and at the same time, a related decision tree is gradationally grown. The gained information t is then used to predict the target through a repetitive process of dividing [203], [208]. To maximize the information gain (IG) at each split, an objective function is defined to optimize via the learning algorithm. The IG of a random variable X obtained from an observation of a random variable AA taking value AA = a is defined in equation 7-1 [208]:

$$IG_{X,A}(X,a) = D_{KL}\big(P_X(x|a) \| P_X(x \vee I)\big) \qquad \textit{Equation 7-1}$$

where,

D_{KL} : Kullback–Leibler divergence which is a directed divergence between two distributions [209]

$P_X(x \vee I)$: Prior distribution

$P_X(x|a)$: Posterior distribution

7.4 RESULTS

7.4.1 Performance of regression models

The MAE (Equation 7-2) of each method which is the average MAE of 10 folds cross-validation between the measured Cobb angle by the surgeons using the radiography images and the ones predicted by each algorithm are shown in Table 7.4. The lowest MAE of 4.6° was obtained by implementing a decision tree model.

$$MAE = \frac{\sum_{i=1}^{n} y_i - x_i \vee}{n} \qquad \textit{Equation 7-2}$$

where,

y_i : Prediction

x_i : True value

n : Total number of data points

Table 7.4 Mean absolute error (MAE) of Cobb angle, average of 10-fold cross validation for each model

*Algorithm with the best result

No.	Regression Algorithm	Cross-Validation MAE (SD) degrees
1	K-nearest neighbours	9.9 (5.1)
2	Radius neighbours	10.5 (4.6)
3	SVM with linear Kernel	10.6 (3.6)
4	Random forests	9.0 (5.3)
5	Linear regression	11.9 (7.5)
6	Linear ridge regression	10.5 (3.5)
7	Lasso regression	9.4 (3.5)
8	Gaussian process	8.9 (4.9)

9	Multilayer perceptron	8.8 (2.4)
10	AdaBoost	6.9 (3.9)
11	***Decision Tree**	**4.6 (3.5)**
12	Bayesian Ridge	9.0 (3.4)
13	Bootstrap aggregating (Bagging)	7.8 (5.3)
14	Extra trees	7.9 (3.2)
15	Gradient Boosting	8.6 (5.6)

7.5 DISCUSSION

This study proposed a radiation-free method based on Machine Learning models, which is able to identify the Cobb angle by implementing the lumbosacral joint efforts during gait as features. The reason behind choosing ML force and torque and AP torque in the lumbosacral joint is the mobility of this part of the spine in lumbar and thoracolumbar scoliosis as reported in [10], [78], [81] and presented in Figures 7.1 and 7.2.

Therefore, the choice of features allowed the algorithm to identify the Cobb angle with an MAE (SD) equal to 4.6°(3.5°) which is the lowest error compared to the previous studies. Observing the value of obtained MAE from different models and compared to the variations in manual measurements which is up to 10° shows that as a preliminary study, the model has the potential of being used as an alternative to X-ray images. In fact, it has been reported that most of the manual measurement variations occur due to the difficulties in selection of the upper and lower end-plate vertebrae [210] .

The value of the MAE in linear models is higher than the other models due to the fact that our data set does not have a fully linear relationship. The models which are the combination of other regression models i.e. AdaBoost (Adaptive Boosting), Bootstrap aggregating (Bagging) and extra trees have provided more accurate predictions as the ensemble model intends to improve the accuracy by reducing the variance. The decision tree provided the lowest value for MAE compared to the others. It can be explained due to its ability in feature selection automatically. In decision tree models, the accuracy of the model is not affected by the presence of multicollinearity (the presence of features that depend on each other) of the features [211].

Most of the previous studies [72], [73], [77], [185], [212] that used Machine Learning models to identify the Cobb angle have chosen radiography or body images for feeding the learning algorithm, which still keeps the need for radiation exposure . However, cumulative radiation exposure, i.e. 10 to 25 spinal X-rays during growth ages, increases the risk of cancer [213]. As reported by Simony *et al.* (2016) [214], the overall rate of cancer on 215 AIS patients was five times higher than the aged matched population and endometrial and breast cancer was most frequent. The dose of radiation applied to the patients in this mentioned study was comparable to modern equipment [214].

Therefore, this underlines the interest of decreasing radiation exposure by developing radiation-free methods to assess the spinal deformity without decreasing the accuracy of the Cobb angle measurement. In fact, using a systematic method would also eliminate the problems of the Cobb angle measurement variations. However, there are still very few studies proposing automated radiation-free methods as an alternative to X-ray. Seo *et al.* [12] proposed a multiple regression analysis model using 21 static posture parameters to predict the Cobb angle with an MAE of 5° tested on only 5 patients without performing any cross-validation, however it is also known that spinal deformity affects mobility and locomotion. Cho *et al.* [212] reported 85.7% accuracy to classify the severity of scoliosis to less and more than 25° of the Cobb angle by applying the support vector machine method on 72 kinematic parameters during gait. Our proposed method as an automated radiation-free method, succeeded in identifying the Cobb angle with an MAE lower than similar studies during gait as a main daily activity.

This method would allow the clinicians and physiotherapists to evaluate the progress of spinal deformity and improve the efficiency of treatments. Therefore, the amount of exposure to radiation could be limited. As shown in Figure 7.3, manual measurement of the Cobb angle based on the radiography images of the spine may decrease the accuracy in measurement of the Cobb angle up to 10° due to the difficulty in visualizing the vertebrae, poor selection of terminal vertebrae and variations in goniometers. For instance, as reported in [53]–[55] an error of 5-10° may occur due to intra-observer and can exceed due to inter-observer variations, measured by the clinicians. Furthermore, radiographic acquisition and measurement methods could also lead to 2° to 7° error [56]. Therefore, an automatic method based on the gait pattern with an MAE of 4.6° could be considered as a reliable model with the potential of improving and implementing in determination of treatments strategies.

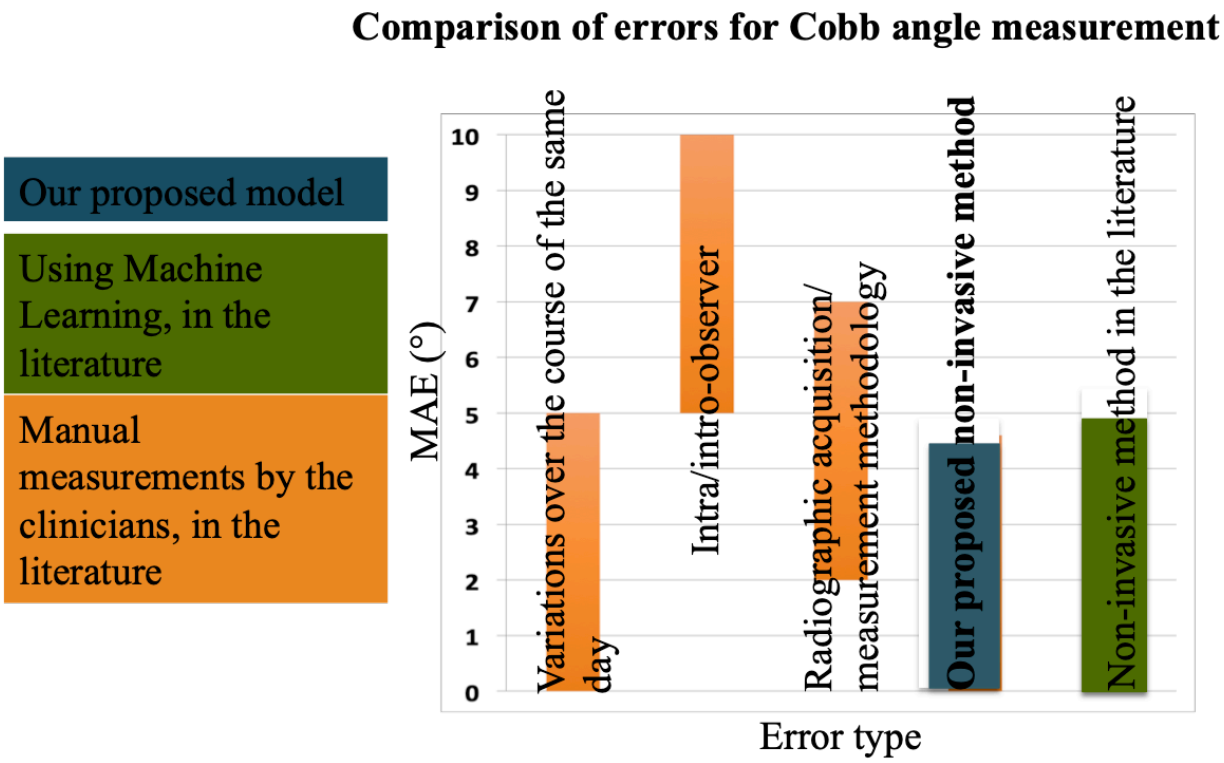

Figure 7.3 Comparison between the Cobb angle measurement errors and the error of the proposed model [53]–[56], [77], [215]

The accuracy of the performance of the algorithm supports that spinal deformity modifies the gait pattern. Therefore, this study also shows the relation between the AP and ML torques and ML force at the lumbosacral joint with the Cobb angle for scoliosis with lumbar/thoracolumbar spine curvature. It can be interpreted by the asymmetry loading on the spine due to the left/right curvature of the spine and its impact on the lateral efforts, and the impact of a lumbar curve on asymmetrical trunk movement in the coronal plane. Furthermore, it proves the fact that the lumbosacral joint is the most mobile part of the spine.

The dataset included in the present work were obtained from adolescents with AIS with thoracolumbar/lumbar curves. Therefore, it is required that the performance of the algorithm be verified on the other patterns of spinal deformity and be adapted for other types of scoliosis where the location of the spinal deformity is not on the lumbosacral (L5-S1) joint.

7.6 CONCLUSION

For the first time, we developed an efficient Machine Learning tool to identify the Cobb angle of AIS with lumbar/thoracolumbar spine curvature with an MAE of 4.6° which can assess the progression of scoliosis with an accuracy compatible with manual radiography measurement. Additionally, the required information for the learning algorithm is provided by a radiation-free method, which is a simple gait analysis evaluation session. The process of Cobb angle identification is performed in a dynamic situation, i.e. walking which is a crucial activity of daily life. The required features are the components of only three efforts in the lumbosacral joint i.e. ML force and torque and AP torque. Consequently, it is not required to have several measurements to feed the learning algorithms and the time of execution for all of the tested algorithms with the cross-validation and only the decision tree algorithm is 30.20s and 0.02s, respectively.

As future work, the algorithm could be implemented as a tool synchronized with the multibody human model and the motion capture system. The multibody model calculates the efforts in real-time and the motion capture system feeds the required information to the multibody human model. It provides the possibility of identification of the Cobb angle in real-time to assist the clinicians and surgeons.

CHAPTER 8 GENERAL DISCUSSION

8.1 Objective accomplishments

The general objective defined by this thesis was achieved. A radiation-free model to identify the severity of idiopathic scoliosis in adolescents based on the intervertebral efforts during gait was developed. This process revealed a relation between intervertebral efforts and spinal deformity. Moreover, it was confirmed that spinal deformity modifies the gait pattern and intervertebral efforts during gait. The severity and the location of the curvature on the spine were also shown to affect the gait pattern and intervertebral efforts. Finally, it was attested that Machine Learning algorithms are capable of identifying the Cobb angle as an automated method.

To accomplish the main objective, first we defined the most relevant intervertebral efforts, which are associated with spinal deformity during gait (SO1/article 1) by comparing 15 AIS with different types and severity of scoliosis to 12 TDA. Mediolateral force and torque and anteroposterior torque, were chosen to be used as indicators to identify the severity of the AIS. These indicators were then utilized to obtain the features to feed Machine Learning algorithms and identify the severity of scoliosis focusing on AIS with lumbar/thoracolumbar curve type (SO2). Achieving the promising results in classification, we continued to identify the Cobb angle of AIS during gait (SO3/article 2 and 3).

The steps to accomplish the general objective are summarized in Figure 8.1.

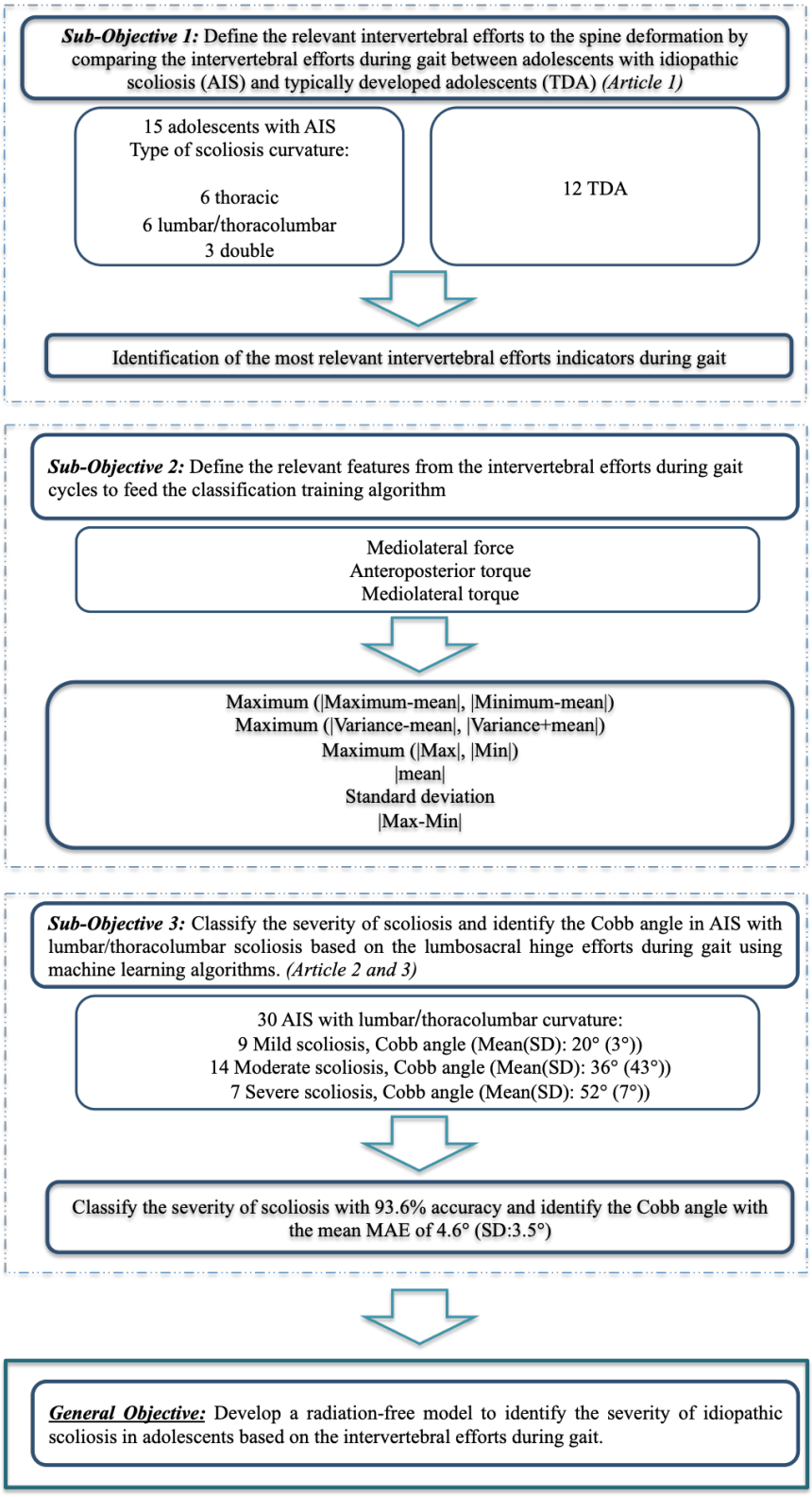

Figure 8.1 Procedures to achieve the general and sub-objectives

The developed model in this study provided an MAE equal to 4.6° (SD: 3.5°) in the identification of the Cobb angle. The performance of the model, in comparison with the classical method i.e., manually measuring the Cobb angle on X-ray images by specialists, is promising since the intra/inter observer measurement variations are between 5° and 10° [53]–[55]. The state of the art method shows that previously, the smallest MAE to identify the Cobb angle using a radiation-free method [77] was 5°, tested on 5 patients only in the static standing position. In the current study, several algorithms were trained and the performance of each algorithm was tested by cross-validation on over 30 samples. Additionally, in comparison with an average error of 4° obtained by automated Cobb angle measurement methods on X-ray images, our proposed method represented less than 5° for MAE as a radiation-free solution. Furthermore, the developed classification model provided an accuracy score of 93.6% categorizing the AIS into three classes of severity, i.e. mild, moderate and severe. To our knowledge, this is the first radiation-free model, capable of classifying the severity of scoliosis into three groups with promising accuracy. It is worth noting that clinicians and surgeons make their decisions for treatments strategies based on the three mentioned classes, devising different treatment procedures for each one. Therefore, our developed methods in both identification of the severity and the Cobb angle have demonstrated the potential for use as a radiation-free method alternative to X-ray images to assess AIS progression and follow-up.

8.2 Limitations

The proposed classification and regression models have been developed only on adolescents with lumbar/thoracolumbar AIS. Given that the location of the spine curvature influences on the lower part of the spine and vertebrae in the lumbosacral joint, the model has yet to be tested and modified for patients with other types of curvature where the deformity is positioned on the upper part of the spine.

8.3 Research Output

The outcomes of this research are published (or submitted for publication) in peer-review journals and conference proceedings. The list of author's contributions and related publications are shown below:

1- Comparison of intervertebral efforts along the spine between adolescents with idiopathic scoliosis and typically developed adolescents:

- B. Samadi, M. Raison, S. Achiche, C. Fortin, "Identification of the most relevant **intervertebral effort indicators during gait of adolescents with idiopathic scoliosis**", *Computer Methods in Biomechanics and Biomedical Engineering*, vol. 23, no. 10, pp. 664–674, Jul. 2020, doi: 10.1080/10255842.2020.1758075 [78].
- B. Samadi, M. Raison, S. Achiche, C. Fortin, ***"Development of an Avatar for the rehabilitation of the trunk and pelvis movements during gait in adolescents with idiopathic scoliosis",*** Congrès étudiant du CRCHU Ste-Justine June 2018, Montréal, Québec, Poster presentation.
- B. Samadi, M. Raison, S. Achiche, C. Fortin, ***"Development of an Avatar for the rehabilitation of the trunk and pelvis movements during gait in adolescents with idiopathic scoliosis",*** Journée scientifique et assemblées annuelles REPAR-INTER May 2018, Québec, Québec, Poster presentation.

2- Classification of the severity of spinal deformity in adolescents with AIS:

- B. Samadi, M. Raison, P. Mahaudens, C. Detrembleur, S. Achiche, ***"Classification of the severity of spinal deformity in adolescents with idiopathic scoliosis using Machine Learning algorithms based on lumbosacral joint efforts during gait"***, Spine Journal, Submission ID: SPINE 162757,2020.

3- Identification of the Cobb angle in adolescents with AIS:

- B. Samadi, M. Raison, P. Mahaudens, C. Detrembleur, S. Achiche, ***"Development of Machine Learning algorithms to identify the Cobb angle in adolescents with lumbar idiopathic scoliosis based on lumbosacral hinge efforts during gait",*** Spine Journal, Submission ID: SPINE 162763,2020.

8.4 Computer implementations

The algorithms and methodologies proposed in this study have been implemented in Python, by using Scikit-learn and Keras libraries. Both are open-source libraries for programming in the Python. Scikit-learn is a Machine Learning library that features various classification, regression

and clustering algorithms [216]. Keras provides a Python interface for Artificial Neural Network [217]. To facilitate applying the proposed model to a similar clinical population for researchers, practitioners and clinicians, all parameters and data are available on a Google drive and will be shared by the author of this thesis as per request.

CHAPTER 9 CONCLUSION AND RECOMMENDATIONS

9.1 Summary of the thesis

In this thesis, we proposed novel approaches toward accomplishing the main objective, which was to develop a radiation-free model to identify the severity of idiopathic scoliosis in adolescents based on the intervertebral efforts during gait. First, a comprehensive and systematic literature review on the challenges related to the main objective and the targeted clinical population was performed. The performed research works and proposed solutions were subsequently reported. Investigating the available proposed methods, the recommendations, and the limitations were helpful in identifying gaps in the field and achieving effective solutions for this challenge. We began with accomplishing the first sub-objective (SO1) through studying the impacts of spinal deformity and posture imbalance on the gait pattern of the AIS and intervertebral efforts along the spine. We included scoliosis with different types of spine curvature and severity to achieve a comprehensive conclusion. The developed multibody dynamics model in [82] was used for this purpose, considering it was designed to compute the intervertebral efforts along the spine. In addition to highlighting the most relevant intervertebral efforts among 3D forces and torques, we concluded that the results could be used to develop an avatar in real-time and be implemented in physiotherapy treatments for adolescents with AIS. This was based on the idea that such a model could serve as a tool to assist clinicians, providing real-time feedback to correct the trunk and pelvis posture during gait. The visual feedback during physiotherapy treatments could subsequently improve the treatment's efficiency based on the postural correction.

To pursue the second and third sub-objectives (SO2/SO3), we utilized the results of SO1, to consider the intervertebral efforts, associated with the spinal deformity as features for training algorithms. To achieve a robust classification algorithm, we focused on one type of scoliosis, i.e. lumbar/thoracolumbar (Lenke 5-6) and selected a database including the lumbosacral intervertebral efforts of these individuals during gait cycles. Our focus on the lumbar/thoracolumbar curvature necessitated the use of the developed multibody model proposed in [17] to compute the efforts at the lumbosacral joint as the most mobile part of the spine [81]. Based on the previous studies [10], [81] and our extensive data analysis, we selected the appropriate parameters as features to feed the training algorithms (SO2). This led to the

development of a model that classified the severity of scoliosis (mild, moderate, severe) with promising accuracy (SO3).

Following the success in the classification model, we considered our results through classification to design a regression model that identifies the value of the Cobb angle measured in degrees. We selected the appropriate features and tested several models to achieve a model with acceptable performance that could be used as an alternative to X-rays for clinical and treatment purposes. Finally, a model to identify the Cobb angle with acceptable accuracy as compared with classical methods was developed based on the radiography images and existing computer-assisted models using both radiology and radiation-free data. Implementing different classification and regression Machine Learning models enabled us to explore the behaviour of each model on our dataset to achieve the best model. Furthermore, it could be used as a guideline for future studies, implementing the method on other types of AIS.

Therefore, our developed method has demonstrated the potential for being used as a radiation-free method alternative to X-ray images that allows for assessing idiopathic scoliosis progression and follow-up.

9.2 Future work and Recommendations

The present model should be tested and modified for other types of scoliosis with the curvature positioned on the middle or thoracic (upper) part of the spine. This is due to the fact that intervertebral efforts on the lumbosacral joint may not be the most relevant indicators of scoliosis for other types of spine curvature.

The proposed model in this study could be synchronized with the multibody dynamics model and motion capture system in the motion labs to identify the Cobb angle in real-time during the gait analysis session.

REFERENCES:

[1] L. G. Lenke *et al.*, "Adolescent idiopathic scoliosis: a new classification to determine extent of spinal arthrodesis," *J Bone Joint Surg Am*, vol. 83-A, no. 8, pp. 1169–1181, Aug. 2001.

[2] L. M. Flood, "DIAGNOSIS AND TREATMENT OF VOICE DISORDERS, 4th ednJ S Rubin, R T Sataloff, G S Korovin Plural Publishing, 2014 ISBN 978-1-59756-553-0 pp 1033 Price $US 350.00," *The Journal of Laryngology & Otology*, vol. 128, no. 9, pp. 843–843, Sep. 2014, doi: 10.1017/S0022215114001753.

[3] U. M. Ahn *et al.*, "The etiology of adolescent idiopathic scoliosis," *Am J. Orthop.*, vol. 31, no. 7, pp. 387–395, Jul. 2002.

[4] S. L. Weinstein, L. A. Dolan, J. C. Cheng, A. Danielsson, and J. A. Morcuende, "Adolescent idiopathic scoliosis," *The Lancet*, vol. 371, no. 9623, pp. 1527–1537, May 2008, doi: 10.1016/S0140-6736(08)60658-3.

[5] M. Rodts and DNP, "Scoliosis Symptoms," *SpineUniverse*. https://www.spineuniverse.com/conditions/scoliosis/symptoms-scoliosis (accessed Sep. 15, 2020).

[6] J. R. Cobb and J. L. Cobb, "Outline for the study of scoliosis," Jan. 1948, Accessed: Nov. 19, 2018. [Online]. Available: https://www.scienceopen.com/document?vid=76a12f1e-c7ef-4cc2-8aec-0904b520cd98.

[7] "Understanding Cobb Angles And What It Means For Scoliosis," *Core Concepts Physiotherapy*. https://www.coreconcepts.com.sg/article/cobb-angle-and-scoliosis/ (accessed Sep. 15, 2020).

[8] G. Giakas, V. Baltzopoulos, P. H. Dangerfield, J. C. Dorgan, and S. Dalmira, "Comparison of Gait Patterns Between Healthy and Scoliotic Patients Using Time and Frequency Domain Analysis of Ground Reaction Forces," *Spine*, vol. 21, no. 19, pp. 2235–2242, Oct. 1996.

[9] J. J. Schimmel, B. E. Groen, V. Weerdesteyn, and M. de Kleuver, "Adolescent idiopathic scoliosis and spinal fusion do not substantially impact on postural balance," *Scoliosis*, vol. 10, no. 1, p. 18, Jun. 2015, doi: 10.1186/s13013-015-0042-y.

[10] P. Mahaudens, X. Banse, M. Mousny, and C. Detrembleur, "Gait in adolescent idiopathic scoliosis: kinematics and electromyographic analysis," *Eur Spine J*, vol. 18, no. 4, pp. 512–521, Apr. 2009, doi: 10.1007/s00586-009-0899-7.

[11] J. H. Yang, S.-W. Suh, P. S. Sung, and W.-H. Park, "Asymmetrical gait in adolescents with idiopathic scoliosis," *Eur Spine J*, vol. 22, no. 11, pp. 2407–2413, Nov. 2013, doi: 10.1007/s00586-013-2845-y.

[12] N. Chockalingam, P. H. Dangerfield, A. Rahmatalla, E.-N. Ahmed, and T. Cochrane, "Assessment of ground reaction force during scoliotic gait," *Eur Spine J*, vol. 13, no. 8, pp. 750–754, Dec. 2004, doi: 10.1007/s00586-004-0762-9.

[13] H. Hatze, "Motion variability--its definition, quantification, and origin," *J Mot Behav*, vol. 18, no. 1, pp. 5–16, Mar. 1986, doi: 10.1080/00222895.1986.10735368.

[14] C. M. Kim and J. J. Eng, "Symmetry in vertical ground reaction force is accompanied by symmetry in temporal but not distance variables of gait in persons with stroke," *Gait Posture*, vol. 18, no. 1, pp. 23–28, Aug. 2003, doi: 10.1016/s0966-6362(02)00122-4.

[15] M. Syczewska, K. Graff, M. Kalinowska, E. Szczerbik, and J. Domaniecki, "Does the gait pathology in scoliotic patients depend on the severity of spine deformity? Preliminary results," *Acta Bioeng Biomech*, vol. 12, no. 1, pp. 25–28, 2010.

[16] M. Syczewska, K. Graff, M. Kalinowska, E. Szczerbik, and J. Domaniecki, "Influence of the structural deformity of the spine on the gait pathology in scoliotic patients," *Gait & Posture*, vol. 35, no. 2, pp. 209–213, Feb. 2012, doi: 10.1016/j.gaitpost.2011.09.008.

[17] M. Yazji *et al.*, "Are the mediolateral joint forces in the lower limbs different between scoliotic and healthy subjects during gait?," *Scoliosis*, vol. 10, no. 2, p. S3, Feb. 2015, doi: 10.1186/1748-7161-10-S2-S3.

[18] J. Cho *et al.*, "Scoliosis Screening through a Machine Learning Based Gait Analysis Test," *Int. J. Precis. Eng. Manuf.*, vol. 19, no. 12, pp. 1861–1872, Dec. 2018, doi: 10.1007/s12541-018-0215-8.

[19] C. G. Schizas, I. A. Kramers-de Quervain, E. Stüssi, and D. Grob, "Gait asymmetries in patients with idiopathic scoliosis using vertical forces measurement only," *Eur Spine J*, vol. 7, no. 2, pp. 95–98, 1998.

[20] I. A. Kramers-de Quervain, R. Müller, A. Stacoff, D. Grob, and E. Stüssi, "Gait analysis in patients with idiopathic scoliosis," *Eur Spine J*, vol. 13, no. 5, pp. 449–456, Aug. 2004, doi: 10.1007/s00586-003-0588-x.

[21] A.-V. Bruyneel, P. Chavet, G. Bollini, and S. Mesure, "Gait initiation reflects the adaptive biomechanical strategies of adolescents with idiopathic scoliosis," *Annals of Physical and Rehabilitation Medicine*, vol. 53, no. 6, pp. 372–386, Aug. 2010, doi: 10.1016/j.rehab.2010.06.005.

[22] J.-S. Chern, C.-C. Kao, P.-L. Lai, C.-W. Lung, and W.-J. Chen, "Severity of spine malalignment on center of pressure progression during level walking in subjects with adolescent idiopathic scoliosis," in *2014 36th Annual International Conference of the IEEE Engineering in Medicine and Biology Society*, Aug. 2014, pp. 5888–5891, doi: 10.1109/EMBC.2014.6944968.

[23] M. Nishida *et al.*, "Position of the major curve influences asymmetrical trunk kinematics during gait in adolescent idiopathic scoliosis," *Gait & Posture*, vol. 51, pp. 142–148, Jan. 2017, doi: 10.1016/j.gaitpost.2016.10.004.

[24] T. Maruyama and K. Takeshita, "Surgical treatment of scoliosis: a review of techniques currently applied," *Scoliosis*, vol. 3, no. 1, p. 6, Apr. 2008, doi: 10.1186/1748-7161-3-6.

[25] A. Patel *et al.*, "Moving Beyond Radiographs: Changes in Gait Patterns after AIS Realignment," *The Spine Journal*, vol. 16, no. 10, p. S243, Oct. 2016, doi: 10.1016/j.spinee.2016.07.155.

[26] E. A. Rapp and P. G. Gabos, "Impact of Scoliosis on Gait," 2016, doi: 10.1007/978-3-319-30808-1_68-1.

[27] P. Mahaudens, C. Detrembleur, M. Mousny, and X. Banse, "Gait in thoracolumbar/lumbar adolescent idiopathic scoliosis: effect of surgery on gait mechanisms," *Eur Spine J*, vol. 19, no. 7, pp. 1179–1188, Jul. 2010, doi: 10.1007/s00586-010-1292-2.

[28] P. Mahaudens, F. Dalemans, X. Banse, M. Mousny, O. Cartiaux, and C. Detrembleur, "Gait in patients with adolescent idiopathic scoliosis. Effect of surgery at 10 years of follow-up," *Gait Posture*, vol. 61, pp. 141–148, Mar. 2018, doi: 10.1016/j.gaitpost.2018.01.007.

[29] L. Aulisa, L. Pitta, R. Padua, E. Ceccarelli, A. Aulisa, and A. Leone, "Biomechanics of the spine," *Rays*, vol. 25, no. 1, pp. 11–18, Mar. 2000.

[30] S. Lupparelli, E. Pola, L. Pitta, O. Mazza, V. De Santis, and L. Aulisa, "Biomechanical factors affecting progression of structural scoliotic curves of the spine," *Stud Health Technol Inform*, vol. 91, pp. 81–85, 2002.

[31] A. B. Schultz, "Biomechanical factors in the progression of idiopathic scoliosis," *Ann Biomed Eng*, vol. 12, no. 6, pp. 621–630, 1984.

[32] C. J. Adam, G. N. Askin, and M. J. Pearcy, "Gravity-Induced Torque and Intravertebral Rotation in Idiopathic Scoliosis," *Spine*, vol. 33, no. 2, p. E30, Jan. 2008, doi: 10.1097/BRS.0b013e318160460f.

[33] C. Hopf, M. Scheidecker, K. Steffan, F. Bodem, and P. Eysel, "Gait analysis in idiopathic scoliosis before and after surgery: a comparison of the pre- and postoperative muscle activation pattern," *E Spine J*, vol. 7, no. 1, pp. 6–11, Feb. 1998, doi: 10.1007/s005860050019.

[34] C. K. Haber and M. Sacco, "Scoliosis: lower limb asymmetries during the gait cycle," *Arch Physiother*, vol. 5, Jul. 2015, doi: 10.1186/s40945-015-0001-1.

[35] B. E. Keenan *et al.*, "Gravity-induced coronal plane joint moments in adolescent idiopathic scoliosis," *Scoliosis*, vol. 10, no. 1, p. 35, Dec. 2015, doi: 10.1186/s13013-015-0060-9.

[36] F. Hefti, "Pathogenesis and biomechanics of adolescent idiopathic scoliosis (AIS)," *J Child Orthop*, vol. 7, no. 1, pp. 17–24, Feb. 2013, doi: 10.1007/s11832-012-0460-9.

[37] H.-R. Weiss *et al.*, "Physical exercises in the treatment of idiopathic scoliosis at risk of brace treatment -- SOSORT consensus paper 2005," *Scoliosis*, vol. 1, p. 6, May 2006, doi: 10.1186/1748-7161-1-6.

[38] S. Negrini, C. Fusco, S. Minozzi, S. Atanasio, F. Zaina, and M. Romano, "Exercises reduce the progression rate of adolescent idiopathic scoliosis: results of a comprehensive systematic review of the literature," *Disabil Rehabil*, vol. 30, no. 10, pp. 772–785, 2008, doi: 10.1080/09638280801889568.

[39] S. Negrini *et al.*, "Why do we treat adolescent idiopathic scoliosis? What we want to obtain and to avoid for our patients. SOSORT 2005 Consensus paper," *Scoliosis*, vol. 1, p. 4, Apr. 2006, doi: 10.1186/1748-7161-1-4.

[40] H. R. Weiss, "The effect of an exercise program on vital capacity and rib mobility in patients with idiopathic scoliosis," *Spine*, vol. 16, no. 1, pp. 88–93, Jan. 1991, doi: 10.1097/00007632-199101000-00016.

[41] S. Athanasopoulos, T. Paxinos, E. Tsafantakis, K. Zachariou, and S. Chatziconstantinou, "The effect of aerobic training in girls with idiopathic scoliosis," *Scand J Med Sci Sports*, vol. 9, no. 1, pp. 36–40, Feb. 1999, doi: 10.1111/j.1600-0838.1999.tb00204.x.

[42] V. Mooney, J. Gulick, and R. Pozos, "A preliminary report on the effect of measured strength training in adolescent idiopathic scoliosis," *J Spinal Disord*, vol. 13, no. 2, pp. 102–107, Apr. 2000, doi: 10.1097/00002517-200004000-00002.

[43] M. S. Wong, A. F. Mak, K. D. Luk, J. H. Evans, and B. Brown, "Effectiveness of audio-biofeedback in postural training for adolescent idiopathic scoliosis patients," *Prosthet Orthot Int*, vol. 25, no. 1, pp. 60–70, Apr. 2001, doi: 10.1080/03093640108726570.

[44] C. Fusco, F. Zaina, S. Atanasio, M. Romano, A. Negrini, and S. Negrini, "Physical exercises in the treatment of adolescent idiopathic scoliosis: An updated systematic review," *Physiotherapy Theory and Practice*, vol. 27, no. 1, pp. 80–114, Jan. 2011, doi: 10.3109/09593985.2010.533342.

[45] N. Smania, A. Picelli, M. Romano, and S. Negrini, "Neurophysiological basis of rehabilitation of adolescent idiopathic scoliosis," *Disability and Rehabilitation*, vol. 30, no. 10, pp. 763–771, Jan. 2008, doi: 10.1080/17483100801921311.

[46] F. Zaina *et al.*, "Bracing for scoliosis in 2014: state of the art," *Eur J Phys Rehabil Med*, vol. 50, no. 1, pp. 93–110, Feb. 2014.

[47] I. a. F. Stokes, "Mechanical effects on skeletal growth," *J Musculoskelet Neuronal Interact*, vol. 2, no. 3, pp. 277–280, Mar. 2002.

[48] V. J. Raso, E. Lou, D. L. Hill, J. K. Mahood, and M. J. Moreau, "Is the Boston brace mechanically effective in AIS?," *Stud Health Technol Inform*, vol. 91, pp. 378–382, 2002.

[49] "Adam's Forward Bend Test," *The Student Physical Therapist*. https://www.thestudentphysicaltherapist.com/adams-forward-bend-test.html (accessed Sep. 23, 2020).

[50] W. P. Bunnell, "An objective criterion for scoliosis screening," *J Bone Joint Surg Am*, vol. 66, no. 9, pp. 1381–1387, Dec. 1984.

[51] W. P. Bunnell, "Selective screening for scoliosis," *Clin. Orthop. Relat. Res.*, no. 434, pp. 40–45, May 2005, doi: 10.1097/01.blo.0000163242.92733.66.

[52] "Self-Assessment in Respiratory Medicine | European Respiratory Society." https://books.ersjournals.com/content/self-assessment-in-respiratory-medicine (accessed Aug. 28, 2020).

[53] R. T. Morrissy, G. S. Goldsmith, E. C. Hall, D. Kehl, and G. H. Cowie, "Measurement of the Cobb angle on radiographs of patients who have scoliosis. Evaluation of intrinsic error," *J Bone Joint Surg Am*, vol. 72, no. 3, pp. 320–327, Mar. 1990.

[54] H. Kim *et al.*, "Scoliosis Imaging: What Radiologists Should Know," *RadioGraphics*, vol. 30, no. 7, pp. 1823–1842, Nov. 2010, doi: 10.1148/rg.307105061.

[55] J. E. H. Pruijs, M. A. P. E. Hageman, W. Keessen, R. van der Meer, and J. C. van Wieringen, "Variation in Cobb angle measurements in scoliosis," *Skeletal Radiol.*, vol. 23, no. 7, pp. 517–520, Oct. 1994, doi: 10.1007/BF00223081.

[56] D. Malfair *et al.*, "Radiographic Evaluation of Scoliosis: Review," *American Journal of Roentgenology*, vol. 194, no. 3_supplement, pp. S8–S22, Mar. 2010, doi: 10.2214/AJR.07.7145.

[57] M. Law, W.-K. Ma, D. Lau, E. Chan, L. Yip, and W. Lam, "Cumulative radiation exposure and associated cancer risk estimates for scoliosis patients: Impact of repetitive full spine radiography," *European Journal of Radiology*, vol. 85, no. 3, pp. 625–628, Mar. 2016, doi: 10.1016/j.ejrad.2015.12.032.

[58] "A.D.A.M." https://www.adam.com/ (accessed Sep. 23, 2020).

[59] H.-H. Ma, C.-L. Tai, L.-H. Chen, C.-C. Niu, W.-J. Chen, and P.-L. Lai, "Application of two-parameter scoliometer values for predicting scoliotic Cobb angle," *BioMedical Engineering OnLine*, vol. 16, no. 1, p. 136, Dec. 2017, doi: 10.1186/s12938-017-0427-7.

[60] T. A. Sardjono, M. H. F. Wilkinson, A. G. Veldhuizen, P. M. A. van Ooijen, K. E. Purnama, and G. J. Verkerke, "Automatic Cobb Angle Determination From Radiographic Images," *Spine*, vol. 38, no. 20, p. E1256, Sep. 2013, doi: 10.1097/BRS.0b013e3182a0c7c3.

[61] B. Samuvel, V. Thomas, M. M.G., and R. K. J., "A Mask Based Segmentation Algorithm for Automatic Measurement of Cobb Angle from Scoliosis X-Ray Image," in *2012 International Conference on Advances in Computing and Communications*, Aug. 2012, pp. 110–113, doi: 10.1109/ICACC.2012.24.

[62] D. J. Pearsall, J. G. Reid, and D. M. Hedden, "Comparison of three noninvasive methods for measuring scoliosis," *Phys Ther*, vol. 72, no. 9, pp. 648–657, Sep. 1992.

[63] P. Patias, E. Stylianidid, M. Pateraki, Y. Chrysanthou, C. Contozis, and Th. Zavitsanakis, "3D DIGITAL PHOTOGRAMMETRIC RECONSTRUCTIONS FOR SCOLIOSIS SCREENING." https://webcache.googleusercontent.com/search?q=cache:7UiWXeWZmvoJ:https://citeseerx.ist.psu.edu/viewdoc/download%3Fdoi%3D10.1.1.222.652%26rep%3Drep1%26type%3Dpdf+&cd=3&hl=en&ct=clnk&gl=ca (accessed Oct. 02, 2020).

[64] L. Pino-Almero, M. F. Mínguez-Rey, R. M. Cibrián-Ortiz de Anda, M. R. Salvador-Palmer, and S. Sentamans-Segarra, "Correlation between Topographic Parameters Obtained by Back Surface Topography Based on Structured Light and Radiographic Variables in the Assessment of Back Morphology in Young Patients with Idiopathic Scoliosis," *Asian Spine J*, vol. 11, no. 2, pp. 219–229, Apr. 2017, doi: 10.4184/asj.2017.11.2.219.

[65] C. J. Goldberg, M. Kaliszer, D. P. Moore, E. E. Fogarty, and F. E. Dowling, "Surface topography, Cobb angles, and cosmetic change in scoliosis," *Spine (Phila Pa 1976)*, vol. 26, no. 4, pp. E55-63, Feb. 2001, doi: 10.1097/00007632-200102150-00005.

[66] J. M. Frerich, K. Hertzler, P. Knott, and S. Mardjetko, "Comparison of Radiographic and Surface Topography Measurements in Adolescents with Idiopathic Scoliosis," *Open Orthop J*, vol. 6, pp. 261–265, Jul. 2012, doi: 10.2174/1874325001206010261.

[67] J. Zhang *et al.*, "A computer-aided Cobb angle measurement method and its reliability," *J Spinal Disord Tech*, vol. 23, no. 6, pp. 383–387, Aug. 2010, doi: 10.1097/BSD.0b013e3181bb9a3c.

[68] H. Wu, C. Bailey, P. Rasoulinejad, and S. Li, "Automatic Landmark Estimation for Adolescent Idiopathic Scoliosis Assessment Using BoostNet," 2017, doi: 10.1007/978-3-319-66182-7_15.

[69] H. Wu, C. Bailey, P. Rasoulinejad, and S. Li, "Automated comprehensive Adolescent Idiopathic Scoliosis assessment using MVC-Net," *Medical Image Analysis*, vol. 48, pp. 1–11, Aug. 2018, doi: 10.1016/j.media.2018.05.005.

[70] M.-H. Horng, C.-P. Kuok, M.-J. Fu, C.-J. Lin, and Y.-N. Sun, "Cobb Angle Measurement of Spine from X-Ray Images Using Convolutional Neural Network," *Comput Math Methods Med*, vol. 2019, p. 6357171, 2019, doi: 10.1155/2019/6357171.

[71] C. Vergari, W. Skalli, and L. Gajny, "A convolutional neural network to detect scoliosis treatment in radiographs," *Int J Comput Assist Radiol Surg*, vol. 15, no. 6, pp. 1069–1074, Jun. 2020, doi: 10.1007/s11548-020-02173-4.

[72] Y. Tu, N. Wang, F. Tong, and H. Chen, "Automatic measurement algorithm of scoliosis Cobb angle based on deep learning," *J. Phys.: Conf. Ser.*, vol. 1187, no. 4, p. 042100, Apr. 2019, doi: 10.1088/1742-6596/1187/4/042100.

[73] J. Zhang, H. Li, L. Lv, and Y. Zhang, "Computer-Aided Cobb Measurement Based on Automatic Detection of Vertebral Slopes Using Deep Neural Network," *Int J Biomed Imaging*, vol. 2017, 2017, doi: 10.1155/2017/9083916.

[74] H. Wu *et al.*, "Prediction of scoliosis progression in time series using artificial intelligence techniques," *Orthopaedic Proceedings*, vol. 90-B, no. SUPP_I, pp. 100–101, Mar. 2008, doi: 10.1302/0301-620X.90BSUPP_I.0880100d.

[75] L. Ramirez, N. G. Durdle, V. J. Raso, and D. L. Hill, "A support vector machines classifier to assess the severity of idiopathic scoliosis from surface topography," *IEEE Transactions on Information Technology in Biomedicine*, vol. 10, no. 1, pp. 84–91, Jan. 2006, doi: 10.1109/TITB.2005.855526.

[76] P. O. Ajemba, L. Ramirez, N. G. Durdle, D. L. Hill, and V. J. Raso, "A support vectors classifier approach to predicting the risk of progression of adolescent idiopathic scoliosis," *IEEE Transactions on Information Technology in Biomedicine*, vol. 9, no. 2, pp. 276–282, Jun. 2005, doi: 10.1109/TITB.2005.847169.

[77] E. J. Seo, A. Choi, S. E. Oh, H. J. Park, D. J. Lee, and J. H. Mun, "Prediction of Cobb-angle for Monitoring System in Adolescent Girls with Idiopathic Scoliosis using Multiple Regression Analysis," *Journal of Biosystems Engineering*, vol. 38, no. 1, pp. 64–71, 2013, doi: 10.5307/JBE.2013.38.1.064.

[78] B. Samadi, M. Raison, S. Achiche, and C. Fortin, "Identification of the most relevant intervertebral effort indicators during gait of adolescents with idiopathic scoliosis," *Comput Methods Biomech Biomed Engin*, pp. 1–11, May 2020, doi: 10.1080/10255842.2020.1758075.

[79] H. Faber, A. J. van Soest, and D. A. Kistemaker, "Inverse dynamics of mechanical multibody systems: An improved algorithm that ensures consistency between kinematics and external forces," *PLOS ONE*, vol. 13, no. 9, p. e0204575, Sep. 2018, doi: 10.1371/journal.pone.0204575.

[80] M. A. Neto and J. Ambrósio, "Stabilization Methods for the Integration of DAE in the Presence of Redundant Constraints," *Multibody System Dynamics*, vol. 10, no. 1, pp. 81–105, Aug. 2003, doi: 10.1023/A:1024567523268.

[81] M. Raison and L. Ballaz, "Lombo-sacral joint efforts during gait: comparison between healthy and scoliotic subjects," *Studies in health technology and informatics*, Nov. 2018, Accessed: Nov. 23, 2018. [Online]. Available: https://www.academia.edu/14823860/Lombo-sacral_joint_efforts_during_gait_comparison_between_healthy_and_scoliotic_subjects.

[82] M. L. Guilbert, M. Raison, C. Fortin, and S. Achiche, "Development of a multibody model to assess efforts along the spine for the rehabilitation of adolescents with idiopathic scoliosis," *J Musculoskelet Neuronal Interact*, vol. 19, no. 1, pp. 4–12, Mar. 2019.

[83] R. B. Davis, S. Õunpuu, D. Tyburski, and J. R. Gage, "A gait analysis data collection and reduction technique," *Human Movement Science*, vol. 10, no. 5, pp. 575–587, Oct. 1991, doi: 10.1016/0167-9457(91)90046-Z.

[84] P. de Leva, "Adjustments to Zatsiorsky-Seluyanov's segment inertia parameters," *J Biomech*, vol. 29, no. 9, pp. 1223–1230, Sep. 1996.

[85] A. Kiefer, A. Shirazi-Adl, and M. Parnianpour, "Stability of the human spine in neutral postures," *Eur Spine J*, vol. 6, no. 1, pp. 45–53, 1997.

[86] T. W. Lu and J. J. O'Connor, "Bone position estimation from skin marker co-ordinates using global optimisation with joint constraints," *J Biomech*, vol. 32, no. 2, pp. 129–134, Feb. 1999.

[87] J.-C. Samin and P. Fisette, *Symbolic Modeling of Multibody Systems*. Springer Science & Business Media, 2013.

[88] "Robotran - Home." http://www.robotran.be/ (accessed Dec. 03, 2018).

[89] T. B. Grivas, E. Vasiliadis, M. Malakasis, V. Mouzakis, and D. Segos, "Intervertebral disc biomechanics in the pathogenesis of idiopathic scoliosis," *Stud Health Technol Inform*, vol. 123, pp. 80–83, 2006.

[90] M. Kuhn and K. Johnson, "Applied predictive modeling," *CERN Document Server*, 2013. https://cds.cern.ch/record/1555660 (accessed Dec. 27, 2020).

[91] M. A. Asher and D. C. Burton, "Adolescent idiopathic scoliosis: natural history and long term treatment effects," *Scoliosis*, vol. 1, no. 1, p. 2, Mar. 2006, doi: 10.1186/1748-7161-1-2.

[92] S. Parent, P. O. Newton, and D. R. Wenger, "Adolescent idiopathic scoliosis: etiology, anatomy, natural history, and bracing," *Instr Course Lect*, vol. 54, pp. 529–536, 2005.

[93] A. Daryabor, M. Arazpour, G. Sharifi, M. A. Bani, A. Aboutorabi, and N. Golchin, "Gait and energy consumption in adolescent idiopathic scoliosis: A literature review," *Ann Phys Rehabil Med*, vol. 60, no. 2, pp. 107–116, Apr. 2017, doi: 10.1016/j.rehab.2016.10.008.

[94] F. Schwab, A. Patel, B. Ungar, J.-P. Farcy, and V. Lafage, "Adult Spinal Deformity—Postoperative Standing Imbalance: How Much Can You Tolerate? An Overview of Key Parameters in Assessing Alignment and Planning Corrective Surgery," *Spine*, vol. 35, no. 25, p. 2224, Dec. 2010, doi: 10.1097/BRS.0b013e3181ee6bd4.

[95] J. A. Janicki and B. Alman, “Scoliosis: Review of diagnosis and treatment,” *Paediatr Child Health*, vol. 12, no. 9, pp. 771–776, Nov. 2007, doi: 10.1093/pch/12.9.771.

[96] J. Costi, I. A. Stokes, M. Gardner-Morse, J. P. Laible, H. Scoffone, and J. Iatridis, “Direct measurement of intervertebral disc maximum shear strain in six degrees of freedom: Motions that place disc tissue at risk of injury,” *J Biomech*, vol. 40, no. 11, pp. 2457–2466, 2007, doi: 10.1016/j.jbiomech.2006.11.006.

[97] P. Mahaudens, X. Banse, M. Mousny, and C. Detrembleur, “Gait in adolescent idiopathic scoliosis: kinematics and electromyographic analysis,” *Eur Spine J*, vol. 18, no. 4, pp. 512–521, Apr. 2009, doi: 10.1007/s00586-009-0899-7.

[98] M. Syczewska, A. Łukaszewska, B. Górak, and K. Graff, “Changes in gait pattern in patients with scoliosis,” *Rehabilitacja Medyczna*, vol. 10, pp. 18–24, Jan. 2006.

[99] A. E. Geissele, M. J. Kransdorf, C. A. Geyer, J. S. Jelinek, and B. E. Van Dam, “Magnetic resonance imaging of the brain stem in adolescent idiopathic scoliosis,” *Spine*, vol. 16, no. 7, pp. 761–763, Jul. 1991, doi: 10.1097/00007632-199107000-00013.

[100] S. Negrini *et al.*, “2016 SOSORT guidelines: orthopaedic and rehabilitation treatment of idiopathic scoliosis during growth,” *Scoliosis and Spinal Disorders*, vol. 13, no. 1, p. 3, Jan. 2018, doi: 10.1186/s13013-017-0145-8.

[101] M. Raison, C.-E. Aubin, C. Detrembleur, P. Fisette, P. Mahaudens, and J.-C. Samin, “Quantification of global intervertebral torques during gait: comparison between two subjects with different scoliosis severities,” *Stud Health Technol Inform*, vol. 158, pp. 107–111, 2010.

[102] G. Abedrabbo *et al.*, “A multibody-based approach to the computation of spine intervertebral motions in scoliotic patients,” *Stud Health Technol Inform*, vol. 176, pp. 95–98, 2012.

[103] I. A. Stokes, H. Spence, D. D. Aronsson, and N. Kilmer, “Mechanical modulation of vertebral body growth. Implications for scoliosis progression,” *Spine*, vol. 21, no. 10, pp. 1162–1167, May 1996.

[104] M. Raison, C.-E. Aubin, C. Detrembleur, P. Fisette, P. Mahaudens, and J.-C. Samin, “Quantification of intervertebral efforts during gait : comparison between subjects with different scoliosis severity,” presented at the IRSSD, 2010, Accessed: Sep. 23, 2019. [Online]. Available: https://dial.uclouvain.be/pr/boreal/object/boreal:96232.

[105] M. Raison, C. E. Aubin, C. Detrembleur, P. Fisette, and J. C. Samin, “Quantification of intervertebral efforts during walking: comparison between a healthy and a scoliotic subject,” *Computer Methods in Biomechanics and Biomedical Engineering*, vol. 11, no. sup001, pp. 189–190, Jan. 2008, doi: 10.1080/10255840802298836.

[106] S. Schmid *et al.*, “Quantifying spinal gait kinematics using an enhanced optical motion capture approach in adolescent idiopathic scoliosis,” *Gait Posture*, vol. 44, pp. 231–237, Feb. 2016, doi: 10.1016/j.gaitpost.2015.12.036.

[107] G. Abedrabbo *et al.*, “A multibody-based approach to the computation of spine intervertebral motions in scoliotic patients,” *Stud Health Technol Inform*, vol. 176, pp. 95–98, 2012.

[108] S. Dupuis, C. Fortin, C. Caouette, I. Leclair, and C.-É. Aubin, “Global postural re-education in pediatric idiopathic scoliosis: a biomechanical modeling and analysis of curve reduction during active and assisted self-correction,” *BMC Musculoskelet Disord*, vol. 19, Jun. 2018, doi: 10.1186/s12891-018-2112-9.

[109] M. Romano *et al.*, “SEAS (Scientific Exercises Approach to Scoliosis): a modern and effective evidence based approach to physiotherapic specific scoliosis exercises,” *Scoliosis*, vol. 10, Feb. 2015, doi: 10.1186/s13013-014-0027-2.

[110] “ALGLIB - C++/C# numerical analysis library,” Nov. 04, 2019. https://www.alglib.net/ (accessed Nov. 04, 2019).

[111] T. W. Lu and J. J. O’Connor, “Bone position estimation from skin marker co-ordinates using global optimisation with joint constraints,” *J Biomech*, vol. 32, no. 2, pp. 129–134, Feb. 1999.

[112] H. P. Gavin, “The Levenberg-Marquardt method for nonlinear least squares curve-fitting problems c ©,” 2013.

[113] T. Sugihara, “Solvability-Unconcerned Inverse Kinematics by the Levenberg–Marquardt Method,” *IEEE Transactions on Robotics*, vol. 27, no. 5, pp. 984–991, Oct. 2011, doi: 10.1109/TRO.2011.2148230.

[114] J. J. Moré, “The Levenberg-Marquardt algorithm: Implementation and theory,” in *Numerical Analysis*, Berlin, Heidelberg, 1978, pp. 105–116, doi: 10.1007/BFb0067700.

[115] “Robotran - Home,” Dec. 03, 2018. http://www.robotran.be/ (accessed Dec. 03, 2018).

[116] M. L. Guilbert, M. Raison, C. Fortin, and S. Achiche, “Development of a multibody model to assess efforts along the spine for the rehabilitation of adolescents with idiopathic scoliosis,” *J Musculoskelet Neuronal Interact*, vol. 19, no. 1, pp. 4–12, Mar. 2019.

[117] M. Yazji *et al.*, “Are the mediolateral joint forces in the lower limbs different between scoliotic and healthy subjects during gait?,” *Scoliosis*, vol. 10, no. 2, p. S3, Feb. 2015, doi: 10.1186/1748-7161-10-S2-S3.

[118] W. P. Bunnell, “An objective criterion for scoliosis screening,” *J Bone Joint Surg Am*, vol. 66, no. 9, pp. 1381–1387, Dec. 1984.

[119] R. B. Davis, S. Õunpuu, D. Tyburski, and J. R. Gage, “A gait analysis data collection and reduction technique,” *Human Movement Science*, vol. 10, no. 5, pp. 575–587, Oct. 1991, doi: 10.1016/0167-9457(91)90046-Z.

[120] P. de Leva, “Adjustments to Zatsiorsky-Seluyanov’s segment inertia parameters,” *J Biomech*, vol. 29, no. 9, pp. 1223–1230, Sep. 1996.

[121] A. Kiefer, A. Shirazi-Adl, and M. Parnianpour, “Stability of the human spine in neutral postures,” *Eur Spine J*, vol. 6, no. 1, pp. 45–53, 1997.

[122] M.-O. Arsenault, “KOLMOGOROV–SMIRNOV TEST,” *Towards Data Science*, Nov. 22, 2017. https://towardsdatascience.com/kolmogorov-smirnov-test-84c92fb4158d (accessed Feb. 24, 2019).

[123] T. K. Kim, “T test as a parametric statistic,” *Korean J Anesthesiol*, vol. 68, no. 6, pp. 540–546, Dec. 2015, doi: 10.4097/kjae.2015.68.6.540.

[124] M. Nishida, K. Watanabe, M. Matsumoto, Y. Toyama, and T. Nagura, "Asymmetric trunk kinematics during gait is seen between concave side and convex side in adolescent idiopathic scoliosis," *Scoliosis*, vol. 10, no. Suppl 1, p. O32, Jan. 2015, doi: 10.1186/1748-7161-10-S1-O32.

[125] K. L. McIntire, M. A. Asher, D. C. Burton, and W. Liu, "Trunk rotational strength asymmetry in adolescents with idiopathic scoliosis: an observational study," *Scoliosis*, vol. 2, p. 9, Jul. 2007, doi: 10.1186/1748-7161-2-9.

[126] J. Kehrer and H. Hauser, "Visualization and Visual Analysis of Multifaceted Scientific Data: A Survey," *IEEE Transactions on Visualization and Computer Graphics*, vol. 19, no. 3, pp. 495–513, Mar. 2013, doi: 10.1109/TVCG.2012.110.

[127] P. Mahaudens, X. Banse, M. Mousny, M. Raison, and C. Detrembleur, "Very short-term effect of brace wearing on gait in adolescent idiopathic scoliosis girls," *Eur Spine J*, vol. 22, no. 11, pp. 2399–2406, Nov. 2013, doi: 10.1007/s00586-013-2837-y.

[128] M. Reuber, A. Schultz, T. McNeill, and D. Spencer, "Trunk muscle myoelectric activities in idiopathic scoliosis.," *Spine (Phila Pa 1976)*, vol. 8, no. 5, pp. 447–456, 1983, doi: 10.1097/00007632-198307000-00002.

[129] S. R. Ward *et al.*, "Architectural analysis and intraoperative measurements demonstrate the unique design of the multifidus muscle for lumbar spine stability," *J Bone Joint Surg Am*, vol. 91, no. 1, pp. 176–185, Jan. 2009, doi: 10.2106/JBJS.G.01311.

[130] P. Mahaudens and M. Mousny, "Gait in adolescent idiopathic scoliosis. Kinematics, electromyographic and energy cost analysis.," *Stud Health Technol Inform*, vol. 158, pp. 101–106, 2010.

[131] K. P. Clark, L. J. Ryan, and P. G. Weyand, "A general relationship links gait mechanics and running ground reaction forces," *J. Exp. Biol.*, vol. 220, no. Pt 2, pp. 247–258, 15 2017, doi: 10.1242/jeb.138057.

[132] A. M. F. Barela, P. B. de Freitas, M. L. Celestino, M. R. Camargo, and J. A. Barela, "Ground reaction forces during level ground walking with body weight unloading," *Braz J Phys Ther*, vol. 18, no. 6, pp. 572–579, 2014, doi: 10.1590/bjpt-rbf.2014.0058.

[133] R. Fujii *et al.*, "Kinematics of the lumbar spine in trunk rotation: in vivo three-dimensional analysis using magnetic resonance imaging," *Eur Spine J*, vol. 16, no. 11, pp. 1867–1874, Nov. 2007, doi: 10.1007/s00586-007-0373-3.

[134] I. A. Kramers-de Quervain, R. Müller, A. Stacoff, D. Grob, and E. Stüssi, "Gait analysis in patients with idiopathic scoliosis," *Eur Spine J*, vol. 13, no. 5, pp. 449–456, Aug. 2004, doi: 10.1007/s00586-003-0588-x.

[135] R. L. Lambach *et al.*, "Evidence for Joint Moment Asymmetry in Healthy Populations during Gait," *Gait Posture*, vol. 40, no. 4, pp. 526–531, Sep. 2014, doi: 10.1016/j.gaitpost.2014.06.010.

[136] M. Nishida, K. Watanabe, M. Matsumoto, Y. Toyama, and T. Nagura, "Asymmetric trunk kinematics during gait is seen between concave side and convex side in adolescent idiopathic scoliosis," *Scoliosis*, vol. 10, no. 1, p. O32, Jan. 2015, doi: 10.1186/1748-7161-10-S1-O32.

[137] F. Hefti, “Pathogenesis and biomechanics of adolescent idiopathic scoliosis (AIS),” *J Child Orthop*, vol. 7, no. 1, pp. 17–24, Feb. 2013, doi: 10.1007/s11832-012-0460-9.

[138] C. K. Haber and M. Sacco, “Scoliosis: lower limb asymmetries during the gait cycle,” *Arch Physiother*, vol. 5, Jul. 2015, doi: 10.1186/s40945-015-0001-1.

[139] “GRAIL | Motekforce Link.” https://www.motekmedical.com/product/grail/ (accessed Feb. 11, 2020).

[140] L. Tg *et al.*, “Etiology of idiopathic scoliosis: current trends in research,” *The Journal of bone and joint surgery. American volume*, Aug. 2000. https://pubmed.ncbi.nlm.nih.gov/10954107/ (accessed Sep. 14, 2020).

[141] R. Morrissy and S. Weinstein, “Lovell and Winter’s Pediatric Orthopedics,” *undefined*, 1996. /paper/Lovell-and-Winter%27s-Pediatric-Orthopedics-Morrissy-Weinstein/9f7a931eb474474ab9b83acb04b344ea6d74540b (accessed Sep. 24, 2020).

[142] V. Chan *et al.*, “A Genetic Locus for Adolescent Idiopathic Scoliosis Linked to Chromosome 19p13.3,” *The American Journal of Human Genetics*, vol. 71, no. 2, pp. 401–406, Aug. 2002, doi: 10.1086/341607.

[143] A. K. Greiner, “Adolescent Idiopathic Scoliosis: Radiologic Decision-Making,” *AFP*, vol. 65, no. 9, p. 1817, May 2002.

[144] D. A. Hoffman, J. E. Lonstein, M. M. Morin, W. Visscher, B. S. Harris, and J. D. Boice, “Breast cancer in women with scoliosis exposed to multiple diagnostic x rays,” *J. Natl. Cancer Inst.*, vol. 81, no. 17, pp. 1307–1312, Sep. 1989.

[145] C. L. J. Nash, E. C. Gregg, R. H. Brown, and K. Pillai, “Risks of exposure to X-rays in patients undergoing long-term treatment for scoliosis.,” *JBJS*, vol. 61, no. 3, pp. 371–374, Apr. 1979.

[146] M. M. Adankon, N. Chihab, J. Dansereau, H. Labelle, and F. Cheriet, “Scoliosis follow-up using noninvasive trunk surface acquisition,” *IEEE Trans Biomed Eng*, vol. 60, no. 8, pp. 2262–2270, Aug. 2013, doi: 10.1109/TBME.2013.2251466.

[147] A. Tabard-Fougère, A. Bonnefoy-Mazure, S. Hanquinet, P. Lascombes, S. Armand, and R. Dayer, “Validity and Reliability of Spine Rasterstereography in Patients With Adolescent Idiopathic Scoliosis,” *Spine*, vol. 42, no. 2, pp. 98–105, Jan. 2017, doi: 10.1097/BRS.0000000000001679.

[148] X. C. Liu, J. G. Thometz, R. M. Lyon, and J. Klein, “Functional classification of patients with idiopathic scoliosis assessed by the Quantec system: a discriminant functional analysis to determine patient curve magnitude,” *Spine*, vol. 26, no. 11, pp. 1274–1278; discussion 1279, Jun. 2001.

[149] I. Weisz, R. J. Jefferson, A. R. Turner-Smith, G. R. Houghton, and J. D. Harris, “ISIS scanning: a useful assessment technique in the management of scoliosis,” *Spine*, vol. 13, no. 4, pp. 405–408, Apr. 1988.

[150] L. Seoud, M. M. Adankon, H. Labelle, J. Dansereau, and F. Cheriet, “Towards Non Invasive Diagnosis of Scoliosis Using Semi-supervised Learning Approach,” in *Image Analysis and Recognition*, Berlin, Heidelberg, 2010, pp. 10–19, doi: 10.1007/978-3-642-13775-4_2.

[151] S. Roy *et al.*, "A Noninvasive 3D Body Scanner and Software Tool towards Analysis of Scoliosis," *BioMed Research International*, May 09, 2019. https://www.hindawi.com/journals/bmri/2019/4715720/ (accessed Jun. 18, 2020).

[152] P. Mahaudens, M. Raison, X. Banse, M. Mousny, and C. Detrembleur, "Effect of long-term orthotic treatment on gait biomechanics in adolescent idiopathic scoliosis," *Spine J*, vol. 14, no. 8, pp. 1510–1519, Aug. 2014, doi: 10.1016/j.spinee.2013.08.050.

[153] A.-V. Bruyneel, P. Chavet, G. Bollini, P. Allard, E. Berton, and S. Mesure, "Dynamical asymmetries in idiopathic scoliosis during forward and lateral initiation step," *Eur Spine J*, vol. 18, no. 2, pp. 188–195, Feb. 2009, doi: 10.1007/s00586-008-0864-x.

[154] "sklearn.preprocessing.StandardScaler — scikit-learn 0.23.1 documentation." https://scikit-learn.org/stable/modules/generated/sklearn.preprocessing.StandardScaler.html (accessed Jul. 20, 2020).

[155] K. E. Bloch, T. Brack, and A. K. Simonds, *Self-Assessment in Respiratory Medicine*. European Respiratory Society, 2015.

[156] "sklearn.neighbors.KNeighborsClassifier — scikit-learn 0.23.1 documentation." https://scikit-learn.org/stable/modules/generated/sklearn.neighbors.KNeighborsClassifier.html#sklearn.neighbors.KNeighborsClassifier (accessed Aug. 03, 2020).

[157] "sklearn.neighbors.RadiusNeighborsClassifier — scikit-learn 0.23.1 documentation." https://scikit-learn.org/stable/modules/generated/sklearn.neighbors.RadiusNeighborsClassifier.html (accessed Jul. 22, 2020).

[158] "sklearn.svm.SVC — scikit-learn 0.23.1 documentation." https://scikit-learn.org/stable/modules/generated/sklearn.svm.SVC.html (accessed Aug. 03, 2020).

[159] "3.2.4.3.1. sklearn.ensemble.RandomForestClassifier — scikit-learn 0.23.1 documentation." https://scikit-learn.org/stable/modules/generated/sklearn.ensemble.RandomForestClassifier.html (accessed Aug. 03, 2020).

[160] "sklearn.linear_model.LogisticRegression — scikit-learn 0.23.1 documentation." https://scikit-learn.org/stable/modules/generated/sklearn.linear_model.LogisticRegression.html# (accessed Aug. 03, 2020).

[161] "1.7. Gaussian Processes — scikit-learn 0.23.1 documentation." https://scikit-learn.org/stable/modules/gaussian_process.html#gaussian-process-classification-gpc (accessed Aug. 03, 2020).

[162] "sklearn.neural_network.MLPClassifier — scikit-learn 0.23.1 documentation." https://scikit-learn.org/stable/modules/generated/sklearn.neural_network.MLPClassifier.html (accessed Aug. 03, 2020).

[163] “sklearn.ensemble.AdaBoostClassifier — scikit-learn 0.23.1 documentation.” https://scikit-learn.org/stable/modules/generated/sklearn.ensemble.AdaBoostClassifier.html (accessed Aug. 03, 2020).

[164] “sklearn.naive_bayes.GaussianNB — scikit-learn 0.23.1 documentation.” https://scikit-learn.org/stable/modules/generated/sklearn.naive_bayes.GaussianNB.html (accessed Aug. 03, 2020).

[165] “sklearn.discriminant_analysis.LinearDiscriminantAnalysis — scikit-learn 0.23.1 documentation.” https://scikit-learn.org/stable/modules/generated/sklearn.discriminant_analysis.LinearDiscriminantAnalysis.html (accessed Aug. 03, 2020).

[166] “sklearn.ensemble.BaggingClassifier — scikit-learn 0.23.1 documentation.” https://scikit-learn.org/stable/modules/generated/sklearn.ensemble.BaggingClassifier.html (accessed Aug. 03, 2020).

[167] “3.2.4.3.3. sklearn.ensemble.ExtraTreesClassifier — scikit-learn 0.23.1 documentation.” https://scikit-learn.org/stable/modules/generated/sklearn.ensemble.ExtraTreesClassifier.html (accessed Aug. 03, 2020).

[168] “1.11. Ensemble methods — scikit-learn 0.23.1 documentation.” https://scikit-learn.org/stable/modules/ensemble.html (accessed Jul. 20, 2020).

[169] “1.17. Neural network models (supervised) — scikit-learn 0.23.1 documentation.” https://scikit-learn.org/stable/modules/neural_networks_supervised.html (accessed Jul. 20, 2020).

[170] “Neural Network Model - an overview | ScienceDirect Topics.” https://www.sciencedirect.com/topics/computer-science/neural-network-model (accessed Jul. 17, 2020).

[171] E. Fix and J. L. Hodges, “Discriminatory Analysis. Nonparametric Discrimination: Consistency Properties,” *International Statistical Review / Revue Internationale de Statistique*, vol. 57, no. 3, pp. 238–247, 1989, doi: 10.2307/1403797.

[172] J. Brownlee, “K-Nearest Neighbors for Machine Learning,” *Machine Learning Mastery*, Apr. 14, 2016. https://machinelearningmastery.com/k-nearest-neighbors-for-machine-learning/ (accessed Jan. 02, 2021).

[173] “An introduction to support Vector Machines | Guide books.” https://dl.acm.org/doi/book/10.5555/345662 (accessed Jul. 20, 2020).

[174] “1.4. Support Vector Machines — scikit-learn 0.23.1 documentation.” https://scikit-learn.org/stable/modules/svm.html (accessed Jul. 20, 2020).

[175] F. Murtagh, “Multilayer perceptrons for classification and regression,” *Neurocomputing*, vol. 2, no. 5, pp. 183–197, Jul. 1991, doi: 10.1016/0925-2312(91)90023-5.

[176] S. E. Dreyfus, “Artificial neural networks, back propagation, and the Kelley-Bryson gradient procedure,” *Journal of Guidance, Control, and Dynamics*, vol. 13, no. 5, pp. 926–928, 1990, doi: 10.2514/3.25422.

[177] S. Schmid *et al.*, "Non-invasive assessment of spinal kinematics during gait in patients with adolescent idiopathic scoliosis," 2015, doi: 10.1016/J.PHYSIO.2015.03.1278.

[178] N. Chockalingam, P. H. Dangerfield, A. Rahmatalla, E.-N. Ahmed, and T. Cochrane, "Assessment of ground reaction force during scoliotic gait," *Eur Spine J*, vol. 13, no. 8, pp. 750–754, Dec. 2004, doi: 10.1007/s00586-004-0762-9.

[179] "A complete guide to the random forest algorithm," *Built In*. https://builtin.com/data-science/random-forest-algorithm (accessed Jan. 02, 2021).

[180] N. C. Jr, G. Ec, B. Rh, and P. K, "Risks of exposure to X-rays in patients undergoing long-term treatment for scoliosis.," *J Bone Joint Surg Am*, vol. 61, no. 3, pp. 371–374, Apr. 1979.

[181] T. G. Lowe *et al.*, "Etiology of Idiopathic Scoliosis: Current Trends in Research*," *JBJS*, vol. 82, no. 8, p. 1157, Aug. 2000.

[182] A. Stewart and G. W. Kneale, "RADIATION DOSE EFFECTS IN RELATION TO OBSTETRIC X-RAYS AND CHILDHOOD CANCERS," *The Lancet*, vol. 295, no. 7658, pp. 1185–1188, Jun. 1970, doi: 10.1016/S0140-6736(70)91782-4.

[183] I. A. F. Stokes, D. D. Aronson, P. J. Ronchetti, H. Labelle, and J. Dansereau, "Reexamination of the Cobb and Ferguson Angles: Bigger Is Not Always Better," *Clinical Spine Surgery*, vol. 6, no. 4, pp. 333–338, Aug. 1993.

[184] J. Wright and A. Feinstein, "Improving the reliability of orthopaedic measurements," *The Journal of Bone and Joint Surgery. British volume*, vol. 74-B, no. 2, pp. 287–291, Mar. 1992, doi: 10.1302/0301-620X.74B2.1544971.

[185] K. Watanabe, Y. Aoki, and M. Matsumoto, "An Application of Artificial Intelligence to Diagnostic Imaging of Spine Disease: Estimating Spinal Alignment From Moiré Images," *Neurospine*, vol. 16, no. 4, pp. 697–702, Dec. 2019, doi: 10.14245/ns.1938426.213.

[186] J. L. Jaremko *et al.*, "Comparison of Cobb angles measured manually, calculated from 3-D spinal reconstruction, and estimated from torso asymmetry," *Comput Methods Biomech Biomed Engin*, vol. 5, no. 4, pp. 277–281, Aug. 2002, doi: 10.1080/10255840290032649.

[187] R. Choi *et al.*, "**CNN-based Spine and Cobb Angle Estimator Using Moire Images** ," *IIEEJ Transactions on Image Electronics and Visual Computing*, vol. 5, no. 2, pp. 135–144, 2017, doi: 10.11371/tievciieej.5.2_135.

[188] W. Wu *et al.*, "Reliability and reproducibility analysis of the Cobb angle and assessing sagittal plane by computer-assisted and manual measurement tools," *BMC Musculoskelet Disord*, vol. 15, p. 33, Feb. 2014, doi: 10.1186/1471-2474-15-33.

[189] L. Wang, Q. Xu, S. Leung, J. Chung, B. Chen, and S. Li, "Accurate automated Cobb angles estimation using multi-view extrapolation net," *Medical Image Analysis*, vol. 58, p. 101542, Dec. 2019, doi: 10.1016/j.media.2019.101542.

[190] T. D.k., P. B.g, and F. Xiong, "Auto-detection of epileptic seizure events using deep neural network with different feature scaling techniques," *Pattern Recognition Letters*, vol. 128, pp. 544–550, Dec. 2019, doi: 10.1016/j.patrec.2019.10.029.

[191] M. W. Browne, "Cross-Validation Methods," *Journal of Mathematical Psychology*, vol. 44, no. 1, pp. 108–132, Mar. 2000, doi: 10.1006/jmps.1999.1279.

[192] R. Bardenet, M. Brendel, B. Kégl, and M. Sebag, "Collaborative hyperparameter tuning," in *Proceedings of the 30th International Conference on International Conference on Machine Learning - Volume 28*, Atlanta, GA, USA, Jun. 2013, p. II-199-II–207, Accessed: Aug. 28, 2020. [Online].

[193] F. Pedregosa *et al.*, "Scikit-learn: Machine Learning in Python," *Journal of Machine Learning Research*, vol. 12, no. 85, pp. 2825–2830, 2011.

[194] "sklearn.neighbors.KNeighborsRegressor — scikit-learn 0.23.2 documentation." https://scikit-learn.org/stable/modules/generated/sklearn.neighbors.KNeighborsRegressor.html (accessed Aug. 29, 2020).

[195] "sklearn.neighbors.RadiusNeighborsRegressor — scikit-learn 0.23.2 documentation." https://scikit-learn.org/stable/modules/generated/sklearn.neighbors.RadiusNeighborsRegressor.html (accessed Aug. 29, 2020).

[196] "sklearn.svm.SVR — scikit-learn 0.23.2 documentation." https://scikit-learn.org/stable/modules/generated/sklearn.svm.SVR.html (accessed Aug. 29, 2020).

[197] "3.2.4.3.2. sklearn.ensemble.RandomForestRegressor — scikit-learn 0.23.2 documentation." https://scikit-learn.org/stable/modules/generated/sklearn.ensemble.RandomForestRegressor.html (accessed Aug. 29, 2020).

[198] "sklearn.linear_model.LinearRegression — scikit-learn 0.23.2 documentation." https://scikit-learn.org/stable/modules/generated/sklearn.linear_model.LinearRegression.html (accessed Sep. 29, 2020).

[199] "sklearn.linear_model.Ridge — scikit-learn 0.23.2 documentation." https://scikit-learn.org/stable/modules/generated/sklearn.linear_model.Ridge.html (accessed Aug. 31, 2020).

[200] "sklearn.linear_model.Lasso — scikit-learn 0.23.2 documentation." https://scikit-learn.org/stable/modules/generated/sklearn.linear_model.Lasso.html (accessed Sep. 29, 2020).

[201] "sklearn.gaussian_process.GaussianProcessRegressor — scikit-learn 0.23.2 documentation." https://scikit-learn.org/stable/modules/generated/sklearn.gaussian_process.GaussianProcessRegressor.html (accessed Aug. 29, 2020).

[202] "sklearn.ensemble.AdaBoostRegressor — scikit-learn 0.23.2 documentation." https://scikit-learn.org/stable/modules/generated/sklearn.ensemble.AdaBoostRegressor.html (accessed Aug. 29, 2020).

[203] "Decision Tree Regression — scikit-learn 0.23.2 documentation." https://scikit-learn.org/stable/auto_examples/tree/plot_tree_regression.html (accessed Aug. 31, 2020).

[204] “sklearn.linear_model.BayesianRidge — scikit-learn 0.23.2 documentation.” https://scikit-learn.org/stable/modules/generated/sklearn.linear_model.BayesianRidge.html (accessed Aug. 31, 2020).

[205] “sklearn.ensemble.BaggingRegressor — scikit-learn 0.23.2 documentation.” https://scikit-learn.org/stable/modules/generated/sklearn.ensemble.BaggingRegressor.html (accessed Aug. 29, 2020).

[206] “3.2.4.3.4. sklearn.ensemble.ExtraTreesRegressor — scikit-learn 0.23.2 documentation.” https://scikit-learn.org/stable/modules/generated/sklearn.ensemble.ExtraTreesRegressor.html (accessed Aug. 29, 2020).

[207] “3.2.4.3.6. sklearn.ensemble.GradientBoostingRegressor — scikit-learn 0.23.2 documentation.” https://scikit-learn.org/stable/modules/generated/sklearn.ensemble.GradientBoostingRegressor.html (accessed Aug. 31, 2020).

[208] J. R. Quinlan, *C4.5: Programs for Machine Learning*. Elsevier, 2014.

[209] S. Kullback and R. A. Leibler, “On Information and Sufficiency,” *The Annals of Mathematical Statistics*, vol. 22, no. 1, pp. 79–86, 1951.

[210] S. Langensiepen *et al.*, “Measuring procedures to determine the Cobb angle in idiopathic scoliosis: a systematic review,” *Eur Spine J*, vol. 22, no. 11, pp. 2360–2371, Nov. 2013, doi: 10.1007/s00586-013-2693-9.

[211] P. Gupta, “Decision Trees in Machine Learning,” *Medium*, Nov. 12, 2017. https://towardsdatascience.com/decision-trees-in-machine-learning-641b9c4e8052 (accessed Jan. 03, 2021).

[212] B. Cho *et al.*, “Automated Measurement of Lumbar Lordosis on Radiographs Using Machine Learning and Computer Vision,” *Global spine journal*, 2020, doi: 10.1177/2192568219868190.

[213] P. Knott *et al.*, “SOSORT 2012 consensus paper: reducing x-ray exposure in pediatric patients with scoliosis,” *Scoliosis*, vol. 9, no. 1, p. 4, Apr. 2014, doi: 10.1186/1748-7161-9-4.

[214] A. Simony, E. J. Hansen, S. B. Christensen, L. Y. Carreon, and M. O. Andersen, “Incidence of cancer in adolescent idiopathic scoliosis patients treated 25 years previously,” *Eur Spine J*, vol. 25, no. 10, pp. 3366–3370, Oct. 2016, doi: 10.1007/s00586-016-4747-2.

[215] B. M, L. H, G. G, S. C, P. B, and D. J, “Diurnal variation of Cobb angle measurement in adolescent idiopathic scoliosis.,” *Spine (Phila Pa 1976)*, vol. 18, no. 12, pp. 1581–1583, Sep. 1993, doi: 10.1097/00007632-199309000-00002.

[216] “scikit-learn: machine learning in Python — scikit-learn 0.23.2 documentation.” https://scikit-learn.org/stable/ (accessed Oct. 20, 2020).

[217] “Keras: the Python deep learning API.” https://keras.io/#why-this-name-keras (accessed Oct. 20, 2020).